Transversal waves and vibrations in axially moving continua

Gaiko, Nick

Important note
To cite this publication, please use the final published version (if applicable).
Please check the document version above.

TRANSVERSAL WAVES AND VIBRATIONS IN AXIALLY MOVING CONTINUA

TRANSVERSAL WAVES AND VIBRATIONS IN AXIALLY MOVING CONTINUA

Proefschrift

ter verkrijging van de graad van doctor
aan de Technische Universiteit Delft,
op gezag van de Rector Magnificus prof. ir. K.C.A.M. Luyben,
voorzitter van het College voor Promoties,
in het openbaar te verdedigen op maandag 20 maart 2017 om 12:30 uur

door

Nick GAIKO

Master of Science in Physics and Mathematics,
geboren te Minsk, Wit-Rusland.

Dit proefschrift is goedgekeurd door de

promotor: Prof. dr. ir. A.W. Heemink
copromotor: Dr. ir. W.T. van Horssen

Samenstelling promotiecommissie:

Rector Magnificus,	voorzitter
Prof. dr. ir. A.W. Heemink,	Technische Universiteit Delft
Dr. ir. W.T. van Horssen,	Technische Universiteit Delft

Onafhankelijke leden:

Prof. dr. A.K. Abramyan,	Russian Academy of Sciences
Prof. dr. I.V. Andrianov,	RWTH Aachen University
Prof. dr. S. Kaczmarcyk,	The University of Northampton
Prof. dr. A.V. Metrikine,	Technische Universiteit Delft
Prof. dr. ir. K. Vuik,	Technische Universiteit Delft

TUDelft

To my Parents

Contents

Chapter 1

Introduction

1.1 Background

Axially moving strings, beams, cables, membranes, and plates have been studied since the early 1950s and are still of great interest to researchers due to their theoretical and industrial importance. They have a wide range of applications in the field of engineering: from large structures to small machine parts. Axially moving continua are found as slender elements in conveyor belts, elevator cables, crane hoist cables, power transmission belts, band saws, and aerial tramways (see Figure 1.1) to name just a few. The dynamics of these engineering devices may be influenced by different kinds of environmental disturbances (rain, wind, or seismic excitations) or by their structural imperfections (the eccentricity of a pulley, the irregular speed of the driving motor, or nonuniform material properties).

In the absence of any driving or damping force, every object tends to oscillate at its natural frequencies. If an object is excited at one or more of the natural frequencies, the response amplitudes of the vibration can reach a relative maximum and the vibratory energy can increase to dangerous levels. This phenomenon is called *resonance*. In most cases resonance leads to failures. The collapse of the Angers bridge on 16 April 1850 is a classic example of the resonance effect, which happened when a battalion of French soldiers was marching across the bridge. In order to prevent such failures, it is important to understand the nature of vibrations.

There are many characteristics in engineering applications to classify vibrations. One of the classifications is based on the degrees of freedom. Vibrations can be divided into axial (or longitudinal), transversal, and torsional. In this thesis, only the transverse vibrations are studied. The minimum number of independent spatial parameters describing the dynamics of axially moving continua is one, which is why strings and beams are commonly used for their modeling. The *critical tension*[1] of a one-dimensional continuum is assumed to be sufficiently large so that the longitudinal variation due to extension of the material is negligible. Moreover, for beam-like problems, torsional rigidity of a beam is also neglected.

---

[1]The maximum tension that a material can resist while being stretched before breaking.

Figure 1.1: The world's largest cabin cable car system, Nu Hoang, transports passengers across Ha Long Bay in Vietnam.

Real-world systems are very complex to model mathematically as their geometry and physics have a strong nonlinear character. To give more insight into the nonlinear dynamics, it is essential to understand the behavior of the associated linear models. These linear models arise when we assume that the transverse displacements of axially moving continua are small compared to their length, which holds for the applications in this dissertation.

One-dimensional axially moving continua are the simplest representatives of distributed parameter gyroscopic systems. The physical parameters and material properties describing such systems are spread along their length. The motion of strings is governed by the wave equation which is represented by second order hyperbolic partial differential equations (PDEs); the motion of beams is governed by the beam equation which is of fourth order in space. The term "gyroscopic" comes from the earlier problems in dynamics of gyroscopes. According to gyroscope theory, axially moving systems are acted upon by the Coriolis force due to the translation of material particles with a certain speed and their rotation at a certain angular velocity. Mathematically the Coriolis force is expressed by the presence of a gyroscopic, skew-symmetric differential operator in the governing equations. Its presence makes the analysis of the partial differential equations more complex.

There is an abundance of analytical methods for the classical problems in mathematical physics determining solutions in a *closed form*[2]. In many cases, it can be difficult or even impossible to find the solution of the problem exactly. Nowadays, with the increasing power and performance of computers, numerical methods are commonly used to tackle complex mathematical models which are generally based on the discretized system models implying implicitly truncation. However, the dynamics of distributed gyroscopic systems is governed by infinite-dimensional systems. In many cases, their discretization with the following truncation leads to inaccurate results on long timescales, consequently illustrating different dynamics from the original system.

Many world processes can be treated as a perturbation of the known tractable mod-

---

[2]A closed-form expression is an analytical expression that can be evaluated in a finite number of operations.

els. Thus, if a problem is not solvable in a closed form, perturbation methods give additional insight. These methods are highly informative and more accurate on long timescales than the discretized models. Nevertheless, perturbation methods also have their disadvantages. For example, the first order approximation of the solution does not always provide a required accuracy, or it is often not the easiest or even a feasible task to construct approximations of higher orders. Thus, the choice of the best method strongly depends on many factors such as the application under consideration, corresponding mathematical model, and its scope of analysis.

1.2 Mathematical models

In this thesis we consider a set of initial-boundary value problems describing the motion of axially moving strings and beams. In applications, these problems may be regarded as models describing the transverse vibrations of conveyor belts and elevator cables in the horizontal and in the vertical direction, respectively.

In Chapter 2, the forced transverse oscillations of a damped axially moving string are considered. The string travels between two pulleys, so its ends are fixed implying Dirichlet boundary conditions (BCs). The initial-boundary value problem in its dimensionless form is given by

$$
\begin{aligned}
\text{PDE}_1 &: u_{tt} + 2v u_{xt} - (1 - v^2) u_{xx} + d(u_t + v u_x) = F(x, t), &&\text{for } 0 < x < 1, \ t > 0, \\
\text{BC}_1 &: u(0, t) = u(1, t) = 0, &&\text{for } t > 0, \\
\text{IC}_1 &: u(x, 0) = \phi(x), \ u_t(x, 0) = \psi(x), &&\text{for } 0 < x < 1,
\end{aligned}
$$

where $u(x, t)$ is a real-valued function representing the transverse displacement of the string, v is the axial velocity, d is the material damping, F is a forcing term. The real-valued functions ϕ, ψ, and F have to satisfy certain smoothness conditions, which will be given in the subsequent chapters.

In Chapter 3, a mass-spring-dashpot system is attached at the downstream boundary of a traveling string. Hence, the boundary conditions have a nonclassical character. The free transverse vibrations of the string are described by the following initial-boundary value problem

$$
\begin{aligned}
\text{PDE}_2 &: u_{tt} - u_{xx} = -2\varepsilon v u_{xt} - \varepsilon^2 v^2 u_{xx}, &&\text{for } 0 < x < 1, \ t > 0, \\
\text{BC}_2 &: u(0, t) = 0, && \\
&\quad m u_{tt}(1, t) + k u(1, t) + u_x(1, t) = \varepsilon[v u_t(1, t) - \eta u_t(1, t)] && \\
&\quad + \varepsilon^2 v^2 u_x(1, t), &&\text{for } t > 0, \\
\text{IC}_2 &: u(x, 0) = \phi(x), \ u_t(x, 0) = \psi(x), &&\text{for } 0 < x < 1,
\end{aligned}
$$

where ε is small, m is an attached mass, k is the elasticity modulus of the spring, and η is the damping factor of the dashpot.

In Chapter 4, different types of boundary supports for a traveling semi-infinite string are considered such as fixed (Dirichlet BC), free (Neumann BC), spring-dashpot, and

mass-spring-dashpot. The last two boundary conditions are non-classical. The equations of the transversal motion of the string are given by

$$\text{PDE}_3 : u_{tt} + 2vu_{xt} - (1-v)^2 u_{xx} = 0, \qquad\qquad \text{for } x < 0, \ t > 0,$$

$\quad \text{BC}_3 : $ 1) $u(0,t) = 0,$ or

$\qquad\qquad$ 2) $u_x(0,t) = 0,$ or

$\qquad\qquad$ 3) $ku(0,t) + \eta u_t(0,t) - vu_t(0,t) + (1-v^2)u_x(0,t) = 0,$ or

$\qquad\qquad$ 4) $mu_{tt}(0,t) + ku(0,t) + \eta u_t(0,) - vu_t(0,t)$

$$\qquad\qquad + (1-v^2)u_x(0,t) = 0, \qquad\qquad \text{for } t > 0,$$

$\quad \text{IC}_3 : u(x,0) = \phi(x), \ u_t(x,0) = \psi(x), \qquad\qquad \text{for } x < 0.$

In Chapter 5, the lateral vibrations of a vertically moving string with harmonically time-varying length are described by

$$\text{PDE}_4 : u_{tt} - [P(x,t;\varepsilon)u_x]_x = -2\varepsilon v u_{xt} - \varepsilon^2(v^2 u_{xx} + \dot{v}u_x), \quad \text{for } 0 < x < l, \ t > 0,$$

$\quad \text{BC}_4 : u(0,t) = u(l,t) = 0, \qquad\qquad\qquad\qquad \text{for } t > 0,$

$\quad \text{IC}_4 : u(x,0) = \phi(x), \ u_t(x,0) = \psi(x), \qquad\qquad \text{for } 0 < x < l_0,$

with $l = l_0 + \beta \sin \Omega t$, where l_0 is the constant mean length, β is the length variation parameter, Ω is the angular frequency and $v = \dot{l} = \frac{dl}{dt}$, and where P is the axial tension in the string.

In Chapter 6, an axially moving beam with a linearly time-varying length is investigated. The boundaries of the beam move in the horizontal direction representing the sway s. The lateral vibrations of the beam are described by

$$\text{PDE}_5 : u_{tt} - [P(x,t;\varepsilon)u_x]_x = -\varepsilon(EIu_{xxxx} + 2vu_{xt})$$

$$\qquad\qquad - \varepsilon^2(v^2 u_{xx} + \dot{v}u_x), \qquad\qquad \text{for } 0 < x < l, \ t > 0,$$

$\quad \text{BC}_5 : u(0,t) = s(H,t), \text{ and } u_{xx}(0,t) = 0,$

$\qquad\qquad u(l,t) = s(H-l,t), \text{ and } u_{xx}(l,t) = 0, \qquad \text{for } t > 0,$

$\quad \text{IC}_5 : u(x,0) = \varepsilon\phi(x), \ u_t(x,0) = \varepsilon\psi(x), \qquad\qquad \text{for } 0 < x < l_0,$

with $l = l_0 + vt$. More details on the above problems will be given in the following chapters.

1.3 Mathematical methods

This section provides analytical techniques that have proved to be useful in the analysis of the linear partial differential equations of hyperbolic type in this thesis.

1.3.1 Modified separation of variables

The method of separation of variables, also known as the Fourier method, is one of the most important techniques to solve linear homogeneous ordinary and partial differential equations. This method also requires linear homogeneous boundary conditions.

According to the Fourier method, the function of the form

$$u(x,t) = X(x)T(t) \tag{1.1}$$

is assumed to be a (product) solution of a partial differential equation in x and t. However, it is not always possible to apply this method, if the algebra of the equation does not allow to separate each of the two variables straightforwardly. Likewise it is not possible to use this method for the hyperbolic type PDEs with a skew-symmetric, non-selfadjoint differential operator. In this case the Fourier method requires a slight modification as follows from [20]. When the product solution is plugged into a PDE, the so-obtained equation will require extra differentiation with respect to some of the independent variables as many times as it is needed for separation of the variables. As a result, the PDE will be reduced to a set of ODEs. This method is frequently used in the thesis to validate the results obtained by other analytical techniques for simplified cases of the problems.

1.3.2 Eigenfunction expansion

The method of eigenfunction expansion is used to solve inhomogeneous problems with homogeneous boundary conditions. According to this method the unknown solution $u(x,t)$ has to be expanded in a generalized Fourier series of the related homogeneous eigenfunctions

$$u(x,t) = \sum_{n=1}^{\infty} c_n(t)u_n(x), \tag{1.2}$$

where $c_n(t)$ are the generalized Fourier coefficients which have to be determined, and $\{u_n\}_{n=0}^{\infty}$ is the sequence of eigenfunctions of a corresponding Sturm-Liouville eigenvalue problem. Remark that the coefficients $c_n(t)$ are not the time-dependent separated solutions from the method of separations of variables for homogeneous problems. For more details on the method of eigenfunction expansion see [43].

1.3.3 Laplace transform method

The Laplace transform method is commonly used for solving ordinary and partial differential equations. The main advantage of this method compared to some other analytical methods such as separation of variables, eigenfunction expansion, or *Green's functions*[3] is that it does not require orthogonality relations of eigenfunctions. The Laplace transform of the unknown solution $u(x,t)$ is defined as

$$\mathscr{L}[u(x,t)] = U(x,s) := \int_0^{\infty} e^{-st}u(x,t)\,dt, \tag{1.3}$$

where x is fixed. The domain of $\mathscr{L}[u](x,s)$ is the set of $s \in \mathbb{R}_+$, such that the improper integral (1.3) converges.

---

[3]A Green's function is the impulse response of an initial-boundary value problem with an inhomogeneous differential equation; see for instance [43].

When the solution of the transformed equation is found, the inverse transform can be applied to find the solution in the original function space. The inverse Laplace transform of $U(x,s)$ is given by the following complex integral

$$\mathscr{L}^{-1}[U(x,s)] = u(x,t) := \frac{1}{2\pi i} \int_{\gamma-i\infty}^{\gamma+i\infty} \mathrm{e}^{st} U(x,s) \, \mathrm{d}s, \tag{1.4}$$

for all $\gamma > 0$ that avoid singularities. In practice, the complex integral can be computed by using the methods of contour integration such as direct integration of a complex-valued function along a contour, the Cauchy integral formula, the residue theorem, or some of these methods combined.

1.3.4 Method of characteristics

The method of characteristics is a powerful tool to solve one-dimensional wave equations. The method reduces a PDE to a family of ODEs which can be integrated with respect to the initial data. In general, the motion of axially moving continua can be governed by an infinite dimensional system of coupled ODEs. Usually it is difficult or even impossible to solve such a system. It was proved in many cases that the method of characteristics can be applied in order to tackle infinite dimensional systems analytically.

According to the method, the general solution is represented by the sum of two waves of fixed shape; one of which moving forward and the other one moving backward. The initial value problem for an infinite space has a solution in the form of the formula of d'Alembert. If a problem is formulated on a semi-infinite or finite domain, some modifications have to be done, which will be given in Chapter 4 and Chapter 5, respectively.

It is worth mentioning that in contrast to the above methods and some other techniques to solve linear PDEs, the method of characteristics can be extended for quasilinear PDEs. This method allows to gain more qualitative insight into a PDE. One of the examples is a traffic flow problem approximating a congested one-directional highway. In this case, the method of characteristics can work in a completely different way compared to linear problems. For instance, one can find shock waves using the crossings of the characteristics resulting in the multi-valued traffic density, what implies a physically impossible phenomenon. The reader can be referred to [43] for this topic.

1.3.5 Multiple timescales

The method of multiple timescales helps to construct uniformly valid approximate solutions for ordinary and partial differential equations on long timescales. The method can be briefly described as follows. First of all, assume that a problem is considered on widely different timescales. In order to avoid resonance in the system, one or more (depending on the problem) new time variables are introduced for each of those timescales and are treated independently. For example, $t = \mathscr{O}(1)^4$, $t_0 = t/\varepsilon, t_1 = \varepsilon t, t_2 = \varepsilon^2 t, \ldots,$

---

[4] $f(t) = \mathscr{O}(g(t))$ as $t \to \infty$ if and only if there exists a positive real number M and a real number t_0 such that $|f(t)| \le M|g(t)|$ for $t \ge t_0$; big $\mathscr{O}$ is also called Landau's symbol.

where ε is a small parameter. Then, it is assumed that the solution $u(x,t)$ of the perturbation problem can be expanded in a power series in ε for a fixed x as follows:

$$u(x,t;\varepsilon) = u_0(x,t_0,t,t_1,t_2,\dots) + \varepsilon u_1(x,t_0,t,t_1,t_2,\dots) + \mathcal{O}(\varepsilon^2). \qquad (1.5)$$

In order to avoid unbounded (or secular) terms in the expansion, secularity conditions have to be found for u_i, where $i \in \mathbb{N} \cup \{0\}$.

1.3.6 Averaging method

The method of averaging is used to study time-varying systems. The idea of this method is quite natural. By averaging the original system, an autonomous (time-invariant) system can be obtained, which is easier to analyze. In order to perform this technique, one should consider the evolution of the time-varying system in two timescales such as fast and slow times. Recall that the average value of a T-periodic function $f(x,t)$ for fixed x is given by

$$f_a(x) = \frac{1}{T} \int_0^T f(x,t)\, \mathrm{d}t. \qquad (1.6)$$

Eventually the approximation method leads to an asymptotic series. For more details on the method, the reader is referred to [26].

1.4 Outline of the thesis

In Chapter 2, the initial-boundary value problem (PDE$_1$-IC$_1$) is studied. The equations of motion are derived by Hamilton's principle. This chapter mainly emphasizes the straightforwardness of the applied Laplace transform method for solving such type of problems.

In Chapter 3, the initial-boundary value problem (PDE$_2$-IC$_2$) is investigated. In this Chapter, an accurate asymptotic approximation of the low-frequency vibrations is constructed by a two-timescales perturbation method. The results are confirmed by an alternative approach, namely the Laplace transform method combined with the approximations of the lower eigenvalues of the problem.

In Chapter 4, the reflection properties and energetics of the semi-infinite traveling string are studied for different types (classical and non-classical) of boundary conditions. The initial-boundary value problem (PDE$_3$-IC$_3$) governs the transverse displacements of the string .The solution is obtained exactly in a form of d'Alembert by the method of characteristics. The obtained results give insight into the most efficient way of placing a boundary support depending on the direction of the transport velocity.

In Chapter 5, the lateral vibrations and resonances of a vertically moving string with time-varying length are studied. The equations of motion of the string are given by (PDE$_4$-IC$_4$). The initial-boundary value problem is solved by the Fourier approach. The infinite dimensional system of coupled ordinary differential equations representing the amplitudes of vibrations is analyzed by Galerkin's method in combination with truncation. Then the dynamic stability is studied from the energy view point, what produce

some conclusions for the first two resonance frequencies. The main result of this chapter is that the truncation method is not applicable for such type of problems.

In Chapter 6, the lateral vibrations and resonances of a swaying axially moving beam with a time-varying length are investigated. The motion of the string is governed by (PDE_5-IC_5). An internal layer analysis is performed mainly with the help of the averaging method. A cascade of autoresonances is detected in the cable system. Because of this reason, a three-timescales perturbation method is used to construct an accurate approximation of the transversal vibrations of the cable. It should be mentioned that the approaches developed in this thesis for the analysis of the linear transverse vibrations of axially moving continua can be extended to a much broader and more complex class of distributed gyroscopic systems.

Chapter 2

Laplace transform and the transverse vibrations of a damped traveling string

In this chapter, we study the forced transverse vibrations of a damped axially moving string fixed between two supports. The problem is studied by the Laplace transform method which seems to be more straightforward then other known exact, analytical techniques. Remark that this method will be frequently used in the subsequent chapters. The obtained results show agreement with previous research and also show the importance of the axial velocity and the viscous damping of the material in vibrations of the string.
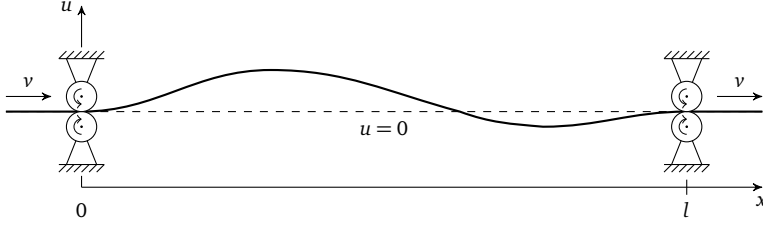
Figure 2.1: An axially moving string with fixed ends.

2.1 Introduction

This chapter starts with a simple model of a traveling string with constant speed between two fixed pulleys and considers its free transverse vibrations (see Figure 2.1). This model can be regarded as one describing the transverse vibrations of a moving belt. In most of the works for traveling systems, damping is usually ignored and only linear elasticity of the belt material is considered. However, belts are usually composed of some viscoelastic materials such as polymers. In order to describe the dynamics of the belt accurately, it is important to take into account such material properties, especially when vibrations of pipes conveying fluids or creep analysis of belts are studied. Thus, in this work we introduce linear viscosity of the belt which is expressed in a damping force acting upon the system. The main aim of this chapter is to show the applicability of the Laplace transform method (see [21, 22, 62]) to the partial differential equations of hyperbolic type with a skew-symmetric differential operator governing axially moving systems. In contrast to other classical methods to solve string-like problems such as the eigenfunction expansion [6, 27] or Green's functions [5], the Laplace transform seems to be more straightforward because it does not require orthogonality of the eigenfunctions.

The current chapter is organized as follows. In Section 2.2, the governing equation is derived using Hamilton's principle and the physical interpretation for the motion of the string is given. Further, the initial-boundary value problem is tackled by the Laplace transform method in Section 2.3. Then, the image of the Laplace transform is mapped inversely into the original function space by Mellin's inverse formula (also known as the Bromwich integral or the Fourier-Mellin integral) in Section 2.4. The complex integral of the inverse Laplace transform is computed by Cauchy's residue theorem and a convolution. Section 2.5 shows some numerical simulations for the simplified problems. Finally, the straightforwardness of the Laplace transform method and the system parameters contribution are discussed in Section 2.6.

2.2 Assumptions and a mathematical model

In order to restrict the complexity of the analysis of the problem, we assume:

- the string is uniform;

- the string is fixed at its ends;
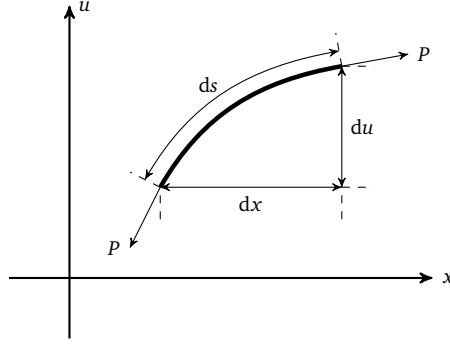
Figure 2.2: An element of the string and the transverse direction u.

- bending stiffness and the effects due to gravity are neglected;

- the equilibrium position is defined to be $u = 0$ along the string;

- only transverse damped, forced oscillations are considered;

- the transverse displacements are sufficiently small such that the non-linear terms in the governing equation can be neglected.

The equation of motion describing the vertical displacement of the string will be obtained by applying the *Hamilton's principle* in the following form (see [4, 8, 19]):

$$\delta \int_{t_1}^{t_2} L \, dt + \int_{t_1}^{t_2} \delta W \, dt = 0, \tag{2.1}$$

where δ is a variation in a function, L is the *Lagrangian*[1], and W is the *virtual work* performed by *non-conservative forces*[2] of the system. To obtain the Lagrangian, we must calculate the *kinetic energy* of the particles in the system at any instant and the corresponding *potential energy*. It should be noted that the virtual momentum transport of mass across the boundaries is included implicitly into the Lagrangian. In some papers (for instance, [33]) this mass transport is written down as a separate integral in (2.1).

The kinetic energy of the system is produced by the the kinetic energy of the string, which is given by

$$K_s := \frac{1}{2} \int_0^l \rho V_{tr}^2 \, dx, \tag{2.2}$$

where $V_{tr} := u_t + V u_x$ is the instantaneous transverse velocity of a material particle.

Next, the total potential energy is the work done by deflecting the string from its equilibrium position. Considering the increase in length of an element of the string

---

[1] The Lagrangian contains the information about the dynamics of the system.
[2] The work done by a non-conservative force in moving a particle between two points depends on the taken path.

from dx to $ds := \sqrt{dx^2 + du^2}$ (see Figure 2.2), the strain e at position x is given by

$$e := \frac{ds}{dx} - 1 = \sqrt{1 + u_x^2} - 1.$$

The square root term can be expanded by the binomial identity as follows

$$\left(1 + u_x^2\right)^{\frac{1}{2}} = 1 + \frac{1}{2}u_x^2 - \frac{1}{8}u_x^4 + \frac{1}{16}u_x^6 - \cdots$$

Eliminating then the higher order terms (by assumption $u_x \ll 1$) in the expansion, the strain becomes $e \approx u_x^2/2$. Hence the contribution of the axial load is given by

$$U_s := \int_0^l Pe \; dx = \frac{1}{2} \int_0^l Pu_x^2 \; dx. \tag{2.3}$$

The Lagrangian is then found to be

$$L := K_s - U_s = \frac{1}{2} \int_0^l \left[\rho(u_t + vu_x)^2 - Pu_x^2\right] dx.$$

The virtual work due to non-conservative forces, such as an external force, f, acting on the string in the plane normal to x and a transverse damping force, f_η, is given by

$$W := \int_0^l (f - f_\eta)u \; dx,$$

where

$$f_\eta := \eta_s V_{tr},$$

and η_s is the viscous damping factor of the string. The damping force opposes its motion, that is why the virual work done by it is negative. *Recall that Hamilton's principle means that among all the possible paths between the end points, the motion will occur along the path that gives an extreme value to the integral*

$$I := \int_{t_1}^{t_2} (L + W) \; dt = \int_{t_1}^{t_2} \int_0^l \left[\frac{1}{2}\rho(u_t + vu_x)^2 - \frac{1}{2}Pu_x^2\right] dxdt$$

$$+ \int_{t_1}^{t_2} \int_0^l (fu - f_\eta u) \; dxdt \tag{2.4}$$

for arbitrary times t_1 and t_2.

Let us assume that u minimizes the Hamiltonian integral (2.4) and consider the true evolution $\bar{u} = u + \phi\mu$ of the system. The term $\phi\mu$ is the variation of the function u, where μ is an arbitrary function that is differentiable and vanishes at the time endpoints t_1 and t_2, that is, $\mu(\cdot, t_1) = 0$ and $\mu(\cdot, t_2) = 0$, and ϕ is a small parameter $0 < \phi \ll 1$.

So the integral (2.4) becomes the (action) functional of ϕ:

$$I(\phi) = \int_{t_1}^{t_2} \int_0^l \left[\frac{1}{2} \rho[u_t + \phi\mu_t + v(u_x + \phi\mu_x)]^2 - \frac{1}{2} P(u_x + \phi\mu_x)^2 \right] \mathrm{d}x\mathrm{d}t$$
$$+ \int_{t_1}^{t_2} \int_0^l [f(u + \phi\mu) - f_\eta(u + \phi\mu)] \, \mathrm{d}x\mathrm{d}t. \tag{2.5}$$

Since (2.4) has a minimum at u, the functional $I(\phi)$ has a minimum at $\phi = 0$, thus,

$$\delta I(\mu) := \left. \frac{\mathrm{d}I(\phi)}{\mathrm{d}\phi} \right|_{\phi=0} = 0.$$

Applying this condition to (2.5) the *first variation* of the action becomes

$$\delta I(\mu) = \int_{t_1}^{t_2} \int_0^l [\rho(u_t + Vu_x)(\mu_t + v\mu_x) - Pu_x\mu_x + (f - f_\eta)\mu] \, \mathrm{d}x\mathrm{d}t = 0. \tag{2.6}$$

Then we need the following derivatives

$$(u_x\mu)'_x = u_{xx}\mu + u_x\mu_x \text{ and } (u_t\mu)'_t = u_{tt}\mu + u_t\mu_t.$$

Substituting these derivatives into the equation (2.6) we obtain

$$\int_{t_1}^{t_2} \int_0^l \left(\rho[-u_{tt}\mu - v^2 u_{xx}\mu + v(u_t\mu_x + u_x\mu_t)] + Pu_{xx}\mu + f\mu - f_\eta\mu \right) \mathrm{d}x\mathrm{d}t$$
$$+ \rho v^2 \int_{t_1}^{t_2} \int_0^l (u_x\mu)'_x \, \mathrm{d}x\mathrm{d}t - P \int_{t_1}^{t_2} \int_0^l (u_x\mu)'_x \, \mathrm{d}x\mathrm{d}t + \rho \int_0^l \int_{t_1}^{t_2} (u_t\mu)'_t \, \mathrm{d}t\mathrm{d}x = 0. \tag{2.7}$$

Now applying integration by parts to the first integral from (2.7) yields

$$\int_{t_1}^{t_2} \int_0^l \left[-\rho(u_{tt} + 2vu_{xt} + v^2 u_{xx}) + Pu_{xx} - f_\eta + f \right] \mu \, \mathrm{d}x\mathrm{d}t$$
$$+ \int_{t_1}^{t_2} \left[(\rho v^2 - P)u_x\mu\big|_{x=0}^{x=l} + \rho v u_t \mu\big|_{x=0}^{x=l} \right] \mathrm{d}t + \rho \int_0^l \left[u_t\mu\big|_{t=t_1}^{t=t_2} + vu_x\mu\big|_{t=t_1}^{t=t_2} \right] \mathrm{d}x = 0. \tag{2.8}$$

The last integral in (2.8) vanishes because the variation is zero at times t_1 and t_2 by definition. Finally, after rearranging, we have

$$\int_{t_1}^{t_2} \int_0^l \left[\rho(u_{tt} + 2vu_{xt} + v^2 u_{xx}) - Pu_{xx} + f_\eta - f \right] \mu \, \mathrm{d}x\mathrm{d}t$$
$$- \int_{t_1}^{t_2} \left[\rho v u_t + (\rho v^2 - P)u_x \right] \mu \Big|_{x=0}^{x=l} \, \mathrm{d}t = 0. \tag{2.9}$$

The equation of motion is contained in the first term of (2.9) and it is given by

$$\rho(u_{tt} + 2vu_{xt} + v^2 u_{xx}) - Pu_{xx} + \eta_s(Vu_x + u_t) = f. \tag{2.10}$$

The second term of (2.9) defines natural boundary conditions.

Equation (2.10) shows that the string is acted upon by the four forces in the transverse direction. The first term in the equation represents the inertial loading, where u_{tt}, $2vu_{xt}$ and $v^2 u_{xx}$ correspond to the *local transverse, Coriolis*[3] and *centripetal acceleration* respectively. The second force Pu_{xx} is the transverse tension of the string. The last two terms were mentioned above as the viscous damping force and an external excitation, respectively.

To continue with the solution of the problem it is convenient to nondimensionalize the obtained governing equation by using the following dimensionless quantities

$$x^* = \frac{x}{L}, \ u^* = \frac{u}{L}, \ t^* = \frac{t}{L}\sqrt{\frac{P}{\rho}}, \ v^* = V\sqrt{\frac{\rho}{P}}, \ \eta^* = \frac{\eta_s L}{\sqrt{P\rho}}, \ f^* = f\frac{L}{P},$$

as obtained in Appendix A.1. Note that we will use these notations without asterisk further for convenience.

So the dimensionless equation of transversal motion is represented by the PDE:

$$u_{tt} + 2vu_{xt} - (1-v^2)u_{xx} + \eta(u_t + vu_x) = f(x,t), \tag{2.11a}$$

for $0 < x < l$, and $t > 0$, subject to the BCs:

$$u(0,t) = u(1,t) = 0, \tag{2.11b}$$

for $t > 0$, and with the ICs:

$$\begin{aligned} u(x,0) &= \phi(x), \\ u_t(x,0) &= \psi(x), \end{aligned} \tag{2.11c}$$

for $0 < x < l_0$.

In the following section we will solve the system (2.11a-2.11b) by applying the Laplace transform directly.

---

[3]Coriolis acceleration in axially moving continua arises from a combination of axial movement of the material particle while it is following a nonstraight path.

2.3   Application of the Laplace transform

By applying the Laplace transform (1.3) to PDE (2.11a), we obtain that $U(x,s)$ satisfies the PDE

$$s^2 U(x,s) - su(x,0) - u_t(x,0) + 2v[sU_x(x,s) - u_x(x,0)] - (1-v^2)U_{xx}(x,s)$$
$$+ \eta[sU(x,s) - u(x,0)] + \eta v U_x(x,s) = \mathscr{L}[f](x,s), \tag{2.12}$$

with the BCs

$$U(0,s) = 0 \text{ and } U(1,s) = 0. \tag{2.13}$$

Using the initial conditions (2.11c), and performing some simplifications, (2.12) becomes

$$U_{xx} - \frac{v(2s+\eta)}{1-v^2}U_x - \frac{s(s+\eta)}{1-v^2}U = F(x,s), \tag{2.14}$$

where

$$F(x,s) := -\frac{1}{1-v^2}\left(\mathscr{L}[f] + 2v\phi' + (s+\eta)\phi + \psi\right). \tag{2.15}$$

Then we will derive the solution of (2.14) with BCs (2.13), which at the same time is the image solution of (2.11a-2.11b). The particular solution can be found by using the method of variation of parameters (see Appendix A.2). By using (A.5), the general solution of (2.14) is given by:

$$U(x,s) = C_1(s)e^{(\alpha-\beta)x} + C_2(s)e^{(\alpha+\beta)x} + \frac{1}{2\beta}\int_0^x F(\xi,s)\left[e^{(\alpha+\beta)(x-\xi)} - e^{(\alpha-\beta)(x-\xi)}\right]d\xi,$$

where C_1 and C_2 follow by solving the system obtained after introducing the BCs (2.13), and

$$\alpha(s) := \frac{v}{2}\frac{2s+\eta}{1-v^2}, \quad \beta(s) := \frac{1}{2}\frac{\sqrt{4s^2+4s\eta+v^2\eta^2}}{1-v^2}. \tag{2.16}$$

Eventually we have

$$U(x,s) = \frac{1}{2\beta}\frac{e^{(\alpha-\beta)x} - e^{(\alpha+\beta)x}}{e^{\alpha+\beta} - e^{\alpha-\beta}}\int_0^1 F(\xi,s)\left[e^{(\alpha+\beta)(1-\xi)} - e^{(\alpha-\beta)(1-\xi)}\right]d\xi$$
$$+ \frac{1}{2\beta}\int_0^x F(\xi,s)\left[e^{(\alpha+\beta)(x-\xi)} - e^{(\alpha-\beta)(x-\xi)}\right]d\xi, \tag{2.17}$$

where as before α and β are given by (2.16), and F by (2.15).

2.4   The inverse transformation

It is convenient to rewrite the image solution (2.17) in the following form

$$U(x,s) = \int_0^1 F(\xi,s)H_1(\xi,x,s)\,d\xi + \int_0^x F(\xi,s)H_2(\xi,x,s)\,d\xi, \tag{2.18}$$

with

$$H_1(\xi,x,s) := \left[e^{\beta(1-\xi)} - e^{-\beta(1-\xi)} \right] \frac{e^{\alpha(x-\xi)}}{2\beta} \frac{e^{-\beta x} - e^{\beta x}}{e^{\beta} - e^{-\beta}}, \tag{2.19}$$

and

$$H_2(\xi,x,s) := \left[e^{\beta(x-\xi)} - e^{-\beta(x-\xi)} \right] \frac{e^{\alpha(x-\xi)}}{2\beta}. \tag{2.20}$$

Note that H_1 and H_2 are *meromorphic functions*[4]. Fixing x and s for the moment, we will write with a slight abuse of notation for the sake of simplicity $H_1(\xi)$ and $H_2(\xi)$ when we mean $H_1(\xi,x,s)$ and $H_2(\xi,x,s)$ respectively. Applying Mellin's formula (1.4) to (2.18) will lead to a convolution in (x,t). Next, the integral from (1.4) can be calculated using the Cauchy's residue theorem:

$$\int_{\gamma-i\infty}^{\gamma+i\infty} e^{st} U \, \mathrm{d}s = 2\pi i \sum_{k=1}^{n} \mathrm{Res}(e^{st} U; s_k),$$

for a non-zero meromorphic function $e^{st} U$, where $\mathrm{Res}(e^{st} U; s_k)$ is the *residue*[5] of $e^{st} U$ at *isolated singularities*[6] $s_1, s_2, \ldots, s_n$.

2.4.1 Singularity analysis

According to Cauchy's residue theorem the only contribution will be due to the poles[7] of a function. Remark that if the external excitation f is specified, it can also contribute into (2.18) with poles. As a first step we calculate the singularities of H_1 and H_2. We split the set of singularities into two sets, one for which is $e^{\beta} - e^{-\beta} = 0$ and the other for which is $\beta = 0$. Considering the real and imaginary parts separately for $\beta = \beta_1 + i\beta_2$ applying to the first set of singularities we have $e^{\beta_1} e^{i\beta_2} - e^{-\beta_1} e^{-i\beta_2} = 0$. Then we need to solve the following two equations $e^{\beta_1} \cos(\beta_2) - e^{-\beta_1} \cos(\beta_2) = 0$ and $e^{\beta_1} \sin(\beta_2) + e^{-\beta_1} \sin(\beta_2) = 0$. For the first equation we consider the case when $\cos(\beta_2)$ is non-zero or when it is zero. Doing this, we obtain that $\beta_1 = 0$ or $\beta_2 = \frac{\pi}{2} + k\pi$. One should observe that β_2 violates the latter equation. Thus, $\sin(\beta_2)$ is equal to zero, resulting in $\beta_2 = k\pi$. As a conclusion we have for all k in $\mathbb{Z}$:

$$\beta_1 = 0, \quad \beta_2 = k\pi, \quad \text{i.e.,} \quad \beta = k\pi i. \tag{2.21}$$

A singularity analysis in Appendix A.3 shows that among all the possible singularities (2.21), only $\beta = k\pi i$ for $k \in \mathbb{Z}\setminus\{0\}$ turn out to be poles which contribute to the Cauchy's residue theorem.

With the work we have done so far, the singularities for s can readily be found. For convenience we rewrite α and β as follows:

$$\alpha(\lambda) = \frac{\eta}{2} \frac{v\lambda}{\sqrt{1-v^2}}, \quad \beta(\lambda) = \frac{\eta}{2} \frac{\sqrt{\lambda^2-1}}{\sqrt{1-v^2}},$$

---

[4]Meromorphic function is a function that is holomorphic, i.e. complex differentiable in a neighborhood of every point in its domain, on an open subset of the complex plane except for a set of the isolated singularities.

[5]The residue is a complex number proportional to the contour integral of a meromorphic function along a path enclosing one of its singularities [44].

[6]An isolated singularity is one that has no other singularities in its neighborhood.

[7]A pole of a meromorphic function is a singularity that behaves like the singularity of s^{-n} at $s = 0$.

where

$$\lambda(s) := \frac{2}{\eta} \frac{1}{\sqrt{1-v^2}} \left(s + \frac{\eta}{2}\right), \tag{2.22}$$

As β is purely imaginary this forces $\sqrt{\lambda^2 - 1}$ to be purely imaginary too. Hence, $\lambda^2 < 1$. As $\beta = k\pi i$ this implies that

$$\frac{\eta}{2} \frac{\sqrt{1-\lambda^2}}{\sqrt{1-v^2}} = k\pi. \tag{2.23}$$

The singularities can be found from (2.23) with the notation (2.22), which gives

$$s^2 + \eta s + k^2\pi^2(1-v^2)^2 + \frac{\eta^2}{4}v^2 = 0. \tag{2.24}$$

Solving (2.24) for s, we obtain

$$s_k = -\frac{\eta}{2} \pm i\omega_k, \tag{2.25}$$

which are simple poles, where

$$\omega_k := \frac{1}{2}\sqrt{1-v^2}\sqrt{4k^2\pi^2(1-v^2)-\eta^2} \tag{2.26}$$

for $k \in \mathbb{Z}\backslash\{0\}$. Since $s_k = s_{-k}$, it is sufficient to consider in (2.25) only non-zero natural k.

2.4.2 Residue calculation

As we have shown in Appendix A the function H_1, given by (2.19), has *simple poles*[8] at s_k for every non-zero natural k. H_1 can be written as the quotient of two analytic functions P and Q. These are given by

$$P(s) := e^{\alpha(s)(x-\xi)}(e^{-\beta(s)x} - e^{\beta(s)x})(e^{\beta(s)(1-\xi)} - e^{-\beta(s)(1-\xi)}), \tag{2.27}$$

and

$$Q(s) := 2\beta(s)(e^{\beta(s)} - e^{-\beta(s)}), \tag{2.28}$$

such that, $H_1(s) = \frac{P(s)}{Q(s)}$. Recall that Q has *simple zeroes* at s_k. Then

$$h(\xi, x, t) := \text{Res}(e^{st}H_1(s); s_k) = \lim_{s \to s_k}(s - s_k)e^{st}H_1(s) = e^{s_k t}\frac{P(s_k)}{Q'(s_k)}. \tag{2.29}$$

After the calculation (2.29) and some simplifications, finally we obtain

$$h(\xi, x, t) = -2e^{-\frac{1}{2}t\eta}\frac{(1-v^2)^2}{\omega_k}\sin(k\pi\xi)\sin(k\pi x)\sin\left(\omega_k\left[t + \frac{v}{1-v^2}(x-\xi)\right]\right). \tag{2.30}$$

---

[8]A pole of order 1.

2.4.3 Convolution

In order to obtain the original solution by using the *convolution theorem*, first we take the inverse Laplace transform of F, which is

$$\mathscr{L}^{-1}[F](\xi, t) = f_0 := f(\xi, t) + \delta(t)[2\nu\phi'(\xi) + \eta\phi(\xi) + \psi(\xi)] + \partial_t\delta(t)\phi(\xi),$$

where δ is the *Dirac delta function*[9]. So according to the convolution theorem we obtain

$$(f_0 * h)(t) := \mathscr{L}^{-1}[Fe^{st}H_1](t) = \int_0^t f_0(\tau)h(t - \tau)\,\mathrm{d}\tau. \tag{2.31}$$

Using the shifting property of the delta function and the definition of the *distributional derivative*, from (2.31) we obtain

$$(f_0 * h)(\xi, x, t) := \int_0^t f(\xi, \tau)h(\xi, x, t - \tau)\,\mathrm{d}\tau + [2\nu\phi'(\xi) + \eta\phi(\xi) + \psi(\xi)]h(\xi, x, t)$$
$$- \phi(\xi)\partial_t h(\xi, x, t), \tag{2.32}$$

where h is given as before by (2.30).

2.4.4 Series representation

Computing the inverse Laplace transform of (2.32), we determine the solution to the initial-boundary value problem (2.11a-2.11b) as follows:

$$u(x, t) = -\frac{1}{1 - \nu^2}\sum_{k=1}^{\infty}\int_0^1 (f_0 * h)(\xi, x, t)\,\mathrm{d}\xi. \tag{2.33}$$

For the purpose of comparing with known results it is more convenient to rewrite (2.33) in the form of a Fourier series:

$$u(x, t) = -(1 - \nu^2)\int_0^t e^{-\frac{1}{2}(t - \tau)\eta}\sum_{k=1}^{\infty}\left[A_k(\tau)\cos\left(\omega_k\left[t - \tau + \frac{\nu x}{1 - \nu^2}\right]\right)\right.$$
$$\left. + B_k(\tau)\sin\left(\omega_k\left[t - \tau + \frac{\nu x}{1 - \nu^2}\right]\right)\right]\sin(k\pi x)\,\mathrm{d}\tau - (1 - \nu^2)\,e^{-\frac{1}{2}t\eta}$$
$$\times\sum_{k=1}^{\infty}\left[C_k\cos\left(\omega_k\left[t + \frac{\nu x}{1 - \nu^2}\right]\right) + D_k\sin\left(\omega_k\left[t + \frac{\nu x}{1 - \nu^2}\right]\right)\right]\sin(k\pi x), \tag{2.34}$$

---

[9]The Dirac delta function is a generalized function defined on the real line that is zero everywhere except at zero; its integral over the entire real line is one.

where A_k, B_k, C_k and D_k are the coefficients of Fourier series:

$$A_k(\tau) = \frac{2}{\omega_k} \int_0^1 f(\xi, \tau) \sin(k\pi\xi) \sin\left(\frac{\omega_k v\xi}{1-v^2}\right) \, d\xi,$$

$$B_k(\tau) = -\frac{2}{\omega_k} \int_0^1 f(\xi, \tau) \sin(k\pi\xi) \cos\left(\frac{\omega_k v\xi}{1-v^2}\right) \, d\xi,$$

$$C_k = -2 \int_0^1 \phi(\xi) \sin(k\pi\xi) \cos\left(\frac{\omega_k v\xi}{1-v^2}\right) \, d\xi$$
$$- \frac{2}{\omega_k} \int_0^1 \left[2v\phi'(\xi) + \frac{3}{2}\eta\phi(\xi) + \psi(\xi)\right] \sin(k\pi\xi) \sin\left(\frac{\omega_k v\xi}{1-v^2}\right) \, d\xi,$$

$$D_k = 2 \int_0^1 \phi(\xi) \sin(k\pi\xi) \sin\left(\frac{\omega_k v\xi}{1-v^2}\right) \, d\xi$$
$$- \frac{2}{\omega_k} \int_0^1 \left[2v\phi'(\xi) + \frac{3}{2}\eta\phi(\xi) + \psi(\xi)\right] \sin(k\pi\xi) \cos\left(\frac{\omega_k v\xi}{1-v^2}\right) \, d\xi.$$

In the next section we will check the validity of the obtained result (2.34) representing the transverse vibrations of the string.

2.5 Comparison and examples

There are a lot of results obtained in previous research for string-like problems (see for instance [13], [2, 13, 21, 22, 27]). To verify (2.34) in some special cases we will consider the following four known problems:

- undamped stationary string;

- undamped axially moving string;

- damped stationary string;

- damped axially moving string.

Note that the numerical results will be obtained for the problems with no external excitation, that is $f = 0$. To analyze the motion of the system we will present some simulations. Remark that the graphs in the following subsections are drawn by plotting values of the amplitude of the transverse vibrations u on the vertical axis and the position along the string $0 \leq x \leq 1$ on the horizontal axis at a certain period of time t.

2.5.1 Undamped stationary string

Starting with the simplest case, when $\eta = 0$ and $v = 0$ we have the wave equation. This represents a uniform vibrating string without external forces. The solution is well-known (see for instance [62]). Let us attempt to illustrate the motion of an undamped
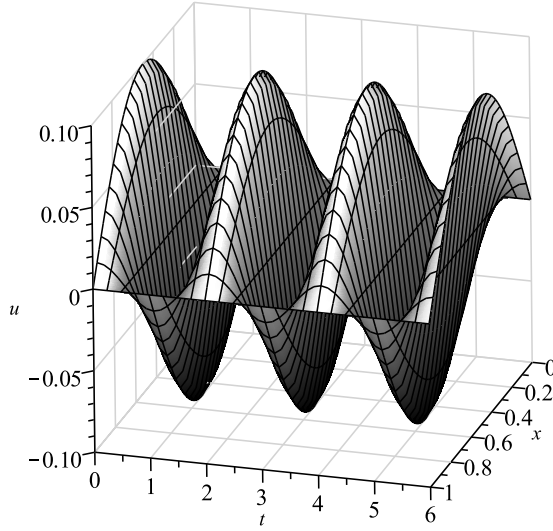
Figure 2.3: Free vibration response of an *undamped stationary string* with $\eta = 0$ and $v = 0$.

stationary string without damping with the initial displacement of $\phi(x) = 0.01 \sin(\pi x)$, and the initial velocity $\psi(x) = 0$ for various values of time t (see Figure 2.3). One can see *standing waves*, because each mode looks like a simple oscillation and the amplitude varies periodically in time.

2.5.2 Undamped axially moving string

Checking for an undamped axially moving string, we assume $\eta = 0$. The result will be the same as one presented in [22]. The following example (see Figure 2.4) involves an undamped axially moving string with the speed $v = 0.3$, and as before with the initial displacement of $\phi(x) = 0.01 \sin(\pi x)$, and no initial velocity. The speed of wave propagation to the right and to the left are not the same for a moving string in contrast to the stationary one, resulting in assymetric transverse vibrations.

2.5.3 Damped stationary string

Setting $v = 0$, the problem is simplified to a damped stationary string system. Figure 2.5 shows the transverse vibrations of a damped stationary string with $\eta = 1$ and the same initial conditions as in the previous two examples. We observe the same standing waves as in the undamped stationary case but with decreased amplitude at equal periods of time.
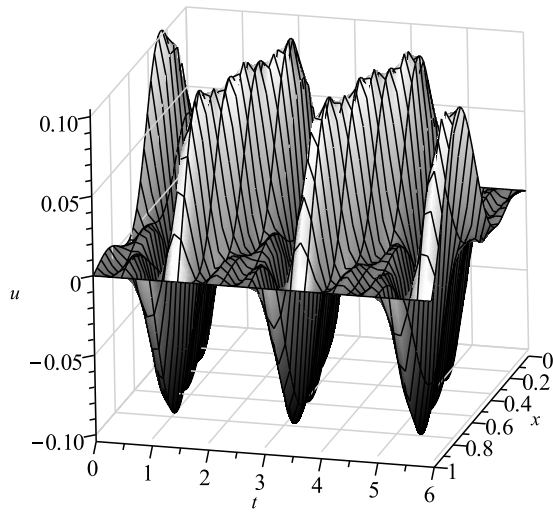
Figure 2.4: Free vibration response of an *undamped axially moving string* with $\eta = 0$ and $v = 0.3$.
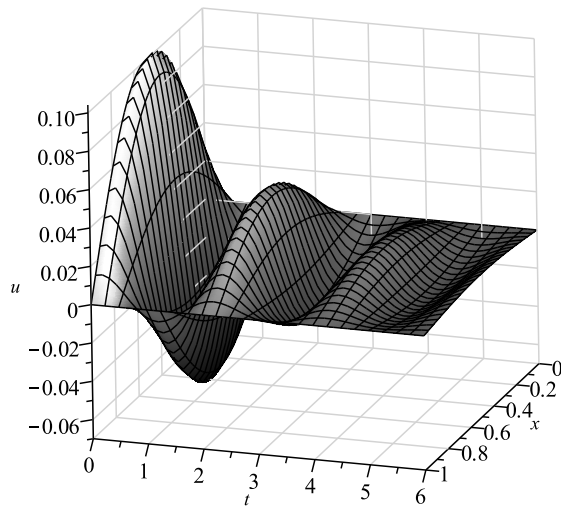
Figure 2.5: Free vibration response of a *damped stationary string* with $\eta = 1$ and $v = 0$.
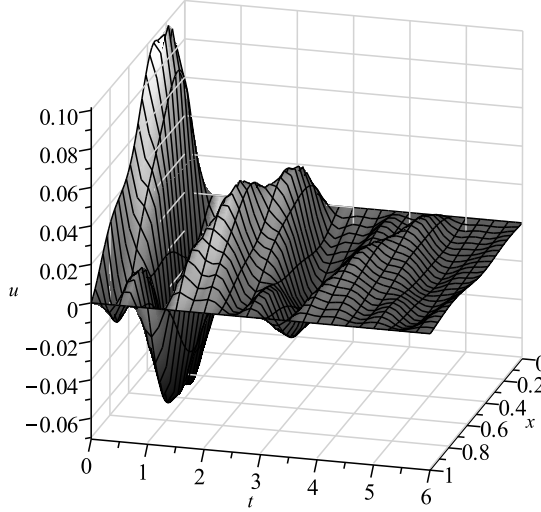
Figure 2.6: Free vibration response of a *damped axially moving string* with $\eta = 1$ and $v = 0.3$.

2.5.4 Damped axially moving string

The last example is based on the analytical solution derived in Section 5 with no external excitation. A damped axially moving string with the speed $v = 0.3$, with the damping $\eta = 1$, and with the initial displacement of $a(x) = 0.01 \sin(\pi x)$, and no initial velocity is considered (see Figure 2.6). From where with the analysis of the previous examples we conclude that the damping and the velocity both reduce the amplitude of oscillations.

2.6 Conclusions

In this chapter, an initial-boundary value problem for a damped axially moving string with constant speed has been investigated. The Laplace transform method was applied because of its straightforwardness. The results show that the poles in the s-domain of the Laplace transform are actually the eigenvalues and the solution is a combination of eigenfunctions. Furthermore, the obtained solution shows agreement with the previous research. The analysis of special cases gives insight to the contribution of the velocity and the viscous damping into string-like problems. As it was expected they reduce the amplitude of oscillations of the string. It should be noted that the Laplace transform method can be extended for string-like problems with non-classical boundary conditions.

Appendix A

A.1 Dimensional analysis

The dimensionless equation of motion of the damped axially moving string can be derived from (2.10) using the *Buckingham theorem* (also known as π-*theorem*). The fundamental dimensions involved are length L, mass M, and time T. Using these the dimensionality of the three variables (x, u, and t) and the five parameters ($\rho, V, P, \eta_{\mathrm{s}}$, and f) of the system are given as follows

$$[x] = L, \; [u] = L, \; [t] = T, \; [\rho] = \frac{M}{L}, \; [V] = \frac{L}{T}, \; [P] = \frac{ML}{T^2}, \; [\eta_{\mathrm{s}}] = \frac{M}{LT}, \; [f] = \frac{M}{T^2}.$$

According to π-theorem we form the products

$$x^{r_1} u^{r_2} t^{r_3} \rho^{r_4} V^{r_5} P^{r_6} \eta_{\mathrm{s}}^{r_7} f^{r_8}$$

and substitute the dimensions, so we arrive at the products

$$L^{r_1} L^{r_2} T^{r_3} \left(\frac{M}{L} \right)^{r_4} \left(\frac{L}{T} \right)^{r_5} \left(\frac{ML}{T^2} \right)^{r_6} \left(\frac{M}{LT} \right)^{r_7} \left(\frac{M}{T^2} \right)^{r_8}.$$

Collecting powers of L, M and T, the following three equations for the r_i (for $i = 1, 2, \ldots, 8$) are obtained:

$$r_1 + r_2 - r_4 + r_5 + r_6 - r_7 = 0,$$
$$r_3 - r_5 - 2r_6 - r_7 - 2r_8 = 0,$$
$$r_4 + r_6 + r_7 + r_8 = 0.$$

As a result, we got three equations for eight unknowns, so five unknowns can be treated as free parameters. For instance, the choices

$$(r_1, r_3, r_5, r_7, r_8) = (1, 0, 0, 0, 0),$$
$$(r_2, r_3, r_5, r_7, r_8) = (1, 0, 0, 0, 0),$$
$$(r_2, r_3, r_5, r_7, r_8) = (0, 1, 0, 0, 0),$$
$$(r_1, r_2, r_5, r_7, r_8) = (0, 0, 1, 0, 0),$$
$$(r_2, r_3, r_5, r_7, r_8) = (0, 0, 0, 1, 0),$$
$$(r_1, r_3, r_5, r_7, r_8) = (0, 0, 0, 0, 1),$$

respectively, yield the dimensionless quantities

$$x^* = \frac{x}{L}, \ u^* = \frac{u}{L}, \ t^* = \frac{t}{L}\sqrt{\frac{P}{\rho}}, \ v^* = V\sqrt{\frac{\rho}{P}}, \ \eta^* = \frac{\eta_s L}{\sqrt{P\rho}}, \ f^* = f\frac{L}{P}.$$

A.2 Variation of parameters

To solve the non-homogeneous PDE (2.14), we will apply the *method of variation of parameters*. Assume that there exists two functions v_1 and v_2 such that a solution to (2.14) is given by

$$U_p(x,s) := v_1 U_1 + v_2 U_2, \tag{A.1}$$

where $U_1 = e^{(\alpha-\beta)x}$ and $U_2 = e^{(\alpha+\beta)x}$. To restrict degrees of freedom we additionally assume without loss of generality that

$$v_1' U_1 + v_2' U_2 = 0. \tag{A.2}$$

Taking the first and the second derivatives of (A.1) with respect to x,

$$U_p' = v_1 U_1' + v_2 U_2', \text{ and } U_p'' = v_1' U_1' + v_1 U_1'' + v_2' U_2' + v_2 U_2'',$$

we plug them and (A.1) into (2.14) and slightly rearrange:

$$
\begin{aligned}
& v_1 \left(U_1'' - \frac{v(2s+\eta)}{1-v^2} U_1' - \frac{s(s+\eta)}{1-v^2} U_1 \right) + v_2 \left(U_2'' - \frac{v(2s+\eta)}{1-v^2} U_2' - \frac{s(s+\eta)}{1-v^2} U_2 \right) \\
& + v_1' U_1' + v_2' U_2' = F.
\end{aligned} \tag{A.3}
$$

Both U_1 and U_2 are the solutions of homogeneous equation (2.14) making the first two terms of (A.3) vanish. Thus, the equations that we need to solve for the unknowns v_1 and v_2 are

$$
\begin{aligned}
v_1' U_1 + v_2' U_2 &= 0, \\
v_1' U_1' + v_2' U_2' &= F.
\end{aligned}
$$

Solving for v_1' and v_2' gives

$$v_1' = -\frac{F U_2}{U_2' U_1 - U_2 U_1'} \text{ and } v_2' = \frac{F U_1}{U_2' U_1 - U_2 U_1'}. \tag{A.4}$$

If we assume that the denominator $U_2' U_1 - U_2 U_1'$ is non-zero and recall that this is the *Wronskian W* of (U_1, U_2) we obtain by integration of (A.4):

$$v_1(x,s) = -\int_0^x \frac{F(\xi,s) U_2(\xi,s)}{W(\xi,s)} \, d\xi, \quad v_2(x,s) = \int_0^x \frac{F(\xi,s) U_1(\xi,s)}{W(\xi,s)} \, d\xi.$$

Substituting (A.2) into (A.1) we obtain a particular solution to the PDE (2.14):

$$U_p(x,s) = \frac{1}{2\beta} \left(e^{(\alpha+\beta)x} \int_0^x F(\xi,s) e^{-(\alpha+\beta)\xi} \, d\xi - e^{(\alpha-\beta)x} \int_0^x F(\xi,s) e^{-(\alpha-\beta)\xi} \, d\xi \right). \tag{A.5}$$

A.3 Singularity analysis

Here we check whether $\beta = 0$ and $\beta = k\pi i$ for $k \in \mathbb{Z}\backslash\{0\}$ actually give a singularity. Remark that we will proceed with modulus of H_1 and H_2 to estimate these functions for the complex values of β.

Around $\beta = 0$

Let us start with the evaluation of $|H_1|e^{-\alpha(x-\xi)}$. We split this into two parts

$$p_1 := \left| \frac{e^{\beta x} - e^{-\beta x}}{e^\beta - e^{-\beta}} \right| \text{ and } p_2 := \left| \frac{e^{\beta(1-\xi)} - e^{-\beta(1-\xi)}}{2\beta} \right|.$$

We first expand p_1. Writing the numerator as a series gives

$$e^{\beta x} - e^{-\beta x} = \sum_{n=0}^\infty \frac{(\beta x)^n}{n!} - \sum_{n=0}^\infty (-1)^n \frac{(\beta x)^n}{n!} = 2\sum_{n=0}^\infty \frac{(\beta x)^{2n+1}}{(2n+1)!}. \tag{A.6}$$

An upper bound of the denominator of p_1 can be found by

$$\frac{1}{|e^\beta - e^{-\beta}|} = \left| 2\sum_{n=0}^\infty \frac{\beta^{2n+1}}{(2n+1)!} \right|^{-1} \le \frac{1}{2|\beta|}.$$

Combining this with (A.6) gives

$$\left| \frac{e^{\beta x} - e^{-\beta x}}{e^\beta - e^{-\beta}} \right| \le \left| \frac{1}{\beta} \sum_{n=0}^\infty \frac{(\beta x)^{2n+1}}{(2n+1)!} \right| = x \left| \sum_{n=0}^\infty \frac{(\beta x)^{2n}}{(2n+1)!} \right|$$
$$\le x \sum_{n=0}^\infty \frac{(|\beta|x)^{2n}}{(2n+1)!}$$
$$\le x \sum_{n=0}^\infty \frac{(|\beta|x)^{2n}}{n!} = x e^{|\beta|^2 x^2}.$$

To ease the calculations for the lower bound we consider the reciprocal of p_1. Proceeding as before gives

$$\left| \frac{e^\beta - e^{-\beta}}{e^{\beta x} - e^{-\beta x}} \right| \le \left| \frac{1}{\beta x} \sum_{n=0}^\infty \frac{\beta^{2n+1}}{(2n+1)!} \right| \le \left| \frac{1}{x} \sum_{n=0}^\infty \frac{\beta^{2n}}{n!} \right| \le \frac{1}{x} \sum_{n=0}^\infty \frac{|\beta|^{2n}}{n!} = \frac{1}{x} e^{|\beta|^2}.$$

Combining the upper and the lower bounds

$$x e^{-|\beta|^2} \le \left| \frac{e^{\beta x} - e^{-\beta x}}{e^\beta - e^{-\beta}} \right| \le x e^{|\beta|^2 x^2}. \tag{A.7}$$

Having found bounds for p_1, we proceed with deriving bounds for p_2. For the upper bound:

$$\left|\frac{e^{\beta(1-\xi)} - e^{-\beta(1-\xi)}}{2\beta}\right| = \left|\frac{1}{2\beta}\sum_{n=0}^{\infty}\frac{\beta^{2n+1}(1-\xi)^{2n+1}}{(2n+1)!}\right| = \frac{1-\xi}{2}\left|\sum_{n=0}^{\infty}\frac{\beta^{2n}(1-\xi)^{2n}}{(2n+1)!}\right| \quad \text{(A.8)}$$

$$\leq \frac{1-\xi}{2}\sum_{n=0}^{\infty}\frac{|\beta|^{2n}(1-\xi)^{2n}}{n!} = \frac{1-\xi}{2}e^{|\beta|^2(1-\xi)^2}. \quad \text{(A.9)}$$

To estimate from below we take the first term giving the bounds

$$\frac{1-\xi}{2} \leq \left|\frac{e^{\beta(1-\xi)} - e^{-\beta(1-\xi)}}{2\beta}\right| \leq \frac{1-\xi}{2}e^{|\beta|^2(1-\xi)^2}. \quad \text{(A.10)}$$

Wrapping up, we obtain by combining (A.7) and (A.10):

$$x\frac{1-\xi}{2}e^{\alpha(x-\xi)}e^{-|\beta|^2} \leq |H_1(\xi)| \leq x\frac{1-\xi}{2}e^{\alpha(x-\xi)}e^{|\beta|^2(x^2+(1-\xi)^2)}.$$

Which is as $\beta \to 0$ asymptotically

$$|H_1(\xi)| \sim x\frac{1-\xi}{2}e^{\alpha(x-\xi)},$$

implying that $\beta = 0$ is at most a removable[1] singularity.

Proceeding with H_2 by a similar technique, for which $\beta = 0$ is the only singularity, we derived the following bounds

$$\frac{x-\xi}{2} \leq \left|\frac{e^{\beta(x-\xi)} - e^{-\beta(x-\xi)}}{2\beta}\right| \leq \frac{x-\xi}{2}e^{|\beta|^2(x-\xi)^2}.$$

From where

$$|H_2(\xi)| \sim \frac{x-\xi}{2}e^{\alpha(x-\xi)}$$

as $\beta \to 0$. As a consequence, $\beta = 0$ is at most a removable singularity for H_2 as well. So it will have no contribution to the integral (2.18), i.e., by the Cauchy's residue theorem we obtain for all $\gamma > 0$, that

$$\int_{\gamma-i\infty}^{\gamma+i\infty} e^{st}H_2(s)\, ds = 0.$$

Consequently, the image solution (2.18) takes the simple form:

$$U(x,s) = \int_0^1 F(\xi,s)H_1(\xi,x,s)\, d\xi. \quad \text{(A.11)}$$

---

[1]A removable singularity of a holomorphic function is a point at which the function is undefined, but it is possible to redefine the function at that point in such a way that the resulting function is regular in a neighborhood of that point.

28

Around $\beta = k\pi i$ for $k \in \mathbb{Z}\backslash\{0\}$

Let us expand $|H_1|e^{-\alpha(x-\xi)}$ around $\beta_0 = k\pi i$. Again we start with the estimation of p_1. The *Taylor series* expansions for the numerator and for the denominator are given by

$$e^{\beta x} - e^{-\beta x} = \sum_{n=0}^{\infty} \frac{x^n}{n!}(\beta - \beta_0)^n(e^{\beta_0 x} - (-1)^n e^{-\beta_0 x}), \tag{A.12}$$

$$e^{\beta} - e^{-\beta} = 2(-1)^k \sum_{n=0}^{\infty} \frac{(\beta - \beta_0)^{2n+1}}{(2n+1)!}. \tag{A.13}$$

Taking the first term in (A.13) the upper bound of p_1 is

$$\left| \frac{e^{\beta x} - e^{-\beta x}}{e^{\beta} - e^{-\beta}} \right| \leq \left| \frac{e^{\beta x} - e^{-\beta x}}{2(\beta - \beta_0)} \right| = \left| \frac{\sinh(\beta x)}{\beta - \beta_0} \right|.$$

To estimate p_1 from below we consider its reciprocal. By taking the first term of (A.12) we estimate the reciprocal from above

$$\left| \frac{e^{\beta} - e^{-\beta}}{e^{\beta x} - e^{-\beta x}} \right| \leq \left| \frac{2(-1)^k}{e^{\beta_0 x} - e^{-\beta_0 x}} \sum_{n=0}^{\infty} \frac{(\beta - \beta_0)^{2n+1}}{(2n+1)!} \right|$$

$$\leq \frac{1}{|\sinh(\beta_0 x)|} \sum_{n=0}^{\infty} \frac{|\beta - \beta_0|^{2n+1}}{(2n+1)!}$$

$$\leq \left| \frac{\beta - \beta_0}{\sinh(\beta_0 x)} \right| \sum_{n=0}^{\infty} \frac{|\beta - \beta_0|^{2n}}{(2n)!}$$

$$\leq \left| \frac{\beta - \beta_0}{\sinh(\beta_0 x)} \right| \sum_{n=0}^{\infty} \frac{|\beta - \beta_0|^{2n}}{n!} = \left| \frac{\beta - \beta_0}{\sinh(\beta_0 x)} \right| e^{|\beta - \beta_0|^2}.$$

Knowing the upper bound of the reciprocal of p_1 we can readily obtain the lower bound of p_1. Summarizing, we obtain

$$\left| \frac{\sinh(\beta_0 x)}{\beta - \beta_0} \right| e^{-|\beta - \beta_0|^2} \leq \left| \frac{e^{\beta x} - e^{-\beta x}}{e^{\beta} - e^{-\beta}} \right| \leq \left| \frac{\sinh(\beta x)}{\beta - \beta_0} \right|. \tag{A.14}$$

We continue with estimation of p_2, which we simply rewrite as

$$\left| \frac{e^{\beta(1-\xi)} - e^{-\beta(1-\xi)}}{2\beta} \right| = \left| \frac{\sinh(\beta[1-\xi])}{\beta} \right|. \tag{A.15}$$

As before we obtain for the lower bound:

$$\left| \frac{e^{\beta(1-\xi)} - e^{-\beta(1-\xi)}}{2\beta} \right| = \frac{1}{2|\beta|} \left| \sum_{n=0}^{\infty} \frac{(1-\xi)^n}{n!}(\beta - \beta_0)^n \left(e^{\beta_0(1-\xi)} - (-1)^n e^{-\beta_0(1-\xi)} \right) \right|$$

$$\geq \left| \frac{e^{\beta_0(1-\xi)} - e^{-\beta_0(1-\xi)}}{2\beta} \right| = \left| \frac{\sinh(\beta_0[1-\xi])}{\beta} \right|.$$

Combining (A.14) with the latter the bounds for $|H_1|$ are given by

$$e^{\alpha(x-\xi)}e^{-|\beta-\beta_0|^2}\left|\frac{\sinh(\beta_0 x)\sinh(\beta_0[1-\xi])}{\beta(\beta-\beta_0)}\right| \le |H_1(\xi)|,$$

and

$$|H_1(\xi)| \le e^{\alpha(x-\xi)}\left|\frac{\sinh(\beta x)\sinh(\beta[1-\xi])}{\beta(\beta-\beta_0)}\right|.$$

Finally, asymptotically as $\beta \to \beta_0$

$$|H_1(\xi)| \sim e^{\alpha(x-\xi)}\left|\frac{\sinh(\beta_0 x)\sinh(\beta_0[1-\xi])}{\beta_0(\beta-\beta_0)}\right|.$$

As a consequence, $\beta = k\pi i$ are *simple poles* for $k \in \mathbb{Z}\backslash\{0\}$.

Chapter 3

Transverse, low-frequency vibrations of a traveling string with boundary damping

In this chapter, we study the free transverse vibrations of an axially moving (gyroscopic) material represented by a perfectly flexible string. The problem can be used as a simple model to describe the low frequency oscillations of elastic structures such as conveyor belts. In order to suppress these oscillations, a spring-mass-dashpot system is attached at the non-fixed end of the string. In this chapter it is assumed that the damping in the dashpot is small and that the axial velocity of the string is small compared to the wave speed of the string. This chapter has two main objectives. The first aim is to give explicit approximations of the solution on long time-scales by using a multiple-timescales perturbation method. The other goal is to construct accurate approximations of the lower eigenvalues of the problem which describe the oscillation and the damping properties of the problem. The eigenvalues follow from a so-called characteristic equation obtained by the direct application of the Laplace transform method to the initial-boundary value problem. Both approaches give a complete and accurate picture of the damping and the low frequency oscillatory behavior of the traveling string.
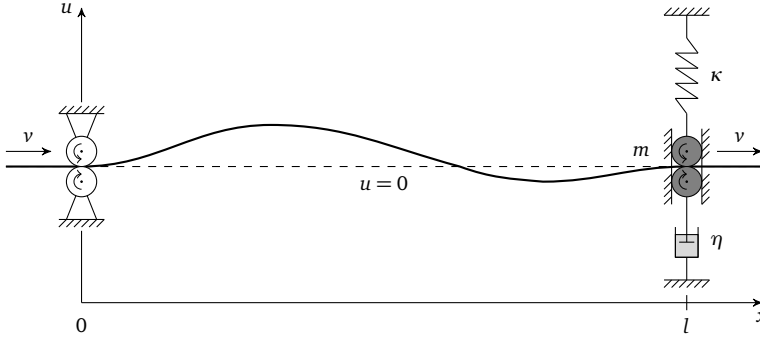
Figure 3.1: Schematic of an axially moving string with a spring-mass-dashpot at the upstream boundary.

3.1 Introduction

While the previous chapter considered the transverse oscillations of an axially moving string with classical fixed boundary conditions, this chapter studies the damping in an elastic string generated at the boundary with an attached mass-spring-dashpot system (see Figure 3.1). The assumptions restricting the formulation of the problem are the same as in Chapter 2. In fact, the translating string is one of the simplest representatives describing the low-frequency dynamic response of distributed gyroscopic systems. For higher-order modes of oscillations, bending stiffness has to be taken into account (see Andrianov and Awrejcewicz [3], Sandilo and van Horssen [51]).

There is an abundance of papers on the analysis of transverse vibrations of axially moving strings. For example, Chen [34] reviewed research on transverse vibrations and their control of axially moving strings. Zhu et al. [63] presented a new spectral analysis for the asymptotic locations of eigenvalues of translating string constrained arbitrarily by a spring-mass-dashpot. Tan and Ying [7] derived an exact response solution for the axially moving string with general boundary conditions by the application of the transfer function formulation and the concept of wave propagation. Van Horssen [21] solved a similar problem exactly by using the Laplace transform method, where the author has also shown that the truncation method is not applicable to moving string problems. Darmawijoyo and van Horssen [9] constructed asymptotic approximations for the stationary string with non-classical boundary conditions by a multiple time-scales perturbation method giving an extension of the classical way to solve such problems. We will use similar approaches with the latter two works for the problem in this paper. Nguyen and Hong [38] developed a control scheme for suppression of transverse and longitudinal vibrations, which also guarantees their asymptotic convergence to zero. Recently Chen and Ferguson [10] considered the axially moving string with constant or time varying length with a viscous damper at one end, for which they found the optimum value to dissipate most input energy.

The main contribution of the current study is the construction of an approximate solution representing the transverse low-frequency vibrations of an axially moving string with boundary damping on a long time-scale. The chapter is organized as follows. As

in the previous chapter, the governing equations are derived using Hamilton's principle in Section 3.2. Next, in Section 3.3 the energy of the system is analyzed showing that the rate of change of the mechanical energy completely depends on the work done at the boundaries. Moving to the main part of the chapter, a formal approximation of the solution is constructed in Section 3.4 using a multiple-timescales perturbation method. Then, the Laplace transform method is employed in Section 3.5 to obtain the so-called characteristic equation, for which explicit approximations of its roots are constructed, thus providing the damping rates and the frequencies of the oscillations modes under consideration. Moreover, an alternative implicit exact solution is derived in Section 3.5 as well. Finally, Section 3.6 concludes the chapter by giving some insight into the relations of physics and mathematics for string-like models.

3.2 Equations of motion

Similar to Section 2.2 in Chapter 2, we derive the equations of motion by using Hamilton's principle. The kinetic energy of the string is given by (2.2). The kinetic energy of the the the pulley with mass is given by

$$K_b := \frac{1}{2} m u_t^2(l, t).$$

The potential energy of the axial load is given by (2.3). The work done by the linear spring at the boundary is

$$U_b := \int_0^{u(l,t)} \kappa \xi \, d\xi = \frac{1}{2} \kappa u^2(l, t).$$

Now the Lagrangian can be written as

$$L := (K_s + K_b) - (U_s + U_b) = \frac{1}{2} \int_0^l \rho (u_t + V u_x)^2 \, dx + \frac{1}{2} m u_t^2(l, t) - \frac{1}{2} \int_0^l P u_x^2 \, dx - \frac{1}{2} \kappa u^2(l, t).$$

To apply the extended form of Hamilton's principle, we still have to consider the virtual work due to the non-conservative damping force at the upstream boundary. Note that the virtual work done by the dashpot is negative, because it opposes the motion of the string. Hence, the virtual energy has the following form

$$W := -F_\eta u(l, t),$$

where the damping force F_η arising in the dashpot is given by $\eta u_t(l, t)$. According to Hamilton's principle, we need to find an extreme value to the integral

$$
\begin{aligned}
I := \int_{t_1}^{t_2} (L + W) \, dt = \frac{1}{2} \int_{t_1}^{t_2} \int_0^l \left[\rho (u_t + V u_x)^2 - P u_x^2 \right] dx \, dt \\
+ \int_{t_1}^{t_2} \left[\frac{1}{2} m u_t^2(l, t) - \frac{1}{2} \kappa u^2(l, t) - F_\eta u(l, t) \right] dt
\end{aligned}
\tag{3.1}
$$

for arbitrary times t_1 and t_2. Let us assume that u minimizes the Hamiltonian integral (3.1) and consider the true evolution $\bar{u} = u + \gamma v$ of the system, where γ is a small positive parameter (i.e., $0 < \gamma \ll 1$). Note that the term γv is the variation of the function u, where v is an arbitrary function that is differentiable and vanishes at the time endpoints t_1 and t_2, i.e., $v(\cdot, t_1) = 0$ and $v(\cdot, t_2) = 0$. Thus, under a small change in the configuration of the system $\bar{u}$, the integral (3.1) becomes the (action) functional of γ:

$$I(\gamma) = \frac{1}{2} \int_{t_1}^{t_2} \int_0^l \left[\rho(u_t + \gamma v_t + V[u_x + \gamma v_x])^2 - P(u_x + \gamma v_x)^2 \right] dxdt$$
$$+ \int_{t_1}^{t_2} \left(\frac{1}{2} m[u_t(l, t) + \gamma v_t(l, t)]^2 - \frac{1}{2} \kappa[u(l, t) + \gamma v(l, t)]^2 - F_\eta[u(l, t) + \gamma v(l, t)] \right) dt.$$
$$(3.2)$$

Since (3.1) has a minimum at u, the functional $I(\gamma)$ has a minimum at $\gamma = 0$. Hence, taking the derivative of (3.2) with respect to its argument γ at 0, the first variation of the action becomes

$$\delta I(v) := \int_{t_1}^{t_2} \int_0^l \left[\rho(u_t + Vu_x)(v_t + V v_x) - Pu_x v_x \right] dxdt + \int_{t_1}^{t_2} [mu_t(l, t)v_t(l, t)$$
$$- \kappa u(l, t)v(l, t) - F_\eta v(l, t)] dt,$$
$$(3.3)$$

which is equal to zero. Applying integration by parts to (3.3) yields

$$\int_{t_1}^{t_2} \int_0^l \left[\rho(u_{tt} + 2Vu_{xt} + V^2 u_{xx}) - Pu_{xx} \right] v \, dxdt + \int_{t_1}^{t_2} [mu_{tt}(l, t) + \kappa u(l, t) + F_\eta]$$
$$\times v(l, t) \, dt - \int_{t_1}^{t_2} \left[\rho Vu_t + (\rho V^2 - P)u_x \right] v \big|_{x=0}^{x=l} \, dt = 0.$$
$$(3.4)$$

The governing equation of motion is contained in the first term of (3.4), and it is given by

$$\rho(u_{tt} + 2Vu_{xt} + V^2 u_{xx}) - Pu_{xx} = 0.$$
$$(3.5)$$

The boundary conditions follow from the rest of the terms in (3.4). As a result, they are given by

$$Pu_x(0, t) - \rho Vu_t(0, t) - \rho V^2 u_x(0, t) = 0,$$
$$(3.6)$$

and

$$mu_{tt}(l, t) + \kappa u(l, t) + \eta u_t(l, t) + Pu_x(l, t) - \rho Vu_t(l, t) - \rho V^2 u_x(l, t) = 0.$$
$$(3.7)$$

Note that (3.6) and (3.7) are the *natural (or force) boundary conditions*. However, (3.6) is not appropriate for our problem, since the string is fixed in transverse direction at the left boundary. Thus, the correct boundary condition at the left boundary is represented by the *essential (or geometric)* one as follows:

$$u(0, t) = 0.$$

Recall from Section 2.2 in Chapter 2, the string is acted upon by the forces due to local transverse, Coriolis, and centripetal accelerations, and by the transverse tension. In turn, the upstream boundary is acted upon by six forces. The first three terms in (3.7) ($mu_{tt}(l,t)$, $\kappa u(l,t)$, and $\eta u_t(l,t)$) represent forces arising in the spring-mass-dashpot system. The last three terms ($Pu_x(l,t)$, $\rho V u_t(l,t)$, and $\rho V^2 u_x(l,t)$) have already been described for (3.5) as the transverse tension of the string, the Coriolis force, and the centripetal force, respectively.

To continue with the formulation of the problem, it is convenient to nondimensionalize the obtained equations of motion of the string, which can be done by using the Buckingham theorem (π-theorem). The fundamental dimensions involved are length L, mass M, and time T. Consequently, the dimensionality of the three variables (u, x, and t) and the six parameters (ρ, V, P, κ, m, and η) of the system are given as follows:

$$[u] = L, \ [x] = L, \ [t] = T,$$

and

$$[\rho] = \frac{M}{L}, \ [V] = \frac{L}{T}, \ [P] = \frac{ML}{T^2}, \ [\kappa] = \frac{M}{T^2}, \ [m] = M, \ [\eta] = \frac{M}{T}.$$

So, using the π-theorem, we obtain the following dimensionless quantities

$$x^* = \frac{x}{L}, \ u^* = \frac{u}{L}, \ t^* = \frac{t}{L}\sqrt{\frac{P}{\rho}}, \ v^* = V\sqrt{\frac{\rho}{P}}, \ m^* = \frac{m}{\rho L}, \ \kappa^* = \frac{\kappa L}{P}, \ \eta^* = \frac{\eta}{\sqrt{\rho P}},$$

where $\sqrt{P/\rho}$ is the wave propagation speed. Hence, (3.5) and (3.7) then read as

$$u_{tt} + 2vu_{xt} + (v^2 - 1)u_{xx} = 0, \tag{3.8}$$

and

$$mu_{tt}(1,t) + \kappa u(1,t) + \eta u_t(1,t) - (v^2 - 1)u_x(1,t) - vu_t(1,t) = 0, \tag{3.9}$$

respectively, where the asterisk notations are omitted for convenience.

3.3 Energy and its rate of change

In this section, we determine the energy of the system and its time-rate of change. It should be noted that we keep working with the dimensionless variables and parameters of the problem.

The total energy per unit length is the sum of the kinetic and potential energy densities:

$$\hat{E}(t) := \frac{1}{2}(u_t + vu_x)^2 + \frac{1}{2}u_x^2.$$

The total mechanical energy of the system is comprised of three contributions such as the energy density $\hat{E}(t)$ contained in all material particles in the region $0 < x < 1$, the potential energy of the spring, and the kinetic energy of the attached mass:

$$E(t) := \frac{1}{2}\int_0^1 \left[(u_t + vu_x)^2 + u_x^2\right]dx + \frac{1}{2}\kappa u^2(1,t) + \frac{1}{2}mu_t^2(1,t). \tag{3.10}$$

By differentiating (3.10) with respect to time t, and by using (3.8) and (3.9), we find that the time-rate of change of the total mechanical energy of the string is given by

$$\frac{\mathrm{d}E(t)}{\mathrm{d}t} = \frac{v}{2}(1-v^2)\left[u_x^2(1,t)-u_x^2(0,t)\right] + \frac{v}{2}u_t^2(1,t) - \eta u_t^2(1,t). \tag{3.11}$$

Here we can see that the time-rate of change of the total energy completely depends on the boundary conditions. The first term on the right-hand side of (3.11) gives the energy flux into the span $(0,1)$ of the string [52], i.e., the string particles pass through fixed boundaries gaining and losing energy. The second term represents the energy flux across the upstream boundary resulting from inertial force due to transverse motion [28]. Finally, the last term is a dissipative one generating damping in the system.

3.4 Formal approximations of the solution

In order to have oscillations that do not decay too fast, and reflections of waves from both of the boundaries of the string, we assume that $\eta = \varepsilon\bar{\eta}$ and $v = \varepsilon\bar{v}$, respectively, where ε is a small positive parameter (i.e., $0 < \varepsilon \ll 1$) and $\bar{v}, \bar{\eta} = \mathcal{O}(1)$. Note that the bar notation for $\bar{\eta}$ and $\bar{v}$ will be omitted further for the sake of convenience. Introducing the initial displacement $\phi(x)$ and the initial velocity $\psi(x)$ of the string, we can now formulate the dimensionless initial-boundary value problem describing the transverse vibrations of an axially moving string with a spring-mass-dashpot system as follows.

The governing PDE is given by

$$u_{tt} - u_{xx} = -2\varepsilon v u_{xt} - \varepsilon^2 v^2 u_{xx}, \tag{3.12a}$$

for $0 < x < 1$, and $t > 0$, subject to the BCs:

$$u(0,t) = 0,$$
$$m u_{tt}(1,t) + \kappa u(1,t) + u_x(1,t) = -\varepsilon\eta u_t(1,t) + \varepsilon v u_t(1,t) + \varepsilon^2 v^2 u_x(1,t), \tag{3.12b}$$

for $t > 0$, and with the ICs:

$$u(x,0) = \phi(x),$$
$$u_t(x,0) = \psi(x), \tag{3.12c}$$

for $0 < x < 1$.

In this section, we construct an approximation of the solution of the initial-boundary value problem (3.12a-3.12c) using a two-timescales perturbation method. According to this method, we have to expand the solution in a Taylor series in ε as $u(x,t) \sim u_0(x,t) + \varepsilon u_1(x,t) + \varepsilon^2 u_2(x,t) + \ldots$, assuming in advance that $u_i(x,t)$ is $\mathcal{O}(1)$ for $i \in \mathbb{N}$. The approximation of the solution will contain secular terms, i.e., unbounded in

time, but it should be pointed out that the solution is bounded on the timescale of $\mathcal{O}(\varepsilon^{-1})$. Consequently, the secular terms have to be avoided on long time-scales in order to construct an accurate approximation. That is why we apply a two-timescales perturbation method by introducing an extra slow time variable $\tau = \varepsilon t$, which will be treated independently from the variable t. Hence, $u(x,t)$ becomes a new function of x, t, and τ, i.e., $u(x,t) = w(x,t,\tau;\varepsilon)$. As a consequence of this, the original time derivatives of the first and the second orders transform as follows:

$$\frac{\mathrm{d}}{\mathrm{d}t} \to \frac{\partial}{\partial t} + \varepsilon \frac{\partial}{\partial \tau}, \text{ and } \frac{\mathrm{d}^2}{\mathrm{d}t^2} \to \frac{\partial^2}{\partial t^2} + 2\varepsilon \frac{\partial^2}{\partial t \partial \tau} + \varepsilon^2 \frac{\partial^2}{\partial \tau^2}. \tag{3.13}$$

Using (3.13), we can rewrite the initial-boundary value problem as

$$w_{tt} - w_{xx} = -2\varepsilon(w_{t\tau} + v w_{xt}) - \varepsilon^2(w_{\tau\tau} + 2v w_{x\tau} + v^2 w_{xx}), \tag{3.14a}$$

for $0 < x < 1$, and $t > 0$, subject to the BCs:

$$
\begin{aligned}
&w(0,t,\tau;\varepsilon) = 0, \\
&mw_{tt}(1,t,\tau;\varepsilon) + \kappa w(1,t,\tau;\varepsilon) + w_x(1,t,\tau;\varepsilon) \\
&\quad = \varepsilon[-2mw_{t\tau}(1,t,\tau;\varepsilon) + (v-\eta)w_t(1,t,\tau;\varepsilon)] \\
&\quad + \varepsilon^2[-mw_{\tau\tau}(1,t,\tau;\varepsilon) + v^2 w_x(1,t,\tau;\varepsilon)(\eta-v)w_\tau(1,t,\tau;\varepsilon)],
\end{aligned} \tag{3.14b}
$$

for $t > 0$, and with the ICs:

$$
\begin{aligned}
&w(x,0,0;\varepsilon) = \phi(x), \\
&w_t(x,0,0;\varepsilon) + \varepsilon w_\tau(x,0,0;\varepsilon) = \psi(x),
\end{aligned} \tag{3.14c}
$$

for $0 < x < 1$, with

$$
\begin{aligned}
&\phi(0) = \phi''(0) = 0, \\
&\psi(0) = \psi'(0) = \psi''(0) = 0, \\
&m(1 - \varepsilon^2 v^2)\phi''(1) + (1 + \varepsilon^2 v^2)\phi'(1) + \kappa\phi(1) = 2\varepsilon m v \psi'(1) - \varepsilon(\eta-v)\psi(1),
\end{aligned} \tag{3.14d}
$$

for $\phi(x) \in C^4([0,1];\mathbb{R})$ and $\psi(x) \in C^3([0,1];\mathbb{R})$. Note that in order to have a sufficiently smooth solution, (3.14d) are the necessary *compatibility conditions*[1]. Substituting then a power series expansion of the form $w(x,t,\tau;\varepsilon) \sim w_0(x,t,\tau) + \varepsilon w_1(x,t,\tau) + \varepsilon^2 w_2(x,t,\tau) + \dots$ into the initial-boundary value problem (3.14a-3.14c) and equating the coefficients of like powers of ε, we obtain $\mathcal{O}(\varepsilon^n)$-problems to solve for $n \in \mathbb{N}$. Additionally, we assume that the initial displacement and the initial velocity can also be expanded in Taylor series in ε as $\phi(x) \sim \phi_0(x) + \varepsilon \phi_1(x) + \varepsilon^2 \phi_2(x) + \dots$ and $\psi(x) \sim \psi_0(x) + \varepsilon \psi_1(x) + \varepsilon^2 \psi_2(x) + \dots$, respectively. In the following subsections, two

---

[1] Compatibility conditions are a set of relations between the PDE, the boundary conditions, and the initial conditions, which are necessary and sufficient for the solution to be differentiable everywhere on the domain of definition of the problem.

initial-boundary value problems of $\mathcal{O}(1)$ and $\mathcal{O}(\varepsilon)$ will be considered in order to construct the formal approximation of the solution for (3.12a-3.12c) of $\mathcal{O}(\varepsilon)$ on a timescale of $\mathcal{O}(\varepsilon^{-1})$. Only the first few modes of oscillations of the string are important from the physical point of view; that is why we are not interested in the higher order mode approximations of the solution.

3.4.1 The $\mathcal{O}(1)$-problem

Collecting the coefficients of $\mathcal{O}(1)$ gives us the following unperturbed initial-boundary value problem:

$$w_{0_{tt}} - w_{0_{xx}} = 0, \tag{3.15a}$$

for $0 < x < 1$, $t > 0$, and $\tau > 0$, subject to the BCs:

$$w_0(0, t, \tau) = 0,$$
$$mw_{0_{tt}}(1, t, \tau) + \kappa w_0(1, t, \tau) + w_{0_x}(1, t, \tau) = 0, \tag{3.15b}$$

for $t > 0$ and $\tau > 0$, and with the ICs:

$$w_0(x, 0, 0) = \phi_0(x),$$
$$w_{0_t}(x, 0, 0) = \psi_0(x), \tag{3.15c}$$

for $0 < x < 1$,

with the compatibility conditions:

$$\phi_0(0) = \phi_0''(0) = \psi_0(0) = \psi_0''(0) = 0,$$
$$m\phi_0''(1) + \phi_0'(1) + \kappa\phi_0(1) = 0,$$
$$m\phi_0'''(1) + \phi_0''(1) + \kappa\phi_0'(1) = 0, \tag{3.16}$$
$$m\psi_0''(1) + \psi_0'(1) + \kappa\psi_0(1) = 0.$$

To find the solution of (3.15a-3.15c), the method of separation of variables will be used here. We look for a nontrivial separated solution of the boundary value problem (3.15a-3.15b) in the form $X(x)T(t, \tau)$. Plugging this into the partial differential (3.15a) and dividing by XT, we obtain a pair of separate differential equations such as $\frac{d^2X}{dx^2} + \mu X = 0$ and $\frac{\partial^2 T}{\partial t^2} + \mu T = 0$, where μ is an arbitrary constant known as the *separation constant*. Their solutions can be easily found as

$$X(x) = C\cos\left(\sqrt{\mu}x\right) + D\sin\left(\sqrt{\mu}x\right), \tag{3.17}$$
$$T(t, \tau) = A(\tau)\cos\left(\sqrt{\mu}t\right) + B(\tau)\sin\left(\sqrt{\mu}t\right), \tag{3.18}$$

where C, D are arbitrary constants, and $A(\tau)$, $B(\tau)$ are arbitrary functions. The next step is to impose the boundary conditions (3.15b) on the separated solution, which gives

$$X(0) = 0, \text{ and } X'(1) = (m\mu - \kappa)X(1). \tag{3.19}$$
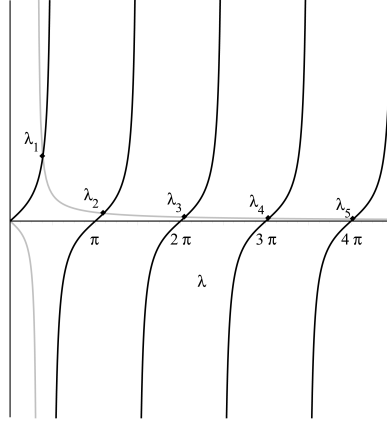
Figure 3.2: Graphical analysis of eigenvalues for $m = 1$ and $\kappa = 1$.

Employing these boundary conditions for (3.17), we obtain a transcendental equation

$$\sqrt{\mu}\cos\left(\sqrt{\mu}\right) = (m\mu - \kappa)\sin\sqrt{\mu}.$$

Any root of this equation would give us an eigenvalue μ_n for the initial-boundary value problem (3.14a-3.14c). Since the *eigenvalues are real-valued and positive* (for the proof we refer the reader to [62]), let us denote them as $\mu = \lambda^2$ for convenience. To find the roots of (3.4.1), we provide a graphical analysis, but first let us rewrite the eigenvalue (3.4.1) with the new notation as follows:

$$\tan\lambda = \frac{\lambda}{m\lambda^2 - \kappa}. \tag{3.20}$$

Proceeding with the graphical analysis (see Figure 3.2), we plot the trigonometric function $\tan\lambda$ and the rational function $\lambda/(m\lambda^2 - \kappa)$ and find their points of intersection. As a result, the eigenvalue μ_n satisfies $(n-1)^2\pi^2 < \mu_n < n^2\pi^2$ for $n \in \mathbb{N}$. Moreover, $\lambda_n \to (n-1)\pi$ as $n \to \infty$, which means that the larger eigenvalues get relatively closer and closer to $(n-1)^2\pi^2$, but recall that we are only interested in the lower eigenvalues; this will give us a finite sum of separated solutions further. Then, the corresponding eigenfunctions follow from (3.17) and (3.19) as $X_n(x) = D_n \sin\left(\lambda_n x\right)$, where D_n is an arbitrary constant.

Thus, separated solutions of (3.15a, 3.15b) are given by

$$w_{0_n}(x, t, \tau) = [A_n(\tau)\cos(\lambda_n t) + B_n(\tau)\sin(\lambda_n t)]\sin(\lambda_n x). \tag{3.21}$$

Now using the *principle of superposition* for (3.21) and the *orthogonality of the eigenfunctions with respect to the inner product* (B.4) derived in Appendix A, we obtain the final solution of (3.15a-3.15c) for the first oscillations modes, which is given by a finite

sum as

$$w_0(x,t,\tau) = \sum_{n=1}^{N} [A_n(\tau)\cos(\lambda_n t) + B_n(\tau)\sin(\lambda_n t)]\sin(\lambda_n x), \qquad (3.22)$$

where $N \in \mathbb{N}$ and

$$A_n(0) = \frac{1}{\alpha_n} \int_0^1 \sigma(x)\phi(x)\sin(\lambda_n x)\,dx, \qquad (3.23)$$

$$B_n(0) = \frac{1}{\alpha_n \lambda_n} \int_0^1 \sigma(x)\psi(x)\sin(\lambda_n x)\,dx, \qquad (3.24)$$

where $\sigma(x)$ is given by (B.3) and

$$\alpha_n := \frac{1}{2}\left[1 + \frac{m\lambda_n^2 + \kappa}{\lambda_n^2}\sin^2\lambda_n\right], \qquad (3.25)$$

and λ_n is given by (3.20). Using the compatibility conditions (3.16) and (3.20), we can show the boundedness of $A_n(0)$ and $B_n(0)$ as follows:

$$|A_n(0)| < \frac{2C_1}{\lambda_n^4}, \text{ and } |B_n(0)| < \frac{2C_2}{\lambda_n^4}, \qquad (3.26)$$

where the constants C_1 and C_2 are given by

$$C_1 = \max_{1 \le n < \infty}\left|\int_0^1 \phi_0^{(iv)}(x)\sin(\lambda_n x)\,dx\right|, \text{ and } C_2 = \max_{1 \le n < \infty}\left|\int_0^1 \psi_0'''(x)\cos(\lambda_n x)\,dx\right|.$$

It should be observed that so far $w_0(x,t,\tau)$ contains undetermined functions $A_n(\tau)$ and $B_n(\tau)$. These functions will be used in the following $\mathcal{O}(\varepsilon)$-problem to avoid secular terms in $w_1(x,t,\tau)$.

3.4.2   The $\mathcal{O}(\varepsilon)$-problem

The initial-boundary value problem for ω_1 is given by

$$w_{1_{tt}} - w_{1_{xx}} = -2w_{0_{t\tau}} - 2\nu w_{0_{xt}}, \qquad (3.27a)$$

for $0 < x < 1$, $t > 0$, and $\tau > 0$, subject to the BCs:

$$w_1(0,t,\tau) = 0,$$
$$mw_{1_{tt}}(1,t,\tau) + \kappa w_1(1,t,\tau) + w_{1_x}(1,t,\tau) = -2mw_{0_{t\tau}}(1,t,\tau) - (\eta - \nu)w_{0_t}(1,t,\tau),$$
$$\qquad (3.27b)$$

for $t > 0$ and $\tau > 0$, and with the ICs:

$$w_1(x,0,0) = \phi_1(x),$$
$$w_{1_t}(x,0,0) = \psi_1(x) - w_{0_\tau}(x,0,0), \qquad (3.27c)$$

for $0 < x < 1$,

with the compatibility conditions:

$$\phi_1(0) = \psi_1(0) = 0,$$
$$\phi_1''(0) = \frac{2v}{1-v^2}\psi_0'(0),$$
$$m\phi_1''(1) + \phi_1'(1) + \kappa\phi_1(1) = 2mv\psi_0'(1) - (\eta - v)\psi_0(1).$$

We will solve this problem by expanding the solution in a Fourier series of eigenfunctions. This approach is commonly used for inhomogeneous problems with homogeneous boundary conditions of classical types such as Dirichlet, Neumann, or Robin (mixed). In case of inhomogeneous boundary conditions, the standard method of shifting the data to make them homogeneous can be used. However, this technique does not work for non-classical boundary conditions such as (3.27b). To make the eigenfunction expansion approach applicable here, a transformation *matching* the partial differential (3.27a) and the boundary condition (3.27b) has to be found. By "matching" we mean that after expanding $w_1(x, t, \tau)$ in a Fourier series, the boundary condition (3.27b) has to be proportional to the partial differential (3.27a) at $x = 1$.

Let us introduce the following transformation

$$w_1(x, t, \tau) = y(x, t, \tau) + xh(t, \tau), \tag{3.28}$$

where y is an arbitrary function and h is to be determined to provide the matching mentioned above. Substituting (3.28) into (3.27a-3.27c), we obtain a new initial-boundary value problem for y:

$$y_{tt} - y_{xx} = -2w_{0_{t\tau}} - 2vw_{0_{xt}} - xh_{tt}, \tag{3.29a}$$

subject to the BCs:

$$y(0, t, \tau) = 0,$$
$$my_{tt}(1, t, \tau) + \kappa y(1, t, \tau) + y_x(1, t, \tau) = -2mw_{0_{t\tau}}(1, t, \tau) - (\eta - v)w_{0_t}(1, t, \tau)$$
$$- mh_{tt}(t, \tau) - (\kappa + 1)h(t, \tau),$$

$$\tag{3.29b}$$

for $t > 0$ and $\tau > 0$, and with the ICs:

$$y(x, 0, 0) = \phi_1(x) - xh(0, 0),$$
$$y_t(x, 0, 0) = \psi_1(x) - w_{0_\tau}(x, 0, 0) - xh_t(0, 0), \tag{3.29c}$$

for $0 < x < 1$. Before solving this problem, we first need to find $h(t, \tau)$. Let us expand the unknown solution $y(x, t, \tau)$ in terms of the eigenfunctions of the problem as follows:

$$y(x, t, \tau) = \sum_{n=1}^{N} y_n(t, \tau) \sin(\lambda_n x). \tag{3.30}$$

Substituting this expansion into (3.29a) and (3.29b), multiplying (3.29a) by m, and taking its limit at $x = 1$, we obtain

$$m\sum_{n=1}^{N}[y_{n_{tt}}(t,\tau) + \lambda_n^2 y_n(t,\tau)]\sin\lambda_n = -2mw_{0_{t\tau}}(1,t,\tau) - 2mvw_{0_{xt}}(1,t,\tau) - mh_{tt}(t,\tau),$$

and

$$m\sum_{n=1}^{N}[y_{n_{tt}}(t,\tau) + \lambda_n^2 y_n(t,\tau)]\sin\lambda_n = -2mw_{0_{t\tau}}(1,t,\tau) - (\eta - v)w_{0_t}(1,t,\tau)$$
$$- mh_{tt}(t,\tau) - (\kappa + 1)h(t,\tau),$$

respectively. One can notice that the left-hand sides of the so-obtained equations are equal to each other. Hence, equating their right-hand sides, we obtain h as follows:

$$h(t,\tau) = \frac{1}{\kappa + 1}[2mvw_{0_{xt}}(1,t,\tau) - (\eta - v)w_{0_t}(1,t,\tau)]. \tag{3.31}$$

Consequently, the initial-boundary value problem (3.29a-3.29c) becomes

$$y_{tt} - y_{xx} = -2w_{0_{t\tau}} - 2vw_{0_{xt}} - xh_{tt}, \tag{3.32a}$$

for $0 < x < 1$, $t > 0$, and $\tau > 0$, subject to the BCs:

$$y(0,t,\tau) = 0,$$
$$my_{tt}(1,t,\tau) + \kappa y(1,t,\tau) + y_x(1,t,\tau) \tag{3.32b}$$
$$= -m[2vw_{0_{xt}}(1,t,\tau) + 2w_{0_{t\tau}}(1,t,\tau) + h_{tt}(t,\tau)],$$

for $t > 0$ and $\tau > 0$, and with the ICs:

$$y(x,0,0) = \phi_1(x) - \frac{x}{\kappa + 1}[2mv\psi_0'(1) - (\eta - v)\psi_0(1)],$$
$$y_t(x,0,0) = \psi_1(x) - w_{0_\tau}(x,0,0) - \frac{x}{\kappa + 1}[2mv\phi_0'''(1) - (\eta - v)\phi_0''(1)], \tag{3.32c}$$

for $0 < x < 1$, where $h_{tt}(t,\tau) = \frac{1}{\kappa+1}[2mvw_{0_{xttt}}(1,t,\tau) - (\eta - v)w_{0_{ttt}}(1,t,\tau)]$. It should be noted that if $m = 0$, then the boundary condition at $x = 1$ becomes the homogeneous classical boundary condition of mixed type. Since the partial differential (3.32a) and the boundary condition (3.32b) now match each other, we can employ the eigenfunction expansion approach to solve the problem (3.32a-3.32c). Thus, substituting the finite series (3.30) into (3.32a), multiplying the so-obtained equation by $\sigma(x)\sin(\lambda_r x)$, where $\sigma(x)$ is given by (B.3), integrating then over the interval $0 < x < 1$, and employing the

orthogonality of eigenfunctions, we rewrite (3.32a) as follows:

$$y_{n_{tt}} + \lambda_n^2 y_n = 2\lambda_n (A_n' + \gamma_n A_n) \sin(\lambda_n t) - 2\lambda_n (B_n' + \gamma_n B_n) \cos(\lambda_n t) \tag{3.33}$$

$$+ \frac{2v}{\alpha_n} \sum_{\substack{p=1 \\ p \neq n}}^{N} \zeta_{np} \left[A_p \sin(\lambda_p t) - B_p \cos(\lambda_p t) \right]$$

$$- \frac{\beta_n}{\kappa + 1} \sum_{\substack{k=1 \\ k \neq n}}^{N} \hat{\zeta}_k \left[A_k \sin(\lambda_k t) - B_k \cos(\lambda_k t) \right],$$

where

$$\beta_n := \frac{2(\kappa + 1) \sin \lambda_n}{\lambda_n^2 + (m\lambda_n^2 + \kappa) \sin^2 \lambda_n}, \tag{3.34}$$

$$\gamma_n := \frac{\eta \lambda_n^2}{(m\lambda_n^2 - \kappa)^2 + (m+1)\lambda_n^2 + \kappa} > 0, \tag{3.35}$$

$$\zeta_{np} := \frac{\lambda_p}{\lambda_n^2 - \lambda_p^2} \left(\lambda_n \lambda_p - [(m\lambda_p^2 - \kappa)^2 + \lambda_p^2] \sin \lambda_n \sin \lambda_p \right), \tag{3.36}$$

$$\hat{\zeta}_k := [2mv(m\lambda_k^2 - \kappa) - (\eta - v)]\lambda_k^3 \sin \lambda_k. \tag{3.37}$$

It can be observed that $y(x, t, \tau)$ now automatically satisfies the boundary conditions. Continuing, we have the possibility of secular terms in the solution of (3.33). However, the functions A_n and B_n can be chosen to prevent this. From (3.33), it follows that they have to satisfy $A_n' + \gamma_n A_n = 0$ and $B_n' + \gamma_n B_n = 0$. The solutions of these equations are readily found as

$$A_n(\tau) = A_n(0) \exp(-\gamma_n \tau), \text{ and } B_n(\tau) = B_n(0) \exp(-\gamma_n \tau), \tag{3.38}$$

where $A_n(0)$ and $B_n(0)$ are given by (3.23) and (3.24), respectively. Note that the finite series representation (3.22) for w_0 and the exponential representation of functions A_n and B_n give insight into the differentiability and the stability of the solution w_0. It is worth noting that the obtained result (3.35) is in agreement with the result found in [9] for the stationary (i.e., $v = 0$) string. Finally, the solution of (3.33) is given by the sum of a homogeneous solution and a particular one:

$$y_n(t, \tau) = D_n(\tau) \cos(\lambda_n t) + E_n(\tau) \sin(\lambda_n t) \tag{3.39}$$

$$+ \frac{2v}{\alpha_n} \sum_{\substack{p=1 \\ p \neq n}}^{N} \frac{\zeta_{np}}{\lambda_n^2 - \lambda_p^2} \left[A_p(\tau) \sin(\lambda_p t) - B_p(\tau) \cos(\lambda_p t) \right]$$

$$- \frac{\beta_n}{\kappa + 1} \sum_{\substack{k=1 \\ k \neq n}}^{N} \frac{\hat{\zeta}_k}{\lambda_n^2 - \lambda_k^2} \left[A_k(\tau) \sin(\lambda_k t) - B_k(\tau) \cos(\lambda_k t) \right],$$

where $D_n(\tau)$ and $E_n(\tau)$ are arbitrary functions which can be used in the $\mathcal{O}(\varepsilon^2)$-problem to avoid secular terms in $\omega(x, t, \tau)$. Now by using the initial conditions (3.32c) and the

orthogonality relations of the eigenfunctions, we obtain $D_n(0)$ and $E_n(0)$ as follows:

$$D_n(0) = \frac{1}{\alpha_n} \int_0^1 \sigma(x) \left(\phi_1(x) - \frac{x}{\kappa+1} \left[2m\nu\psi_0'(1) - (\eta - \nu)\psi_0(1) \right] \right) \sin(\lambda_n x) \, dx$$

$$+ \frac{2\nu}{\alpha_n} \sum_{\substack{p=1 \\ p \neq n}}^{N} \frac{\lambda_p}{(\lambda_n^2 - \lambda_p^2)^2} \zeta_{np} B_p(0) - \frac{\beta_n}{\kappa+1} \sum_{\substack{k=1 \\ k \neq n}}^{N} \frac{\lambda_k^3}{\lambda_n^2 - \lambda_k^2} \hat{\zeta}_k B_k(0),$$

$$\lambda_n E_n(0) = \frac{1}{\alpha_n} \int_0^1 \sigma(x) \left(\psi_1(x) - \frac{x}{\kappa+1} \left[2m\nu\phi_0'''(1) - (\eta - \nu)\phi_0''(1) \right] \right) \sin(\lambda_n x) dx$$

$$- \frac{2\nu}{\alpha_n} \sum_{\substack{p=1 \\ p \neq n}}^{N} \frac{\zeta_{np}}{\lambda_n^2 - \lambda_p^2} A_p(0) + \frac{\beta_n}{\kappa+1} \sum_{\substack{k=1 \\ k \neq n}}^{N} \frac{\hat{\zeta}_k}{\lambda_n^2 - \lambda_k^2} A_k(0) + \gamma_n A_n(0),$$

where $A_n(0)$, $B_n(0)$, α_n, β_n, γ_n, ζ_{np}, $\hat{\zeta}_k$, and σ are given by (3.23), (3.24), (3.25), (3.34), (3.35), (3.36), (3.37), and (B.3), respectively. By using (3.26), we can easily show the boundedness of $D_n(0)$ and $E_n(0)$ as $|D_n(0)| < \frac{C_3}{\lambda_n^3}$ and $|E_n(0)| < \frac{C_4}{\lambda_n^3}$, where C_3 and C_4 are positive constants.

The solution of the $\mathscr{O}(\varepsilon)$-problem now readily follows from (3.28), (3.30), (3.31), and (3.39), yielding

$$w_1(x, t, \tau) = \sum_{n=1}^{N} \left[y_n(t, \tau) + \frac{\beta_n}{\kappa+1} \sum_{j=1}^{Q} H_j(t, \tau) \right] \sin(\lambda_n x), \qquad (3.40)$$

where λ_n is given by (3.20), $N, Q \in \mathbb{N}$, and

$$H_j(t, \tau) := \frac{\hat{\zeta}_j}{\lambda_j} \left[B_j(\tau) \cos(\lambda_j t) - A_j(\tau) \sin(\lambda_j t) \right],$$

where $A_j(\tau)$ and $B_j(\tau)$ are given by (3.38).

Concluding, we have constructed a formal approximation

$$u(x, t) = w(x, t, \tau) \sim w_0(x, t, \tau) + \varepsilon w_1(x, t, \tau),$$

where $w_0(x, t, \tau)$ and $w_1(x, t, \tau)$ are given by Equations (3.22) and (3.40), respectively. Moreover, they are twice continuously differentiable with respect to x and t and infinitely many times with respect to τ. As was mentioned before, we are not interested in higher order approximations; that is why we take $D_n(\tau) = D_n(0)$ and $E_n(\tau) = E_n(0)$ in (3.39). Otherwise, $D_n(\tau)$ and $E_n(\tau)$ can be found from the solvability conditions of the $\mathscr{O}(\varepsilon^2)$-problem.
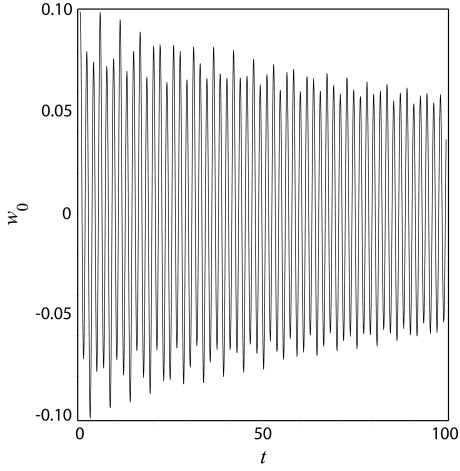
(a) $x = 0.5$: (b) $x = 1$:
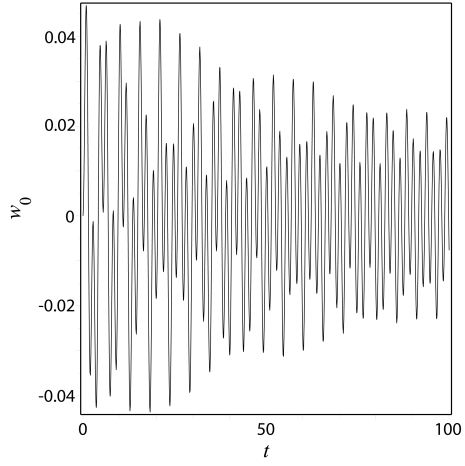
Figure 3.3: Transverse displacements w_0 at (a) $x = 0.5$ and at (b) $x = 1$ against time t with the initial displacement $\phi(x) = 0.1\sin(\pi x)$ and the initial velocity $\psi(x) = 0.05\sin(\pi x)$ for $\varepsilon = 0.1$, $\eta = 0.5$, $m = 1$, $\kappa = 1$, and $N = 10$.
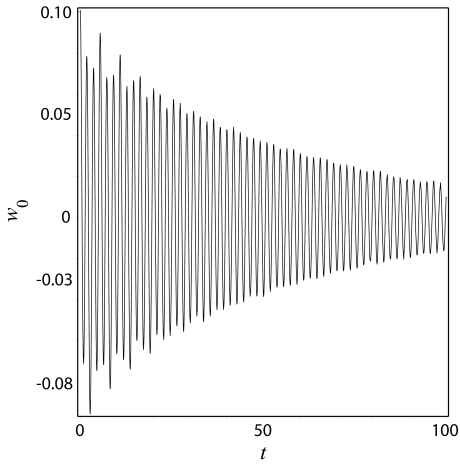
(a) $x = 0.5$: (b) $x = 1$:
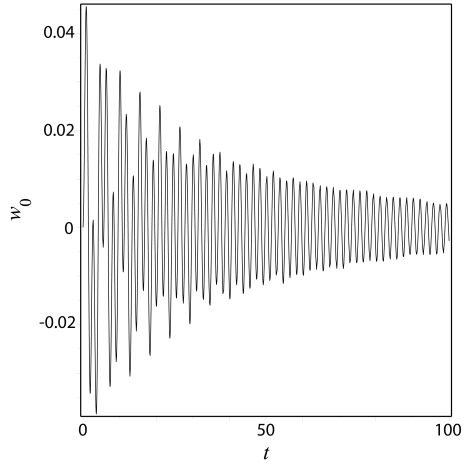
Figure 3.4: Transverse displacements w_0 at (a) $x = 0.5$ and at (b) $x = 1$ against time t with the initial displacement $\phi(x) = 0.1\sin(\pi x)$ and the initial velocity $\psi(x) = 0.05\sin(\pi x)$ for $\varepsilon = 0.1$, $\eta = 2$, $m = 1$, $\kappa = 1$, and $N = 10$.

3.4.3 Numerical results

It is interesting to see the behavior of the asymptotic approximation w_0 indicating the damping characteristics of the solution u of the initial-boundary value problem (3.12a-

3.12c). Figures 3.3 and 3.4 illustrate the vibration response at the middle ($x = 0.5$) and at the end ($x = 1$) points of the string for two different values of the damping factor η (i.e., Figure 3.3 is plotted for $\eta = 0.5$, and Figure 3.4 is plotted for $\eta = 2$); the initial conditions are specified as $u(x,0) = 0.1\sin(\pi x)$ and $u_t(x,0) = 0.05\sin(\pi x)$. These figures show that the amplitudes of the transverse vibrations decrease faster for increasing values of η as expected.

3.5   Alternative solution by the Laplace transform

In this section, the Laplace transform method is applied directly to the initial-boundary value problem (3.12a-3.12c) to obtain an implicit exact solution. Moreover, the approximations of the roots, which are actually eigenvalues, of a so-called *characteristic equation* are constructed (see, for instance, Chapter 6 in [30]). These results can be used to verify the approximate solution derived by the two-timescales perturbation method in the previous section.

3.5.1   Implicit solution

Applying the Laplace transform to (3.12a-3.12c) and introducing the following notations

$$h_1(x,s) := -2\varepsilon v\phi'(x) - s\phi(x) - \psi(x),$$
$$h_2(s) := m[s\phi(1) + \psi(1)] + \varepsilon(\eta - v)\phi(1),$$

where the prime notation indicates differentiation with respect to the argument, we obtain the following boundary value problem for $0 < x < 1$ and $s > 0$ to solve

$$(1 - \varepsilon^2 v^2)U_{xx}(x,s) - 2\varepsilon vsU_x(x,s) - s^2 U(x,s) = h_1(x,s), \tag{3.41a}$$

with the BCs

$$U(0,s) = 0,$$
$$(1 - \varepsilon^2 v^2)U_x(1,s) + (ms^2 + \varepsilon[\eta - v]s + \kappa)U(1,s) = h_2(s), \tag{3.41b}$$

for $s > 0$, where $U(x,s)$ is the Laplace transform of $u(x,t)$ and s is the transform variable. The nonhomogeneous second-order differential (3.41a) can easily be solved by standard techniques. Thus, the solution of (3.41a, 3.41b) is given by

$$U(x,s) = K(s)\Phi(x,s) + \frac{1}{s}\int_0^x h_1(\xi,s)\Phi(x-\xi,s)\,\mathrm{d}\xi, \tag{3.42}$$

where

$$K(s) := \frac{1}{\hat{\beta}(s)} \int_0^1 \frac{h_1(\xi,s)}{e^{\hat{\alpha}(s)\xi}} \left[\cosh\left(\hat{\beta}(s)\xi\right) - \frac{\Theta_{m\eta\kappa}(s)}{\Omega_{m\eta\kappa}(s)} \sinh\left(\hat{\beta}(s)\xi\right) \right] d\xi - \frac{1}{e^{\hat{\alpha}(s)}} \frac{h_2(s)}{\Omega_{m\eta\kappa}(s)},$$

$$\Phi(x,s) := e^{\hat{\alpha}(s)x} \sinh\left(\hat{\beta}(s)x\right),$$

$$\Omega_{m\eta\kappa}(s) := (ms^2 + \varepsilon\eta s + \kappa) \sinh\left(\hat{\beta}(s)\right) + s \cosh\left(\hat{\beta}(s)\right), \tag{3.43}$$

$$\Theta_{m\eta\kappa}(s) := (ms^2 + \varepsilon\eta s + \kappa) \cosh\left(\hat{\beta}(s)\right) + s \sinh\left(\hat{\beta}(s)\right),$$

$$\hat{\alpha}(s) := \frac{\varepsilon v s}{1 - \varepsilon^2 v^2}, \text{ and } \hat{\beta}(s) := \frac{s}{1 - \varepsilon^2 v^2}.$$

Next, to obtain the solution of (3.12a-3.12c), the inverse Laplace transform of U will be used, which will lead to a convolution in the (x,t)-domain. The inverse Laplace transform can be calculated using Cauchy's residue theorem. It should be noted in advance that $s = 0$ is not a pole of U; that is why the only contribution to the inversion of (3.42) by Cauchy's residue theorem will be due to the poles of $K(s)\Phi(x,s)$. These poles are determined by the roots of the so-called characteristic equation

$$\Omega_{m\eta\kappa}(s) = 0, \tag{3.44}$$

where $\Omega_{m\eta\kappa}(s)$ is given by (3.43). *In Appendix B, it is shown that* (3.44) *has infinitely many roots which appear in complex conjugate pairs. Moreover, these roots are simple poles.* This fact is used here to calculate the residues of $K(s)\Phi(x,s)$.

Let us denote the roots of (3.44) with a positive imaginary part by $s_n := s_n^{re} + i s_n^{im}$, where $s_n^{re}, s_n^{im} \in \mathbb{R}$ for $n \in \mathbb{N}$. Thus, inverting $K(s)\Phi(x,s)$ by incorporating Cauchy's residue theorem and the convolution theorem, we obtain the *implicit solution* of the problem (3.12a-3.12c) as follows:

$$u(x,t) = \sum_{n=1}^N e^{s_n^{re} t} \left(\left[R_n \Phi_n(x) + \overline{R_n \Phi_n}(x) \right] \cos(s_n^{im} t) + i \left[R_n \Phi_n(x) - \overline{R_n \Phi_n}(x) \right] \sin(s_n^{im} t) \right), \tag{3.45}$$

where the upper bar stands for complex conjugation, and R_n and $\Phi_n(x)$ are given by

$$R_n := \frac{\Theta_{m\eta\kappa}(s_n)}{\partial_s\left(\hat{\beta}(s)\Omega_{m\eta\kappa}(s)\right)\big|_{s=s_n}} \int_0^1 [2\varepsilon v\phi'(\xi) - s_n\phi(\xi) + \psi(\xi)] \frac{\sinh\left(\hat{\beta}(s_n)\xi\right)}{e^{\hat{\alpha}(s_n)\xi}} \, d\xi$$

$$- \frac{m[s_n\phi(1) + \psi(1)] + \varepsilon(\eta - v)\phi(1)}{\partial_s\left(e^{\hat{\alpha}(s)}\Omega_{m\eta\kappa}(s)\right)\big|_{s=s_n}}, \tag{3.46}$$

$$\Phi_n(x) := e^{\hat{\alpha}(s_n)x} \sinh\left(\hat{\beta}(s_n)x\right), \tag{3.47}$$

where the derivatives with respect to s in the denominators of (3.46) are found to be

$$\partial_s\left(\hat{\beta}(s)\Omega_{m\eta\kappa}(s)\right)\big|_{s=s_n} = \frac{\Omega_{m\eta\kappa}(s_n)}{1 - \varepsilon^2 v^2} + \hat{\beta}(s_n)\left[\frac{\Theta_{m\eta\kappa}(s_n)}{1 - \varepsilon^2 v^2} + \hat{\Omega}_{m\eta}(s_n)\right],$$

$$\partial_s\left(e^{\hat{\alpha}(s)}\Omega_{m\eta\kappa}(s)\right)\big|_{s=s_n} = e^{\hat{\alpha}(s_n)}\left[\frac{\varepsilon v\Omega_{m\eta\kappa}(s_n)}{1 - \varepsilon^2 v^2} + \frac{\Theta_{m\eta\kappa}(s_n)}{1 - \varepsilon^2 v^2} + \hat{\Omega}_{m\eta}(s_n)\right],$$

where $\hat{\Omega}_{m\eta}(s) := (2ms + \varepsilon\eta)\sinh\left(\hat{\beta}(s)\right) + \cosh\left(\hat{\beta}(s)\right)$.

3.5.2 Formal approximations of the eigenvalues

In this subsection we construct approximations of the roots of (3.44) by assuming that these roots can be expanded in a Taylor series in ε as $s_n(\varepsilon) \sim s_{0,n} + \varepsilon s_{1,n} + \varepsilon^2 s_{2,n} + \ldots$, where $s_{k,n} = s_{k,1,n} + i s_{k,2,n}$ with $s_{k,1,n}, s_{k,2,n} \in \mathbb{R}$ for $k \in \mathbb{N} \cup \{0\}$, and $s_{k,1,n}, s_{k,2,n} = \mathcal{O}(1)$ for $k \in \mathbb{N}$. These roots, i.e., the approximations of the roots, describe the low frequency vibrations of the string. So, we substitute the Taylor series expansion of $s_n(\varepsilon)$ into (3.44) and equate the coefficients of like powers of ε in order to obtain $\mathcal{O}(\varepsilon^n)$-equations for $n \in \mathbb{N}$. The solutions of the so-obtained equations will be used to construct approximations of the roots of the characteristic equation. From the described above procedure the $\mathcal{O}(1)$-problem follows as

$$(m s_{0,n}^2 + \kappa) \sinh s_{0,n} + s_{0,n} \cosh s_{0,n} = 0. \tag{3.48}$$

The solutions of (3.48) are given by

$$s_{0,n} = i s_{0,2,n}, \tag{3.49}$$

where $s_{0,2,n}$ is the n-th positive root of $(m s^2 - \kappa) \sin s - s \cos s = 0$, which is the same equation as (3.4.1) if one takes the separation constant μ equal to s^2. Recall that it has also been shown there that $(n-1)\pi < s_n < n\pi$ for $n \in \mathbb{N}$ and $s_n \to (n-1)\pi$ as $n \to \infty$. Then, the $\mathcal{O}(\varepsilon)$-equation gives the following solution

$$s_{1,n} = s_{1,1,n} = -\frac{\eta s_{0,2,n}^2}{(m s_{0,2,n}^2 - \kappa)^2 + (m+1) s_{0,2,n}^2 + \kappa}. \tag{3.50}$$

So far, we have constructed a formal approximation of the roots of (3.44) as $s_n(\varepsilon) = s_n^{\text{re}}(\varepsilon) + i s_n^{\text{im}}(\varepsilon) + \mathcal{O}(\varepsilon^2)$, where the damping rate $s_n^{\text{re}}(\varepsilon)$ is given by $\varepsilon s_{1,1,n} + \mathcal{O}(\varepsilon^2)$, and the frequency $s_n^{\text{im}}(\varepsilon)$ is given by $s_{0,2,n} + \mathcal{O}(\varepsilon)$ for $n \in \mathbb{N}$. Moreover, the damping rate $\varepsilon s_{1,1,n}$ confirms the result obtained in Section 4, which is given by (3.35) and (3.38).

n	s_n^{num}	$s_n(\varepsilon)$
1	$-0.0353 + 1.2074i$	$-0.0354 + 1.2078i$
2	$-0.00829 + 3.4480i$	$-0.00826 + 3.4482i$
3	$-0.00241 + 6.4409i$	$-0.00241 + 6.4410i$
4	$-0.00110 + 9.5305i$	$-0.00110 + 9.5305i$
5	$-0.000625 + 12.646i$	$-0.000628 + 12.646i$
6	$-0.000402 + 15.772i$	$-0.000400 + 15.772i$
7	$-0.000280 + 18.903i$	$-0.000279 + 18.903i$
8	$-0.000208 + 22.037i$	$-0.000207 + 22.037i$
9	$-0.000158 + 25.173i$	$-0.000158 + 25.173i$
10	$-0.000126 + 28.310i$	$-0.000125 + 28.310i$

Table 3.1: First ten numerical (s_n^{num}) and asymptotic ($s_n(\varepsilon) \sim s_{0,n} + \varepsilon s_{1,n}$) approximations of the eigenvalues s_n for $\varepsilon = 0.1$, $\eta = 1$, $\kappa = 1$, and $m = 1$.

Next, Table 3.1 provides the first ten Maple numeric (s_n^{num}) and asymptotic ($s_n(\varepsilon) \sim s_{0,n} + \varepsilon s_{1,n}$) approximations of the roots of the (3.44), where the real part stands for the damping rate and the imaginary part represents the oscillatory behavior. Here, the numerical and asymptotic results are very close to each other. Additionally, it is clear that the stability of the solution (3.45) is determined by the real part of the eigenvalues. Hence, the negative real part of $s_n(\varepsilon)$ implies that the solution (3.45) is *asymptotically stable* for the low frequency vibrations of the string.

It can be observed that the damping rates of the first oscillations modes decrease faster for increasing values of η, and the contribution of the axial speed v arises for the higher order modes of oscillations. The axial speed mainly influences on the oscillatory behavior of the string, and does not much influence its damping rates.

In addition, the approximation of the eigenfunctions (3.47) corresponding to the roots of the (3.44) can be given. Substituting the Taylor series expansion of $s_n(\varepsilon)$ into (3.47) and expanding the result with respect to ε, we obtain the formal approximation of the eigenfunctions as follows:

$$\Phi_n(x; \varepsilon) = \sinh(s_{0,n}x) + \varepsilon x[s_{1,n}\cosh(s_{0,n}x) + vs_{0,n}\sinh(s_{0,n}x)] + \mathcal{O}(\varepsilon^2),$$

where $s_{0,n}$ and $s_{1,n}$ are given by (3.49) and (3.50), respectively. However, these eigenfunctions, corresponding to different eigenvalues, are not orthogonal over the interval $0 \leq x \leq 1$.

3.6 Conclusions

This chapter has considered the transverse vibrations of an axially moving string with a fixed end and a spring-mass-dashpot system attached to a non-fixed end. These oscillations were described by the initial-boundary value problem (3.12a-3.12c), developed by employing the extended Hamilton's principle. Then, the total mechanical energy of the system was derived analytically. Its time-rate of change shows that the energy dissipation completely depends on the work done at the boundaries.

Both objectives of this chapter have been achieved, i.e., approximations of the solution on a long time-scale and approximations of the eigenvalues have been constructed. More precisely, the approximate solution of order ε on a time-scale of order ε^{-1} was constructed by a two-timescales perturbation method. Furthermore, the numerical results (graphed in Figures 3.3 and 3.4) show that the increase of the damping factor considerably reduces the amplitude of the transverse vibrations. It should be noted that string-like models for elastic structures (bending stiffness is neglected) are only applicable to the lower frequencies, i.e., $\sqrt{\mu} = \lambda$ should be of $\mathcal{O}(1)$. To obtain good approximations of the frequencies of the higher order modes, bending stiffness has to be included. For a similar beam-like problem the reader is referred to the paper of Sandilo and van Horssen [51], where the authors showed that damping in the system depends on the position of the damper and the direction of the axial velocity, which is not the case for our (string-like) model. In addition, explicit approximations of the damping rates and the frequencies of the oscillations modes were constructed. The numerical results in Table 3.1 and Figure 5 confirm the damping behavior of the solution obtained by

the two-timescales perturbation method. Lastly, the obtained alternative solution by the Laplace transform method can be used to check the response derived from the multiple-timescales approach. It is easy to see that $\mathcal{O}(1)$-part of eigenfunctions in (3.5.2) satisfies the orthogonality property (B.2) allowing to compare the results of both approaches up to $\mathcal{O}(\varepsilon)$, and seeing that they are identical.

Appendix B

B.1 Orthogonality of eigenfunctions

Let $X_1(x)$ and $X_2(x)$ be two different solutions corresponding to different eigenvalues λ_1 and λ_2, respectively. Using *Green's formula* [43], we obtain

$$\int_0^1 (L[X_1]X_2 - X_1 L[X_2])\, dx = -\left(X_1 \frac{dX_2}{dx} - X_2 \frac{dX_1}{dx} \right)\Bigg|_{x=0}^{x=1}, \tag{B.1}$$

where $L[X_i] = \frac{d^2 X_i}{dx^2}$ for $i = 1, 2$. The left-hand side of (B.1) can be rewritten as follows:

$$\int_0^1 (L[X_1]X_2 - X_1 L[X_2])\, dx = (\lambda_1 - \lambda_2) \int_0^1 X_1 X_2\, dx.$$

The right-hand side of (B.1), using the boundary condition (3.19), takes the form

$$\left(X_1(x) \frac{dX_2(x)}{dx} - X_2(x) \frac{dX_1(x)}{dx} \right)\Bigg|_{x=0}^{x=1} = m(\lambda_1 - \lambda_2)X_1(1)X_2(1).$$

Equating the last two equations and rearranging terms, we obtain

$$\int_0^1 [1 + 2m\delta(x-1)]X_1 X_2\, dx = 0, \tag{B.2}$$

where $\delta(x-1)$ is the Dirac delta function which is zero everywhere except at $x = 1$, where it is infinite, and it is also constrained to satisfy the identity $\int_0^1 \delta(x-1)\, dx = 1/2$. The latter shows that $X_1(x)$ and $X_2(x)$ are orthogonal with weight

$$\sigma(x) := 1 + 2m\delta(x-1). \tag{B.3}$$

Hence, the inner product of two real-valued continuous functions f and g can be defined as follows:

$$\langle f(x), g(x) \rangle := \int_0^1 \sigma(x)f(x)g(x)\, dx. \tag{B.4}$$

Thus, we state that *two different eigenfunctions corresponding to different eigenvalues are orthogonal with respect to the inner product* (B.4).

B.2 Roots of the characteristic equation

Real-valued roots

First, we study the real-valued roots of the so-called characteristic (3.44). Considering the continuous function $\Omega_{m\eta\kappa}(s)$ in the exponential representation, it can be seen that $\Omega_{m\eta\kappa}(s) \to \infty$ as $s \to \infty$ and $\Omega_{m\eta\kappa}(s) \to -\infty$ as $s \to -\infty$. This implies that (3.44) has at least one real-valued root, and we notice that $s = 0$ is one of these roots. For the further analysis on the number of real-valued roots, it is more convenient to rewrite (3.44) in the following form

$$(ms^2 + \kappa)\tanh(cs) = -s\,(\varepsilon\eta\tanh(cs) + 1),\tag{B.5}$$

where $c := (1 - \varepsilon^2 v^2)^{-1} > 0$, $m > 0$, $\kappa > 0$, and $0 < \varepsilon\eta \ll 1$.

Now we consider two cases, i.e., when s is positive and when it is negative. For $s > 0$, the left-hand side of (B.5) is positive and the right-hand side is negative, which leads to a contradiction. Next, recall that ε and $\varepsilon\eta$ were assumed to be small positive constants, and $|\tanh(cs)| < 1$. Hence, for negative s, it follows that $\varepsilon\eta\tanh(cs) + 1 > 0$, which shows that the left-hand side of (B.5) is negative and the right-hand side is positive, providing again a contradiction. Summing everything up, $s = 0$ is the only real-valued root of the characteristic (3.44). However, *it is not a pole of $U(x,s)$ given by* (3.42), which implies that there are no real-valued roots of (B.5) contributing to Cauchy's residue theorem.

Complex-valued roots

Here we show that $\Omega_{m\eta\kappa}(s)$ has infinitely many zeros in the complex s-plane by using *Hadamard's theorem*. First of all, note that $\Omega_{m\eta\kappa}(s)$ is an *entire function*[1]. To apply Hadamard's theorem, we then need to define its order. Recall that the order of $\Omega_{m\eta\kappa}(s)$ is the infimum of all k such that $\Omega_{m\eta\kappa}(s) = \mathcal{O}(\exp(|s|^k))$ as $s \to \infty$. We can determine it using the limit superior

$$k := \limsup_{s\to\infty} \frac{\log(\log\|\Omega_{m\eta\kappa}\|_{\infty,B_r})}{\log r},\tag{B.6}$$

where B_r is the disk of radius r and $\|\Omega_{m\eta\kappa}\|_{\infty,B_r}$ denotes the supremum norm of $\Omega_{m\eta\kappa}(s)$ on B_r. To find the order of $\Omega_{m\eta\kappa}(s)$, it is not necessary to consider the whole function itself, but the highest order term in $\Omega_{m\eta\kappa}(s)$ can be chosen for this purpose. Hence, we need to find the order of

$$f(s) := s^2 \sinh(cs).$$

The logarithm of the supremum norm of $f(s)$ is given by

$$\log\|f\|_{\infty,B_r} = \log\left(r^2 \sinh(cr)\right) = 2\log r + \log(\sinh(cr)).\tag{B.7}$$

---

[1] A complex-valued function that is holomorphic over the whole complex plane.

Substituting (B.7) into (B.6) and applying l'Hôpital's rule, we obtain

$$k = \lim_{r \to \infty} \frac{2 + cr}{2 \log r - \log 2 + cr} = \lim_{r \to \infty} \frac{2/r + c}{(2/r) \log r - (1/r) \log 2 + c} = \frac{c}{c} = 1.$$

As a consequence, the order of $\Omega_{m\eta\kappa}(s)$ is $k = 1$. Thus, the fact that $\Omega_{m\eta\kappa}(s)$ is an entire function of finite order k admits *Hadamard's canonical factorization*

$$\Omega_{m\eta\kappa}(s) = s e^{g(s)} \prod_{n=1}^{\infty} \left(1 - \frac{s}{s_n}\right) \exp\left(\sum_{j=1}^{p} \frac{1}{j} \left(\frac{s}{s_n}\right)^j\right), \tag{B.8}$$

where $g(s)$ is a polynomial in s of degree q, which satisfies $q \leq k$, and p is the smallest non-negative integer, such that the series $\sum_{n=1}^{\infty} \frac{1}{|s_n|^{p+1}}$ converges.

Finally, it follows from the factorization (B.8) that the characteristic (3.44) has an *infinite number of roots s_n* (for $n \in \mathbb{Z} \backslash \{0\}$), which appear in conjugate pairs and $|s_n| \to \infty$ as $|n| \to \infty$. Moreover, all the eigenvalues s_n have geometric multiplicity equal to one implying that *these roots are simple poles* for $K(s)\Phi(x,s)$ in (3.42). The reader is referred to [44] for further details on these theorems in complex analysis.

Chapter 4

Wave reflections and energetics for a semi-infinite traveling string with a non-classical boundary support

In this chapter, the free, linear, transverse vibrations of a semi-infinite axially moving string are considered in order to study the reflection of an incident wave and the damping properties of different types of boundary conditions such as free, fixed, spring-dashpot, and mass-spring-dashpot. To obtain the response to the initial conditions, the method of d'Alembert is applied. Furthermore, analytical expressions for the time-rate of change of the total mechanical energy of the system are derived. The obtained results give insight into the most efficient way of placing a boundary support depending on the direction of the transport velocity. Moreover, for nonclassical boundary conditions, the dynamics of the string is described by the relative values of the system parameters.
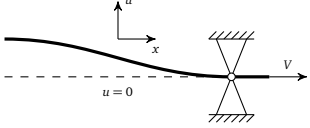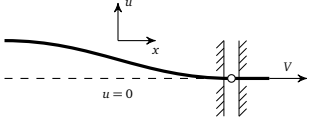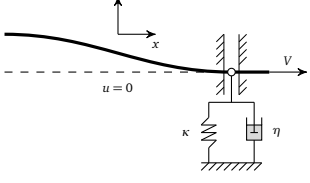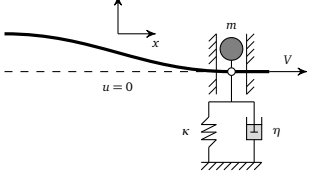
Type	Diagram	Equation
Fixed		$u(0,t) = 0$
Free		$u_x(0,t) = 0$
Spring-Dashpot		$\kappa u(0,t) + \eta u_t(0,t) + P u_x(0,t)$ $= \rho V[u_t(0,t) + V u_x(0,t)]$
Mass-Spring-Dashpot		$m u_{tt}(0,t) + \kappa u(0,t) + \eta u_t(0,t)$ $= \rho V[u_t(0,t) + V u_x(0,t)] - P u_x(0,t)$

Table 4.1: List of various boundary conditions. The symbols are defined in the text.

4.1 Introduction

The previous chapter showed an example of boundary damping as a passive approach to suppress vibrations. This chapter investigates boundary damping more thoroughly by considering different types of boundary supports for the string (see the schematic diagrams in Table 4.1). In reality, engineering slender elements have finite length, where the waves are reflected at both boundaries. The interaction among the reflected waves does not allow to study the effectiveness of a boundary support as a standalone device in a simple way, while the semi-infinite span of the string does. Therefore, a semi-infinite string is chosen as a model for consideration in this chapter. This simple model can be used to determine how much energy of the wave is dissipated at the boundary. More precisely, by looking at the reflected wave profile and the energetics of the model under consideration, one can examine the efficiency of a placed boundary support as a vibration suppressor.

There are a plenty of examples studying the reflection phenomena in stationary strings with classical boundary conditions by the classical d'Alembert solution in the literature (see for instance, [31, 62]). Recently, Akkaya and van Horssen [53] employed the same method to obtain the exact solutions for the semi-infinite stationary string with nonclassical boundary conditions. Additionally, the authors analyzed reflection and damping properties of the considered boundary conditions. Apart from these,

a lot of research has been done on the dynamic analysis of axially moving strings (see the reference paper [34]). For example, Swope and Ames [42] derived a response for a moving threadline by the methods of d'Alembert and characteristics. Tan and Ying [7] used the transfer function formulation and the wave propagation concept to derive the exact response solution for the translating string with general boundary conditions. Lee and Mote [52] analyzed the energetics of translating continua for fixed, free, and damped boundary conditions. Chen and Ferguson [10] studied the energy dissipation by a viscous damper attached at one end of a moving string.

In contrast to previous research for traveling strings defined on a finite domain, this chapter focuses on the reflection and damping properties of a single boundary of different types. The chapter is organized as follows. Section 4.2 introduces the equations of motion describing the transverse vibrations of an axially moving semi-infinite string and different types of boundary conditions. In Section 4.3, the method of d'Alembert is used to obtain the response to the initial conditions. Additionally, the reflections of waves at different types of boundary supports are analyzed. Next, Section 4.4 presents the total energy and its time-rate of change providing more insight into the stability of the system. Finally, Section 4.5 emphasizes the advantages of the used method for the solution and summarizes the results obtained in Sections 4.3 and 4.4.

4.2 Equations of motion

The transverse equation of motion of the semi-infinite string can be obtained by the application of *Hamilton's principle* (see, for instance, [8, 35, 40]):

$$u_{tt} + 2V u_{xt} + (V^2 - c^2) u_{xx} = 0,$$

where u is the transverse displacement and $c = \sqrt{P/\rho}$ is the wave propagation speed. To avoid the divergence instability [52] in the string and to have a reflection of the incident wave at the boundary, we assume that the transport speed V is less than the critical one, i.e., $|V| < c$. To put the governing equation in a non-dimensional form, we incorporate the following dimensionless quantities:

$$x^* = \frac{x}{L}, \ u^* = \frac{u}{L}, \ t^* = \frac{tc}{L}, \ v^* = \frac{V}{c},$$

where L is a free length. Hence, the non-dimensional equation of transversal motion of the string then reads as

$$u_{tt} + 2v u_{xt} - (1 - v^2) u_{xx} = 0,$$

where the asterisk notations are omitted for convenience. Remark that (4.1a) is defined on $D := (-\infty, 0) \times (0, \infty)$ for the variables (x, t).

Table 4.1 presents a set of boundary conditions which will be considered in the following sections. These conditions can be classified into two general types such as *classical* (fixed and free) and *nonclassical* (spring-dashpot and mass-spring-dashpot) boundary conditions. It should be noted that the nonclassical boundary conditions were also derived by Hamilton's principle [35].

4.3 Reflections at the boundary

In general, the nature of the reflected wave is determined by the nature of the boundary. In this section, we investigate the response to the intial conditions for different types of boundary supports. First, we use the general solution and the method of characteristics to obtain the solution of the Cauchy problem in the form of d'Alembert. Then, we employ the boundary conditions listed in Table 4.1 to obtain an extension of the d'Alembert solution to the full domain of the problem definition.

4.3.1 Solution of the Cauchy problem

Here, we consider the following initial value problem:

$$u_{tt} + 2\nu u_{xt} - (1 - \nu^2) u_{xx} = 0, \tag{4.1a}$$

for $x < 0$, and $t > 0$, subject to the Cauchy initial conditions:

$$\begin{aligned} u(x,0) &= \phi(x), \\ u_t(x,0) &= \psi(x), \end{aligned} \tag{4.1b}$$

for $x < 0$, where $\phi(x) \in C^2((-\infty, 0]; \mathbb{R})$ and $\psi(x) \in C^1((-\infty, 0]; \mathbb{R})$.

Let us introduce the following notations:

$$\lambda_1 := 1 - \nu, \ \lambda_2 := 1 + \nu. \tag{4.2}$$

The general solution of the one-dimensional wave equation is well-known (e.g., [62, 42]). Using the characteristics with speeds λ_1 and λ_2, we write the general solution for the problem (4.1a-4.1b) in the following form:

$$u(x,t) = F(x - \lambda_2 t) + G(x + \lambda_1 t), \tag{4.3}$$

where F and G are two arbitrary, twice differentiable functions. The initial conditions are satisfied if

$$F(x) = \frac{1}{2} \lambda_1 \phi(x) + \frac{1}{2} \int_x^0 \psi(\xi) \, \mathrm{d}\xi + K, \tag{4.4}$$

$$G(x) = \frac{1}{2} \lambda_2 \phi(x) - \frac{1}{2} \int_x^0 \psi(\xi) \, \mathrm{d}\xi - K, \tag{4.5}$$

where K is a constant of integration. The substitution of (4.4) and (4.5) into (4.3) gives the solution of the Cauchy problem (4.1a-4.1b) in the form of d'Alembert:

$$u(x,t) = \frac{1}{2} \left[\lambda_1 \phi(x - \lambda_2 t) + \lambda_2 \phi(x + \lambda_1 t) \right] + \frac{1}{2} \int_{x - \lambda_2 t}^{x + \lambda_1 t} \psi(\xi) \, \mathrm{d}\xi. \tag{4.6}$$
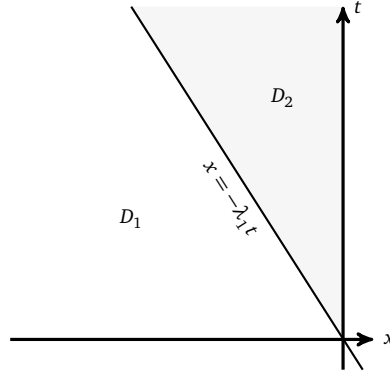
Figure 4.1: Space-time diagram of a characteristic emanating from the boundary.

Recall that the functions ϕ and ψ are defined for negative arguments. From (4.6), one can see that these functions have to be defined not only for negative arguments but also for positive ones. Note that the argument $(x-\lambda_2 t)$ in (4.3) is always negative. That is why we will consider only the characteristic with the speed λ_1. Accordingly, we split the domain D in two subdomains $D_1 = \{(x,t) \in D \,|\, |x| > \lambda_1 t\}$ and $D_2 = \{(x,t) \in D \,|\, |x| < \lambda_1 t\}$ by the characteristic line $x = -\lambda_1 t$ (see Figure 4.1). It is clear that $x - \lambda_2 t < 0$ and $x + \lambda_1 t < 0$ for $(x,t) \in D_1$. Consequently, in the subdomain D_1, the solution for the problems is represented by (4.6). Thus, D_2 is our subdomain of interest further. To find the solution in this subdomain, we will employ the boundary conditions listed in Table 4.1 in the following subsections.

4.3.2 Fixed boundary

A fixed support of the string at $x = 0$ is represented by the homogeneous boundary condition:

$$u(0,t) = 0. \tag{4.7}$$

This is a well-known example of a complete wave reflection, where the incident wave is totally reflected with an opposite sign. This is confirmed by the substitution of the general solution (4.3) into (4.7) giving

$$G(\lambda_1 t) = -F(-\lambda_2 t), \tag{4.8}$$

which implies an odd extension for positive arguments when $v = 0$. Let us introduce the following notation

$$s := \lambda_1 t > 0. \tag{4.9}$$

Now, using (4.4) and (4.8), we obtain the extension of G for positive arguments as follows:

$$G(s) = -\frac{1}{2}\lambda_1 \phi\left(-\frac{\lambda_2}{\lambda_1}s\right) - \frac{1}{2}\int_{-\frac{\lambda_2}{\lambda_1}s}^{0} \psi(\xi)\,\mathrm{d}\xi - K.$$
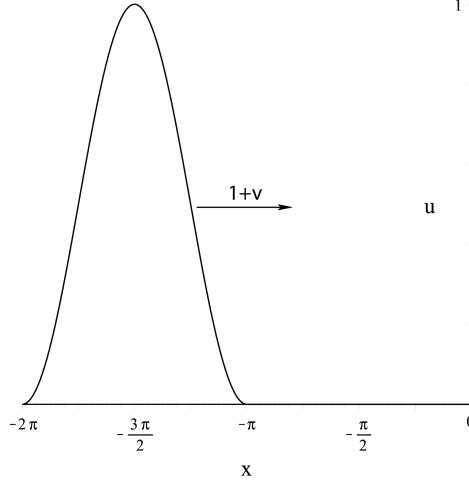
Figure 4.2: Incident wave at initial time $t = 0$.

As a final step, we plug this expression into (4.3) obtaining the solution in D_2 as follows:

$$u(x,t) = \frac{\lambda_1}{2}\left[\phi(x - \lambda_2 t) - \phi\left(-\frac{\lambda_2}{\lambda_1}[x + \lambda_1 t]\right)\right] + \frac{1}{2}\int_{x-\lambda_2 t}^{0} \psi(\xi)\, \mathrm{d}\xi$$

$$-\frac{1}{2}\int_{-\frac{\lambda_2}{\lambda_1}(x+\lambda_1 t)}^{0} \psi(\xi)\, \mathrm{d}\xi. \tag{4.10}$$

Note that the constant of integration K is canceled out. So, the pair of formulas (4.6) and (4.10) give the complete solution for the boundary condition (4.7) in the domain $D_1 \cup D_2$. In order to provide a continuous solution in $D = (-\infty, 0) \times (0, \infty)$, extra *compatibility conditions* for ϕ and ψ have to be introduced:

$$\phi(0) = \psi(0) = 0,$$
$$(1 - v^2)\phi''(0) = 2v\psi'(0). \tag{4.11}$$

Remark that the smoothness and compatibility conditions for the functions ϕ and ψ provide well-posedness of the initial-boundary value problem.

We illustrate the constructed solution (4.10) by considering the initial pulse propagating to the right and incident on a fixed boundary (depicted in Figure 4.2). The incident wave is described by the following initial conditions

$$u(x,0) = \phi(x) := [\mathscr{H}(x + 2\pi) - \mathscr{H}(x + \pi)]\sin^2(x), \tag{4.12}$$
$$u_t(x,0) = \psi(x) := -(1 + v)\phi'(x), \tag{4.13}$$

where $\mathscr{H}$ is the Heaviside step function. Moreover, it can be observed that the functions ϕ and ψ satisfy the compatibility conditions (4.11) providing continuous solution.

(a) (b)

Figure 4.3: Left-propagating reflected wave in the semi-infinite string traveling with (a) positive and (b) negative directions of v at time instants $t = 6$ and $t = 36$, respectively. The lines correspond to $v = \pm 0.2$ (solid), $v = \pm 0.5$ (dash-dot), $v = \pm 0.8$ (dash). The string is *fixed* at its end $x = 0$.

Figure 4.3 shows the reflected waves in the axially moving semi-infinite string with a fixed boundary for (a) positive and (b) negative directions[1] of v at different instants of time $t = 6$ and $t = 36$, respectively. It is clear that the incident wave needs more time to reach the boundary if the axial velocity of the string has an opposite direction and less time otherwise. Remark that the chosen time instants provide complete profiles of the reflected wave. One can also see in Figure 4.3 that the reflected waves have the same amplitudes as the incident wave. Furthermore, the wavelength changes with the change of the transport velocity there. In general, the wavelength is a ratio of a traveling distance to a number of waves in this distance. Particularly in the given example the number of waves equals one, consequently the wavelength is defined only by the traveling distance $x = -\lambda_1 t$, where λ_1 is given by (4.2). That is why the wavelengths in Figure 4.3(b) are bigger than in Figure 4.3(a) with respect to the correspondent velocities, and the relation of the wavelength and velocity is opposite for the opposite directions of v.

4.3.3 Free boundary

Next, we consider the case of a freely supported end of the string at $x = 0$. This case is represented by the homogeneous Neumann boundary condition:

$$u_x(0, t) = 0. \tag{4.14}$$

Remark that the transverse displacements of the reflected and the incident waves must have the same sign in order to satisfy (4.14). Substituting (4.3) into (4.14) yields

$$G'(\lambda_1 t) = -F'(-\lambda_2 t). \tag{4.15}$$

---

[1]The sign of the velocity direction is defind by its direction with respect to the end of the string.
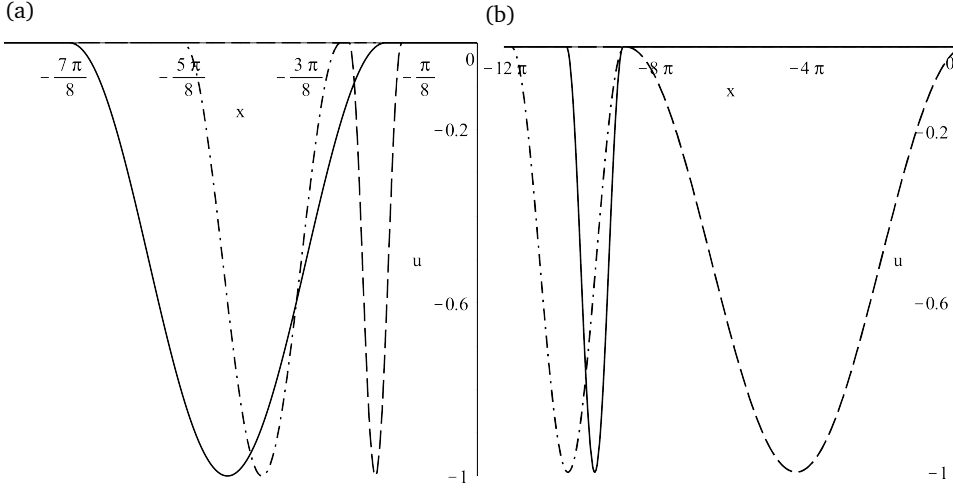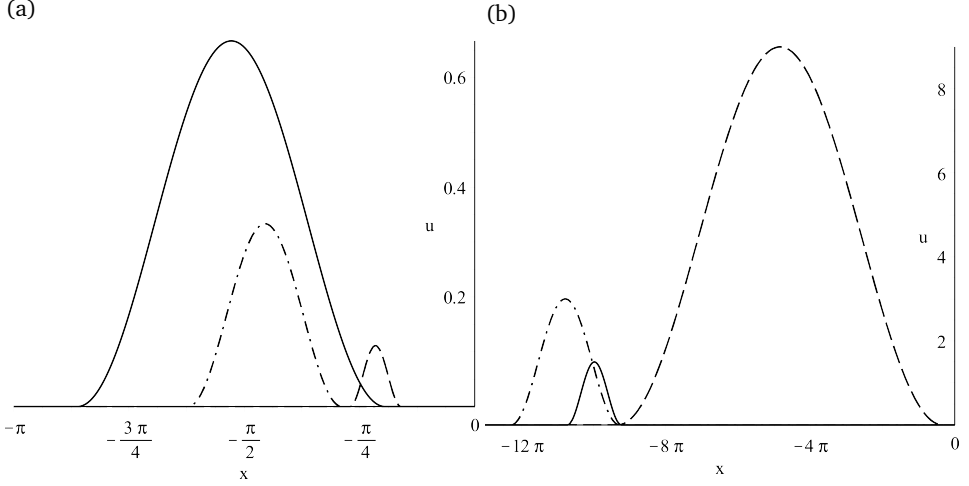
Figure 4.4: Left-propagating reflected wave in the semi-infinite string traveling with (a) positive and (b) negative directions of v at time instants $t = 6$ and $t = 32$, respectively. The lines correspond to $v = \pm 0.2$ (solid), $v = \pm 0.5$ (dash-dot), $v = \pm 0.8$ (dash). The string is *free* at its end.

Integrating (4.15) with respect to s, which is given by (4.9), we have a well-defined function G for positive arguments:

$$G(s) = \frac{1}{2\lambda_2}\left((\lambda_2^2 - \lambda_1^2)\phi(0) + \lambda_1^2 \phi\left(-\frac{\lambda_2}{\lambda_1}s\right) + \lambda_1 \int_{-\frac{\lambda_2}{\lambda_1}s}^{0} \psi(\xi)\,d\xi \right) - K.$$

Hence, the solution for the free boundary condition is given by

$$u(x,t) = \frac{1}{2\lambda_2}\left[(\lambda_2^2 - \lambda_1^2)\phi(0) + \lambda_1\lambda_2\phi(x - \lambda_2 t) + \lambda_1^2 \phi\left(-\frac{\lambda_2}{\lambda_1}[x + \lambda_1 t]\right) \right]$$
$$+ \frac{1}{2}\int_{x - \lambda_2 t}^{0} \psi(\xi)\,d\xi + \frac{\lambda_1}{2\lambda_2}\int_{-\frac{\lambda_2}{\lambda_1}(x + \lambda_1 t)}^{0} \psi(\xi)\,d\xi \qquad (4.16)$$

in D_2.

Thus, formulas (4.6) and (4.16) give a solution of the initial-boundary value problem (4.1a-4.1b), and (4.14) in the domain $D_1 \cup D_2$. In addition, the following compatibility conditions for ϕ and ψ provide a continuous solution in D:

$$\phi'(0) = \phi''(0) = \psi'(0) = 0. \qquad (4.17)$$

Figure 4.4 depicts the reflected waves in the axially moving semi-infinite string with (a) positive and (b) negative directions of v at different times $t = 6$ and $t = 32$, respectively. The initial conditions are again given by (4.12,4.13). Clearly, the reflected waves depicted in Figures 4.4(a) and (b) have the same forms (shapes) as the incident wave (plotted in Figure 4.2). However, in Figure 4.4(a), the amplitude of the reflected wave decreases with the increase of v; in Figure 4.4(b), on the contrary, this characteristic increases when the magnitude of v approaches that of the critical speed ($v = -1$).
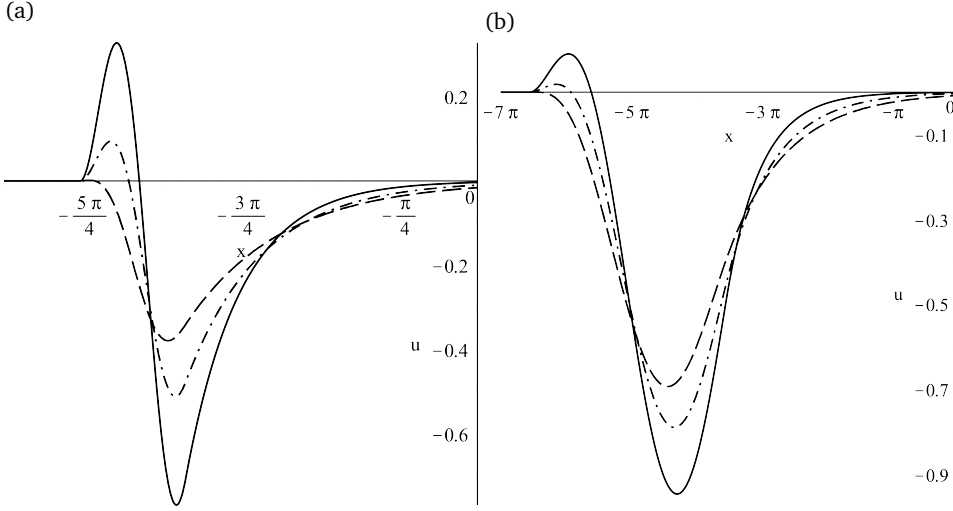
Figure 4.5: Left-propagating reflected wave in the semi-infinite string traveling with (a) $v = 0.5$ and (b) $v = -0.5$ at time instants $t = 10$ and $t = 20$, respectively. The *spring-dashpot* system is attached at the end of the string, where $\kappa = 1$ and $\eta = 0.1$(solid), 0.5(dash-dot), 0.9(dash).

4.3.4 Spring-dashpot boundary

In this subsection, we consider a spring-dashpot system attached to the boundary at $x = 0$. Incorporating the following dimensionless quantities

$$\kappa^* = \frac{\kappa L}{P}, \ \eta^* = \frac{\eta}{\sqrt{\rho P}},$$

the nondimensional boundary condition is given by

$$\kappa u(0, t) + \eta u_t(0, t) = v u_t(0, t) - (1 - v^2) u_x(0, t). \tag{4.18}$$

Let us introduce the following notations for convenience:

$$\alpha := \frac{\lambda_2(\eta - v - \lambda_1)}{\lambda_1(\eta - v + \lambda_2)}, \text{ and } \beta := \frac{k}{\lambda_1(\eta - v + \lambda_2)}. \tag{4.19}$$

Incorporating the spring-dashpot boundary condition (4.18) into (4.3) and by using (4.19), we obtain the following equation

$$G'(s) + \beta G(s) = \alpha F'\left(-\frac{\lambda_2}{\lambda_1}s\right) - \beta F\left(-\frac{\lambda_2}{\lambda_1}s\right).$$

This differential equation can easily be solved by using the *integrating factor* $e^{\beta s}$ yielding

$$G(s) = \exp(-\beta s)\left(G(0) + \frac{\lambda_1}{\lambda_2}\int_{-\frac{\lambda_1}{\lambda_2}s}^{0}\exp\left(-\beta\frac{\lambda_1}{\lambda_2}\xi\right)[\alpha F'(\xi) - \beta F(\xi)]\,d\xi\right)$$

$$= \frac{1}{2\lambda_2}\left[(\lambda_2^2 + \alpha\lambda_1^2)\exp(-\beta s)\phi(0) - \alpha\lambda_1^2\phi\left(-\frac{\lambda_2}{\lambda_1}s\right)\right] - \frac{\lambda_1}{2\lambda_2}\left[\int_{-\frac{\lambda_2}{\lambda_1}s}^{0}\psi(\xi)\,d\xi\right.$$

$$\left. + \beta\left(1 - \alpha\frac{\lambda_1}{\lambda_2}\right)\int_{-\frac{\lambda_2}{\lambda_1}s}^{0}\exp\left(-\beta\left[s + \frac{\lambda_1}{\lambda_2}\xi\right]\right)\left(\lambda_1\phi(\xi) + \int_{\xi}^{0}\psi(\tau)d\tau\right)d\xi\right] - K.$$

The solution in D_2 for the string with an attached spring-dashpot can be obtained from (4.3), and it is given by

$$u(x,t) = \frac{1}{2\lambda_2}\left[(\lambda_2^2 + \alpha\lambda_1^2)\exp(-\beta[x + \lambda_1 t])\phi(0) - \alpha\lambda_1^2\phi\left(-\frac{\lambda_2}{\lambda_1}[x + \lambda_1 t]\right) + \lambda_1\lambda_2\right.$$

$$\left. \times \phi(x - \lambda_2 t)\right] + \frac{\beta\lambda_1}{2\lambda_2}\left(\alpha\frac{\lambda_1}{\lambda_2} - 1\right)\int_{-\frac{\lambda_2}{\lambda_1}(x+\lambda_1 t)}^{0}\exp\left(-\beta\left[x + \lambda_1 t + \frac{\lambda_1}{\lambda_2}\xi\right]\right)\left(\lambda_1\phi(\xi)\right.$$

$$\left. + \int_{\xi}^{0}\psi(\tau)d\tau\right)d\xi + \frac{1}{2}\int_{x-\lambda_2 t}^{0}\psi(\xi)\,d\xi - \frac{\alpha\lambda_1}{2\lambda_2}\int_{-\frac{\lambda_2}{\lambda_1}(x+\lambda_1 t)}^{0}\psi(\xi)\,d\xi. \qquad (4.20)$$

So, the formulas (4.6) and (4.20) represent the solution of the initial-boundary value problem (4.1a-4.1b), and (4.18) in the domain $D_1 \cup D_2$. The following compatibility conditions for ϕ and ψ provide a continuous solution in D:

$$(1 - v^2)\phi'(0) + k\phi(0) = (v - \eta)\psi(0),$$
$$(v - \eta)(1 - v^2)\phi''(0) = [1 - v^2 + 2v(v - \eta)]\psi'(0) + k\psi(0).$$

Figure 4.5 illustrates the reflected waves in the axially moving semi-infinite string with (a) $v = 0.5$ and (b) $v = -0.5$ at different instants of time $t = 10$ and $t = 20$, respectively. The spring-dashpot system has the following parameters $\kappa = 1$ and $\eta = 0.1, 0.5, 0.9$. The initial conditions are again given by (4.12,4.13). One can see that the amplitude of the reflected wave decreases more in the case when v is positive for increasing values of η. In case (b), the length of the reflected wave considerably increases compared to the incident wave. Apparently, the wave-form distortion is created by the spring-dashpot attached to the boundary.

4.3.5 Mass-spring-dashpot boundary

Starting first with the dimensionalization of the last boundary condition in Table 4.1, we incorporate the following dimensionless quantities

$$m^* = \frac{m}{\rho L}, \ \kappa^* = \frac{\kappa L}{P}, \ \eta^* = \frac{\eta}{\sqrt{\rho P}}.$$

Hence, the dimensionless boundary condition for the mass-spring-dashpot case is given by

$$mu_{tt}(0,t) + \kappa u(0,t) + \eta u_t(0,t) = vu_t(0,t) - (1-v^2)u_x(0,t), \tag{4.21}$$

where the asterisk is omitted again for convenience. To continue with the solution, it is convenient to introduce the following notations

$$\zeta^2 := \frac{(1+\eta)^2}{4m\kappa}, \quad \omega^2 := \frac{\kappa}{m(1-v)^2}, \tag{4.22}$$

$$R(s) := \frac{1}{\lambda_1^2}\left(-\lambda_2^2 F''(s) + \frac{(\eta-1)\lambda_2}{m}F'(s) - \frac{\kappa}{m}F(s)\right). \tag{4.23}$$

With the new notations (4.22) and (4.23), we plug (4.3) into (4.21) and obtain the following equation for G to solve:

$$G''(s) + 2\zeta\omega G'(s) + \omega^2 G(s) = R\left(-\frac{\lambda_2}{\lambda_1}s\right), \tag{4.24}$$

where G has to satisfy the conditions obtained from (4.5):

$$G(0) = \frac{1}{2}\phi(0) - K, \quad G'(0) = \frac{1}{2}\phi'(0) + \frac{1}{2}\psi(0). \tag{4.25}$$

The differential equation (4.24) can be readily solved by the method of variation of parameters (for details see [53, 62]). The corresponding characteristic equation for (4.24) is given by

$$\mu^2 + 2\zeta\omega\mu + \omega^2 = 0, \tag{4.26}$$

from where three cases follow as:

$$\mu_j = \begin{cases} \omega(-\zeta \pm \sqrt{\zeta^2-1}) & \text{if } \zeta > 1, \\ -\omega\zeta & \text{if } \zeta = 1, \\ \omega(-\zeta \pm i\sqrt{1-\zeta^2}) & \text{if } \zeta < 1, \end{cases}$$

where $j = 1, 2$, corresponding to *over-damping*, *critical damping*, and *under-damping* of the system, respectively. Before considering these three cases, it should be remarked that the functions ϕ and ψ have to satisfy the following compatibility condition

$$m(1-v^2)\phi''(0) + (1-v^2)\phi'(0) + k\phi(0) = 2mv\psi'(0) + (v-\eta)\psi(0),$$

in order to provide a continuous solution in D.

Overdamped system

For the case when the damping ratio $\zeta > 1$, the characteristic equation (4.26) has two linearly independent real-valued roots $\mu_{1,2} = \omega(-\zeta \pm \sqrt{\zeta^2-1})$. By using these roots and the method of variation of parameters, we obtain the following solution

$$G(s) = C_1 e^{\mu_1 s} + C_2 e^{\mu_2 s} + \frac{\lambda_1}{\lambda_2}\frac{1}{\mu_2 - \mu_1}\int_{-\frac{\lambda_2}{\lambda_1}s}^{0}\left[\exp\left(\mu_2\left[\frac{\lambda_1}{\lambda_2}\tau + s\right]\right)\right.$$
$$\left. - \exp\left(\mu_1\left[\frac{\lambda_1}{\lambda_2}\tau + s\right]\right)\right]R(\tau)d\tau,$$

(a)

(b)

Figure 4.6: The *overdamped* reflected wave propagating in the semi-infinite string that travels with (a) $v = 0.5$ and (b) $v = -0.5$ at time instants $t = 14$ and $t = 28$, respectively. The *mass-spring-dashpot* system is attached at the end of the string, where $m = 0.9$, $\kappa = 1$, and $\eta = 0.9$(solid), 1.5(dash-dot), 2.1(dash), respectively.

where C_1 and C_2 follow from (4.25):

$$C_1 = \frac{\psi(0) + \psi'(0) - \mu_2 \phi(0) + 2K\mu_2}{2(\mu_1 - \mu_2)},$$

$$C_2 = \frac{\psi(0) + \psi'(0) - \mu_1 \phi(0) + 2K\mu_1}{2(\mu_1 - \mu_2)}.$$

Thus, we obtained the extension of the function G for positive arguments. Now, the solution for the overdamped system in D_2 can be found from (4.3). However, the final analytical expression has a cumbersome representation. That is why we present here only numerical results which are depicted in Figure 4.6. It should be noted that in the following two cases (critically damped and underdamped), the final analytical expressions for the transverse displacements in D_2 of the string will be also omitted because of the same reason. So, Figure 4.6 shows the reflected waves in the semi-infinite string traveling with (a) $v = 0.5$ and (b) $v = -0.5$ at times $t = 14$ and $t = 28$, respectively. The mass-spring-dashpot system has the following parameter values $m = 0.9$, $\kappa = 1$, and $\eta = 0.9$, 1.5, 2.1. The initial pulse is depicted in Figure 4.2.

Critically damped system

In this case, when $\zeta = 1$, we have one repeated real root $\mu_1 = \mu_2 = -\omega\zeta$. Hence, the solution of (4.24) follows as

$$G(s) = (C_3 + C_4 s)e^{-\zeta\omega s} + \frac{\lambda_1}{\lambda_2} \int_{-\frac{\lambda_2}{\lambda_1}s}^{0} \left(\frac{\lambda_1}{\lambda_2}\tau + s\right) \exp\left(-\zeta\omega\left[\frac{\lambda_1}{\lambda_2}\tau + s\right]\right) R(\tau)d\tau, \quad (4.27)$$
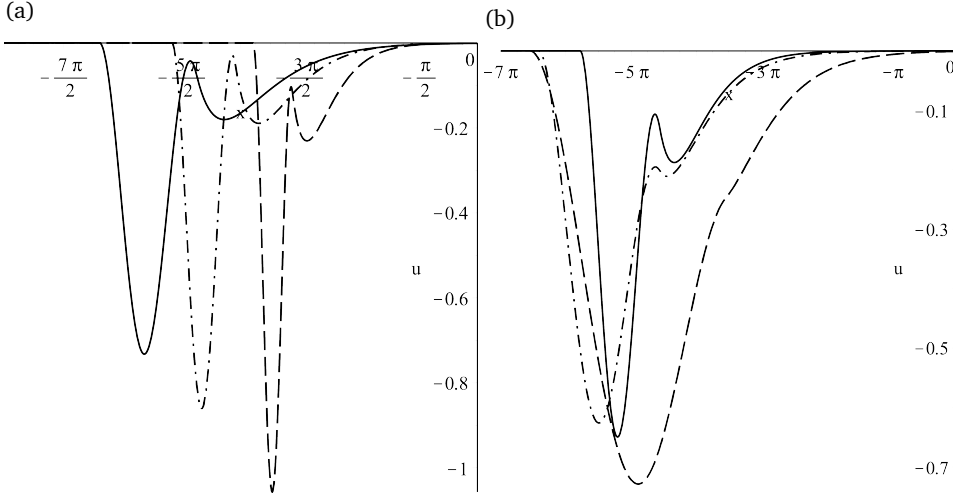
Figure 4.7: The *critically damped* reflected wave propagating in the semi-infinite string that travels with (a) positive and (b) negative directions of v at time instants $t = 16$ and $t = 28$, respectively. The lines correspond to $v = \pm 0.1$ (solid), $v = \pm 0.3$ (dash-dot), $v = \pm 0.5$ (dash). The mass-spring-dashpot system is attached at the end of the string, where $m = 1$, $\kappa = 1$, and $\eta = 1$.

where, from (4.25),

$$C_3 = \frac{1}{2}\phi(0) - K,$$

$$C_4 = \frac{1}{4}\phi(0) + \frac{1}{2}\psi(0) + \frac{1}{2}\psi'(0) - \zeta\omega K.$$

Figure 4.7 represents the reflected waves in the semi-infinite string traveling with (a) positive and (b) negative directions of v at times $t = 16$ and $t = 28$, respectively. The mass-spring-dashpot system has the following parameter values $m = 1$, $\kappa = 1$, and $\eta = 1$. The initial conditions are given by (4.12) and (4.13).

Underdamped system

When $\zeta < 1$, the roots of (4.26) are a complex conjugate pair $\mu_{1,2} = \omega(-\zeta \pm i\sqrt{1-\zeta^2})$. The solution of (4.24) is obtained as follows:

$$G(s) = e^{-\zeta\omega s}\left[C_5\cos(\omega\sqrt{1-\zeta^2}s) + C_6\sin(\omega\sqrt{1-\zeta^2}s)\right] + \frac{\lambda_1}{\lambda_2}\frac{1}{\omega\sqrt{1-\zeta^2}}$$

$$\times \int_{-\frac{\lambda_2}{\lambda_1}s}^{0} \exp\left(-\zeta\omega\left[\frac{\lambda_1}{\lambda_2}\tau + s\right]\right)\sin\left(\omega\sqrt{1-\zeta^2}\left[\frac{\lambda_1}{\lambda_2}\tau + s\right]\right)R(\tau)\mathrm{d}\tau,$$

where

$$C_5 = \frac{1}{2}\phi(0) - K, \text{ and } C_6 = \frac{\psi'(0) + \psi(0) + \zeta\omega\phi(0) - 4\zeta\omega K}{2\omega\sqrt{1-\zeta^2}}.$$
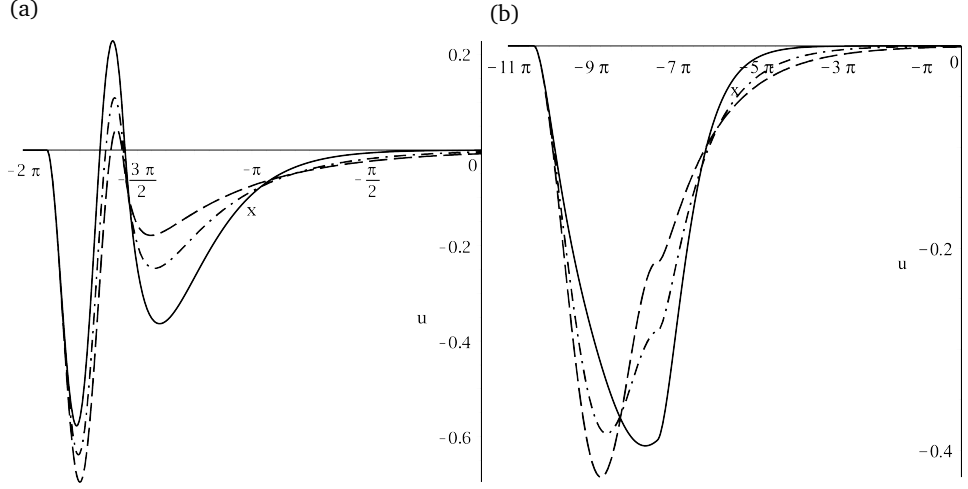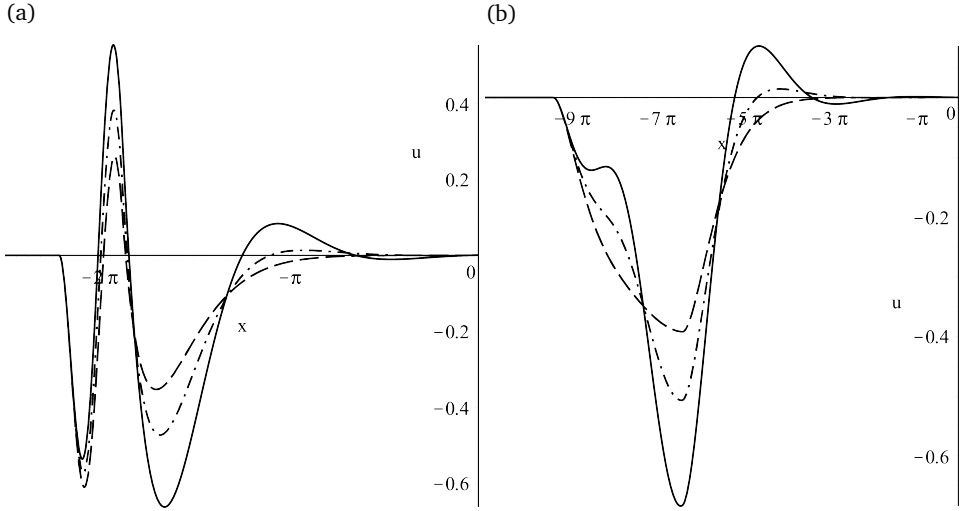
Figure 4.8: The *underdamped* reflected wave propagating in the semi-infinite string that travels with (a) $v = 0.5$ and (b) $v = -0.5$ at time instants $t = 16$ and $t = 26$, respectively. The mass-spring-dashpot system is attached at the end of the string, where $m = 1$, $\kappa = 1$, and $\eta = 0.1$(solid), 0.5(dash-dot), 0.9(dash), respectively.

In Figure 4.8, the reflected waves in the string traveling with (a) $v = 0.5$ and (b) $v = -0.5$ are given at times $t = 16$ and $t = 26$, respectively. The mass-spring-dashpot system has the following parameter values $m = 1$, $\kappa = 1$, and $\eta = 0.1$, 0.5, 0.9. The initial conditions are the same as before and are given by (4.12,4.13).

To sum the considered cases up, the reflected waves illustrated in Figures 4.6, 4.7, and 4.8 have relatively the same behavior. For case (b), where v is negative, the amplitudes of these waves are slightly smaller than the ones in case (a). However, their lengths are considerably bigger for negative v compared to a positive one. Lastly, the incident wave experiences quite similar distortions in all three cases created by the mass-spring-dashpot during the reflection process.

4.4   Energy and its rate of change

In this section, we analyze the total mechanical energy of the semi-infinite string for the different types of boundary conditions as presented in Table 4.1. In the following subsections, the expressions for the rate of change of energy provide information whether the energy grows or decays.

Figure 4.9: The total mechanical energy of the semi-infinite string traveling with (a) positive and (b) negative directions of v. The lines correspond to $v = \pm 0.2$ (solid), $v = \pm 0.5$ (dash-dot), $v = \pm 0.8$ (dash). The string is *fixed* at its end at $x = 0$.

4.4.1 Fixed boundary

The total mechanical energy of the semi-infinite string with a fixed end consists of the kinetic and potential energy densities in the following way (see, e.g., [35, 52, 65, 66]):

$$E(t) = \frac{1}{2} \int_{-\infty}^{0} \left[(u_t + v u_x)^2 + u_x^2 \right] \mathrm{d}x. \tag{4.28}$$

Note that the energy is given in a dimensionless form. It is also well-known that this energy of the semi-infinite string system can be obtained by multiplying the governing equation (4.1a) by the velocity $u_t + v u_x$, and then by integrating the so-obtained equation with respect to x from $-\infty$ to 0, and by integrating with respect to t. The time-rate of change of the energy results from differentiating (4.28) with respect to time t and by using the boundary condition (4.7):

$$\frac{\mathrm{d}E(t)}{\mathrm{d}t} = \frac{v}{2}(1 - v^2)u_x^2(0, t). \tag{4.29}$$

Here, one can see that the energy increases for $v > 0$, and decays if the velocity is negative. These observations can be numerically confirmed using (4.6), (4.10), (4.12,4.13) and the following expression, obtained after integration of (4.29),

$$E(t) = E(0) + \frac{v}{2}(1 - v^2) \int_0^t u_x^2(0, s)\mathrm{d}s.$$

Thus, the total energy of the semi-infinite string, which is fixed at its end, traveling with (a) positive and (b) negative v is shown in Figure 4.9. One can observe that the
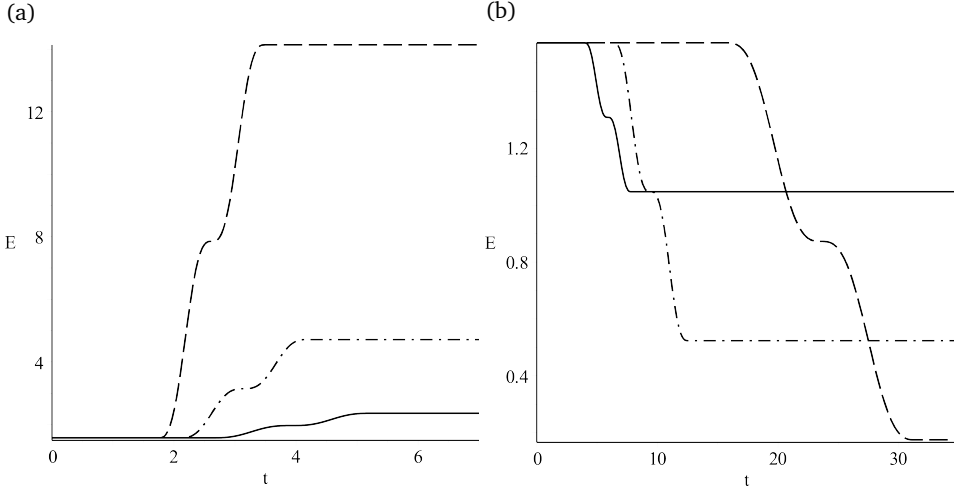
(a)   (b)
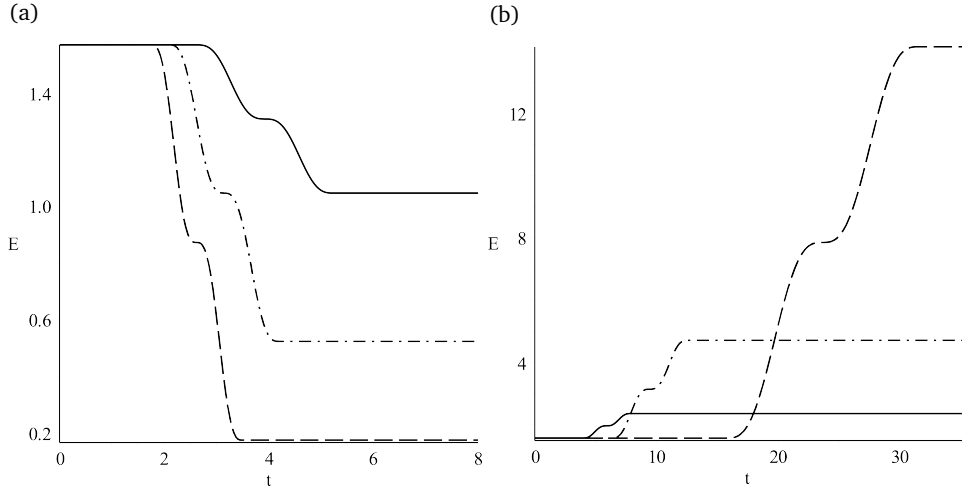
Figure 4.10: The total mechanical energy of the semi-infinite string traveling with (a) positive and (b) negative directions of v. The lines correspond to $v = \pm 0.2$ (solid), $v = \pm 0.5$ (dash-dot), $v = \pm 0.8$ (dash). The string is *free* at its end at $x = 0$.

total energy and its rate of change grow with time as the axial velocity increases in case (a), and they decrease in case (b) for increasing absolute value of the axial velocity with negative direction.

4.4.2 Free boundary

Likewise in the case of a fixed boundary support, the total mechanical energy of the semi-infinite string with a free end is described by (4.28). Using (4.14) and (4.28), we can write the rate of change of energy in the following way:

$$\frac{\mathrm{d}E(t)}{\mathrm{d}t} = -\frac{v}{2}u_t^2(0, t).$$

From where it can be seen straightforwardly that the energy decays for a positive velocity and grows otherwise. To illustrate this we plot the following analytical expression (using again the initial values (4.12) and (4.13)):

$$E(t) = E(0) - \frac{v}{2}\int_0^t u_s^2(0, s)\mathrm{d}s.$$

   In Figure 4.10, the total energy of the semi-infinite string is given, which is free at its end, traveling with (a) positive and (b) negative v. Here, the conclusions for the total energy behavior are opposite to the ones drawn for the fixed support, i.e., the energy decays in case (a) and it grows in case (b). However, the time-rate of change of energy behaves similar as for the case with a fixed boundary.

Figure 4.11: The total mechanical energy of the semi-infinite string traveling with (a) $v = 0.5$ and (b) $v = -0.5$. The *spring-dashpot* system is attached at the end of the string at $x = 0$, where $\kappa = 1$ and $\eta = 0.1$(solid), 0.5(dash-dot), 0.9(dash), respectively.

4.4.3 Spring-dashpot boundary

When the spring-dashpot system is attached to the boundary, we have an additional contribution of potential energy of the spring to the total energy (4.28) of the string:

$$E(t) = \frac{1}{2} \int_{-\infty}^{0} \left[(u_t + v u_x)^2 + u_x^2 \right] dx + \frac{1}{2} \kappa u^2(0, t). \tag{4.30}$$

Proceeding in the same way as in the first two cases, that is, by differentiating (4.30) and by using the boundary condition (4.18), we obtain the following rate of change of energy

$$\frac{dE(t)}{dt} = \frac{v}{2}(1 - v^2) u_x^2(0, t) + \left(\frac{v}{2} - \eta \right) u_t^2(0, t). \tag{4.31}$$

It can be noticed that if v is negative, then the energy decays. Otherwise, the energy behavior depends on the relation between v and η. These conclusions are confirmed in Figure 4.11 by using the initial conditions (4.12) and (4.13), and by using the following expression for the total energy:

$$E(t) = E(0) + \int_0^t \left[\frac{v}{2}(1 - v^2) u_x^2(0, s) + \left(\frac{v}{2} - \eta \right) u_s^2(0, s) \right] ds.$$

4.4.4 Mass-spring-dashpot boundary

Compared to the previous case, we have an extra contribution of the attached mass to the boundary at $x = 0$. Hence, to describe the total mechanical energy of the string

72

Figure 4.12: The *overdamped* system. The total mechanical energy of the semi-infinite string traveling with (a) $v = 0.5$ and (b) $v = -0.5$. The *mass-spring-dashpot* system is attached at the end of the string at $x = 0$, where $m = 0.9$, $\kappa = 1$, and $\eta = 0.9$(solid), 1.6(dash-dot), 2.1(dash), respectively.
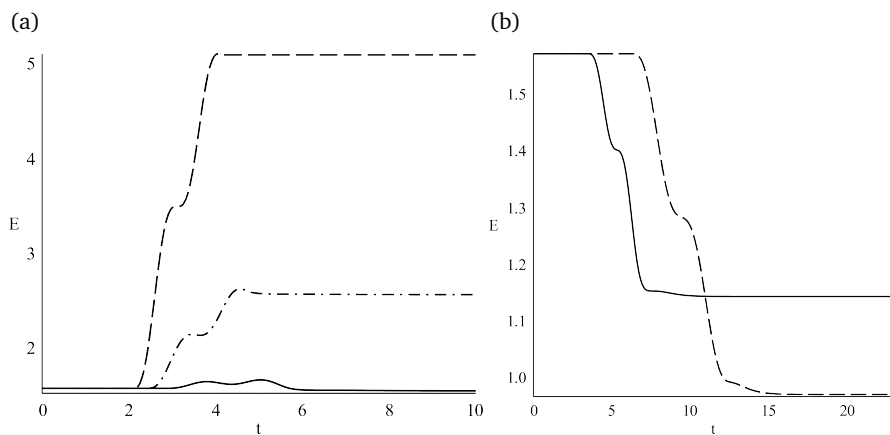
Figure 4.13: The *critically damped* system. The total mechanical energy of the semi-infinite string traveling with (a) positive and (b) negative directions of v. The lines correspond to $v = \pm 0.1$ (solid), $v = \pm 0.3$ (dash-dot), $v = \pm 0.5$ (dash). The *mass-spring-dashpot* system is attached at the end of the string at $x = 0$, where $m = 1$, $\kappa = 1$, and $\eta = 1$.
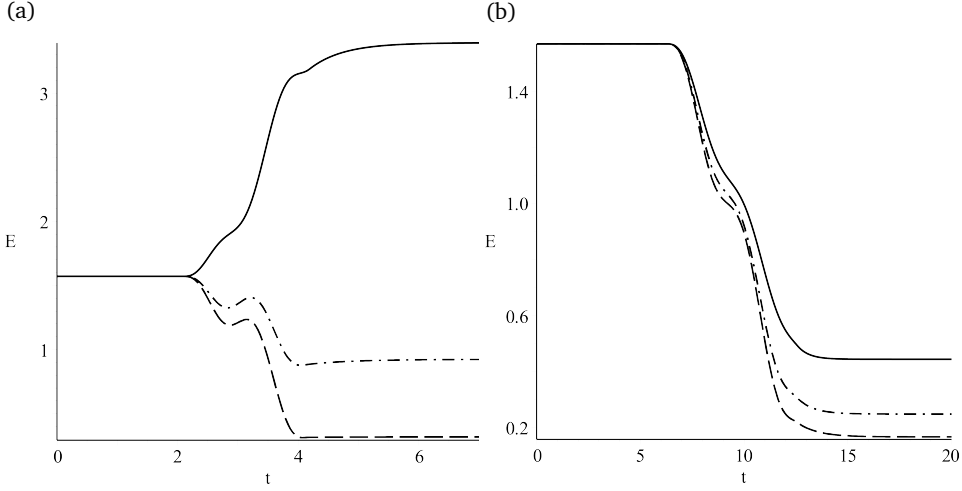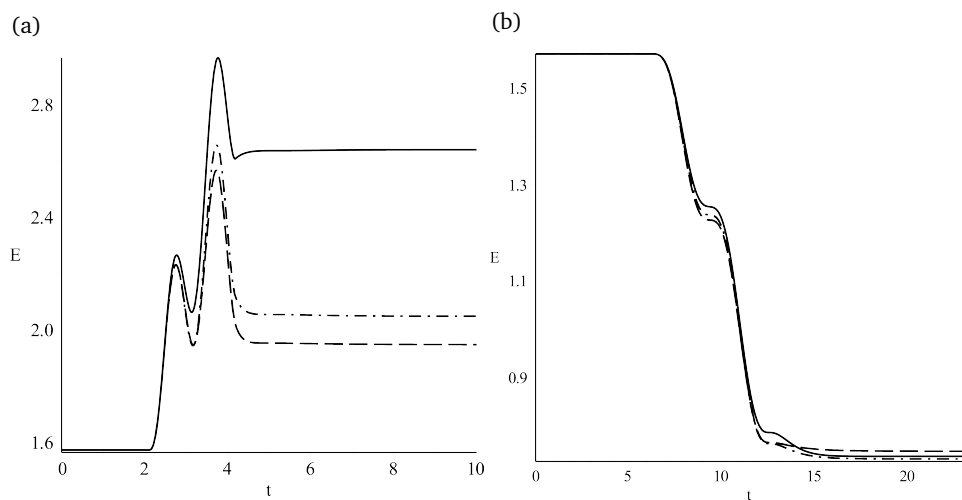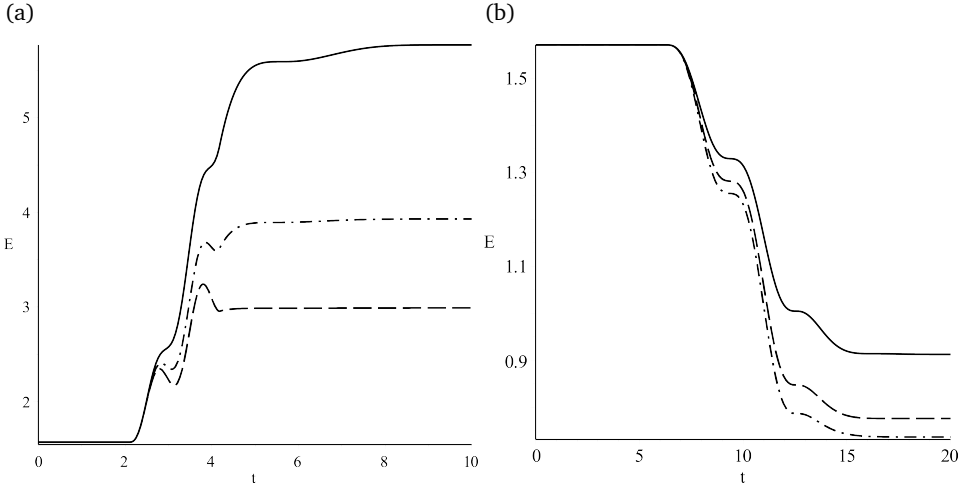
Figure 4.14: The *underdamped* system. The total mechanical energy of the semi-infinite string traveling with (a) $v = 0.5$ and (b) $v = -0.5$. The *mass-spring-dashpot* system is attached at the end of the string at $x = 0$, where $m = 1$, $\kappa = 1$, and $\eta = 0.1$(solid), 0.5(dash-dot), 0.9(dash), respectively.

with the attached mass to the spring-dashpot system, we add the kinetic energy of this mass to (4.30), yielding

$$E(t) = \frac{1}{2}\int_{-\infty}^{0}\left[(u_t + vu_x)^2 + u_x^2\right]dx + \frac{1}{2}\kappa u^2(0,t) + \frac{1}{2}mu_t^2(0,t). \qquad (4.32)$$

By differentiating (4.32) with respect to time t and using (4.21), we find the same expression for the time-rate of change of the total energy as for the massless spring-dashpot system given by (4.31). Figures 4.12-4.14 show the total energy of the semi-infinite string traveling with (a) positive and (b) negative axial velocity v for the overdamped, critically damped, and underdamped cases, respectively. These figures are similar. The rate of increase or decrease in the energy varies depending on the magnitudes of v and η.

4.5 Conclusions

The exact response to initial conditions of a semi-infinite traveling string for different types of boundary conditions is analytically obtained by using the method of d'Alembert. This work can be extended to real life problems of "finite length". By knowing how much energy is transferred at each boundary, one can estimate the total vibratory energy of the whole studied system and so its stability. It should be also mentioned that the obtained analytical results were verified by a slightly different approach based on the freedom of choice of the initial displacement and velocity in D_2 in Figure 4.1 (for details see [53]).

We chose the method of d'Alembert due to its simplicity and elegancy. Particularly, being based on the concept of wave propagation, this method allows an easier physical

interpretation. Moreover, it does not require the information on the frequency spectrum and eigenfunctions. Last but not least, this approach is well suitable not only for classical boundary conditions but also for nonclassical ones.

The total energy and its time-rate of change are derived analytically. The numerical results indicate the importance of the placement of a damper depending on the direction of the transport velocity. In particular, fixed and free boundary conditions have opposite contribution to the total energies, although their rates of change behave similarly. As a result, the string should be simply supported in the upstream region and freely supported in the downstream region. Next, a spring-dashpot system can be efficiently attached to the boundary in both downstream and upstream regions. More precisely, the total energy decreases more in the upstream region than in the downstream one, but the rate of change of the energy in case (a) is faster. Additionally, there is a possibility of growth of energy in the downstream case if $v/2 > \eta$. Lastly, if the mass-spring-dashpot system is attached to the end of the string, we distinguish between overdamped, critically damped, and underdamped systems depending on the relations among the system parameters (m, κ, and η). In all of three cases the mass-spring-dashpot should be placed in the upstream region due to the energy decay there.

Chapter 5

Lateral oscillations of a vertically translating string with small time-harmonic length variation

In this chapter, the free transverse vibrations of a vertically moving string with a harmonically time-varying length are studied. The string length variations are assumed to be small. By using the multiple-timescales perturbation method in combination with a Fourier series approach, we determine the resonance frequencies and derive an infinite dimensional system of coupled ordinary differential equations. This system describes the long time behavior of the amplitudes of the oscillations. Then, the eigenvalues of the obtained system are studied by the truncation method, and the applicability of this method is discussed. The dynamic stability of the solution is investigated by an energy analysis. Additionally, resonance detuning is considered.
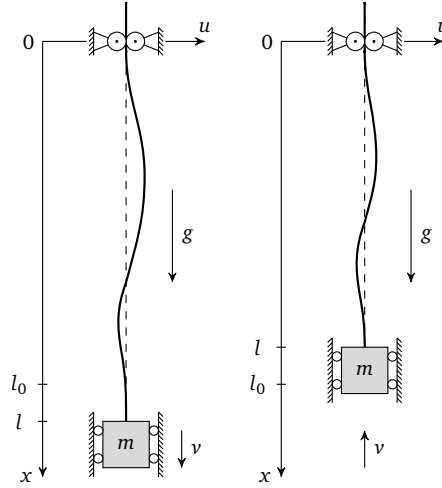
Figure 5.1: Schematics of an extended (a) or retracted (b) cable with an attached mass at $x = l(t)$.

5.1 Introduction

In practice, the gravitational force acting upon a horizontally traveling string is sufficiently small in comparison to its tension force. That is why gravitational effects have reasonably been neglected in the previous chapters. For vertically moving systems, however, gravity plays a role that cannot be ignored. In this chapter, a vertically traveling string with a time-varying length is considered. A rigid body of mass m is attached at the lower end of the cable. The string length fluctuates about a constant mean length l_0 as follows $l(t) = l_0 + \beta \sin(\Omega t)$, where $\beta = \varepsilon \beta_0$ is the length variation parameter and Ω is the angular frequency of the length variation. This system can be regarded as a toy model for elevator cable dynamics with an attached elevator car. A schematic model of this system is illustrated in Figure 5.1, where a positive or negative transport velocity determines the extension (a) or the retraction (b) of the cable, respectively. The main objective of this chapter is to study the dynamic stability of the string oscillations when the frequency of length fluctuation Ω coincides with one of the string's natural frequencies resulting in resonance.

It is worth mentioning that similar problems investigating dynamics of the translating media with varying length or/and velocity have been studied by many researchers. For example, Yamamoto et al. [54] provided a theoretical analysis of free and forced vibrations of a string with time varying length by a power series expansion of the solution. The solution showed agreement with the experimental analysis for the forced vibration. Cooper [24] studied the behavior of the solution for the vibrating string with a moving boundary. Zhu and Ni [56] investigated energetics and stability of translating beam and string models with an arbitrarily varying length. Then Zhu et al. [57] presented the general control laws for the same type of problems in order to dissipate vibratory en-

ergies of translating beams and strings. Some works have been performed particularly for the investigation of the elevator cable dynamics and control (see, e.g., [55, 58, 59, 60]). Kaczmarczyk and Ostachowicz derived a mathematical model [49] and presented a simulation [50] of the transient vibration phenomena in deep mine hoisting cables. Chen and Yang [32] investigated the stability of axially accelerating viscoelastic beams by the method of multiple scales. Sandilo and van Horssen [46] constructed formal asymptotic approximations of the vibrations of a vertical string with changing linearly in time length. The same authors also studied autoresonance phenomena [45] in a similar type of problem with harmonic excitation at the top end. The interior layer analysis provided three timescales for the construction of the asymptotic approximations of the transversal vibrations. It should be noted that the current work is a continuation of [46] and of the paper by Gaiko and van Horssen [36], where the first resonance frequency was analyzed. Compared to previous research, this work in general proposes an analytical approach for a complete analysis of the dynamics of time-variable distributed gyroscopic systems in resonance.

The rest of the chapter is organized as follows. Section 5.2 introduces the equation of free lateral vibrations of the string with changing length. In Section 5.3, the multiple-timescales perturbation method combined with a Fourier series representation of the solution is used. This approach allows to determine resonance frequencies and to obtain secularity conditions for amplitudes of vibrations. Moreover, detuning of the resonance frequencies is also considered. Section 5.4 proceeds with the truncation of the obtained infinite dimensional system and eigenvalue analysis. Further, in Section 5.5, the rate of change of the energy is derived and some conclusions for resonances and their detuning are drawn. Finally, Section 5.6 summarizes all the results.

5.2   Assumptions and a mathematical model

In order to restrict the complexity of the analysis of the problem, it is necessary to make some assumptions:

- the string is uniform, that is, the linear density ρ is constant;

- bending stiffness is neglected;

- only free lateral vibrations, $u(x, t)$, are considered;

- the ends of the string are fixed in the horizontal direction;

- the mass of the string is small compared to the mass of the rigid body, hence providing "constant" pretension in the string. It is worth mentioning that this assumption limits the coefficients of a corresponding eigenvalue problem to be constant, thus simplifying the analysis of the eigenmodes;

- the axial velocity, $v(t) := \dot{l}(t)$, of the string is smaller than the velocity of the wave propagation, where the overdot denotes time differentiation;

- the axial string acceleration, $\dot{v}(t)$, is much smaller than the gravitational acceleration, g.

The transverse equation of motion of an elevator cable can be derived from Hamilton's principle (see [49, 46]) and it is given by

$$\rho \frac{D^2 u(x,t)}{Dt^2} - \frac{\partial}{\partial x}\left(P(x,t)\frac{\partial u(x,t)}{\partial x}\right) = 0, \tag{5.1}$$

where $\frac{D}{Dt}$ and $\frac{D^2}{Dt^2}$ are the differential operators given by

$$\begin{aligned}
\frac{D}{Dt} &\equiv \frac{\partial}{\partial t} + v\frac{\partial}{\partial x}, \\
\frac{D^2}{Dt^2} &\equiv \frac{\partial^2}{\partial t^2} + 2v\frac{\partial^2}{\partial x \partial t} + v^2\frac{\partial^2}{\partial x^2} + \dot{v}\frac{\partial}{\partial x},
\end{aligned} \tag{5.2}$$

where the over dot notation is the differentiation with respect to t and the axial force is given by

$$P(x,t) = mg + \rho(l-x)g - m\dot{v} - \rho(l-x)\dot{v}, \tag{5.3}$$

arising from the superposition of the lower end mass and the cable's weights and longitudinal accelerations. It is worth noting that the axial force can be tensile or compressive depending on the deceleration ($\dot{v} < 0$) or acceleration ($\dot{v} > 0$), respectively, of the cable. With the notations (5.2) and (5.3), (5.1) can be rewritten in the following form

$$\rho(u_{tt} + 2vu_{xt} + v^2 u_{xx}) + \rho g u_x - (m + \rho[l-x])(g - \dot{v})u_{xx} = 0. \tag{5.4}$$

Note that the subscripts denote partial differentiations. According to the assumptions stated above, we rewrite the equation (5.4) in a nondimensional form by using the following dimensionless parameters

$$x^* = \frac{x}{L}, \; u^* = \frac{u}{L}, \; l^* = \frac{l}{L}, \; \mu^* = \frac{\rho L}{m + \rho L}, \; t^* = t\sqrt{\frac{g}{L\mu^*}}, \; v^* = v\sqrt{\frac{\mu^*}{gL}}. \tag{5.5}$$

As a result, the equation of motion (5.4) takes the following form

$$u_{tt} + 2vu_{xt} + v^2 u_{xx} + \mu u_x - (\mu^{-1} + l - x - 1)(\mu - \dot{v})u_{xx} = 0. \tag{5.6}$$

where the asterisks are omitted for convenience.

5.3 Resonance and secularity conditions

In this section we obtain the non-secularity conditions, describing the long time behavior of the amplitudes of the oscillations. To describe these oscillations, it is convenient to convert the time-varying spatial domain of the problem, $[0, l(t)]$, to a stationary domain. After that we extend all functions to an infinite space domain in accordance with the orthogonality properties. Lastly, by using the two-timescales perturbation method, we find the frequencies which cause resonances in the system, and derive the non-secularity conditions for the amplitudes of the cable vibrations.

5.3.1 Spatial transformation

We consider the following initial-boundary value problem comprised of the governing equation (5.6) subject to the homogeneous[1] Dirichlet boundary conditions with the initial displacement $\phi(x)$ and velocity $\psi(x)$:

$$u_{tt} + 2vu_{xt} + \left(v^2 - [\mu - \dot{v}][\mu^{-1} + l - x - 1]\right)u_{xx} + \mu u_x = 0, \tag{5.7a}$$

for $0 < x < l$ and $t > 0$, subject to the BCs:

$$u(0,t) = u(l,t) = 0, \tag{5.7b}$$

for $t > 0$, with the ICs:

$$\begin{aligned} u(x,0) &= \phi(x), \\ u_t(x,0) &= \psi(x), \end{aligned} \tag{5.7c}$$

for $0 < x < l(0)$.

In order to simplify the integration of (5.7a-5.7c), it is convenient to transform the time-varying spatial domain $[0, l(t)]$ to the fixed one $[0,1]$ by introducing a new independent nondimensional spatial coordinate $\xi = \frac{x}{l(t)}$. As a consequence, some extra changes in the initial-boundary value problem have to be performed. Since the function $u(x,t)$ becomes a new function $\tilde{u}(\xi,t)$, all the partial derivatives have to be transformed in accordance with a new variable ξ as follows:

$$u_x = \frac{1}{l}\tilde{u}_\xi, \; u_{xx} = \frac{1}{l^2}\tilde{u}_{\xi\xi}, \; u_{xt} = \frac{1}{l}\tilde{u}_{\xi t} - \frac{v}{l^2}\xi\tilde{u}_{\xi\xi} - \frac{v}{l^2}\tilde{u}_\xi,$$

$$u_t = \tilde{u}_t - \frac{v}{l}\xi\tilde{u}_\xi, \; u_{tt} = \tilde{u}_{tt} - 2\frac{v}{l}\xi\tilde{u}_{\xi t} + \frac{v^2}{l^2}\xi^2\tilde{u}_{\xi\xi} - \frac{l\dot{v} - 2v^2}{l^2}\xi\tilde{u}_\xi.$$

Substituting these derivatives into (5.7a-5.7c), we obtain the following problem:

$$\tilde{u}_{tt} + \frac{v^2}{l^2}(\xi^2 - 2\xi + 1)\tilde{u}_{\xi\xi} + 2\frac{v}{l}(1 - \xi)\tilde{u}_{\xi t} - (\mu^{-1} + l[1 - \xi] - 1)(\mu - \dot{v})\frac{1}{l^2}\tilde{u}_{\xi\xi}$$

$$+ \frac{1}{l}\left(\mu - \frac{2v^2}{l} - \frac{l\dot{v} - 2v^2}{l}\xi\right)\tilde{u}_\xi = 0, \tag{5.8a}$$

for $0 < \xi < 1$ and $t > 0$, with the BCs:

$$\tilde{u}(0,t) = \tilde{u}(1,t) = 0, \tag{5.8b}$$

---

[1] Remark that in case of the nonhomogeneous boundary conditions of the cable, it is possible to transform them to homogeneous (see [35, 59]).

80

for $t > 0$, with the ICs:

$$\tilde{u}(\xi, 0) = \tilde{\phi}(\xi),$$
$$\tilde{u}_t(\xi, 0) = \tilde{\psi}(\xi) + \frac{v(0)}{l(0)}\xi\tilde{\phi}'(\xi),$$

(5.8c)

for $0 < \xi < 1$, where the prime notation means the differentiation with respect to the argument. Further, we substitute the expression for $l(t)$ into (5.8a-5.8c) and use the assumptions, following from (5.5), that $\mu := \varepsilon\mu_0$ and $v(t)$ are $\mathcal{O}(\varepsilon)$, and $\dot{v}(t)$ is $\mathcal{O}(\varepsilon^2)$. By neglecting the terms higher than $\mathcal{O}(\varepsilon)$, we obtain the following initial-boundary value problem:

$$\tilde{u}_{tt} - \frac{1}{l_0^2}\tilde{u}_{\xi\xi} = \varepsilon\left\{\frac{1}{l_0^2}\left[\mu_0 l_0(1-\xi) - \mu_0 + \beta_0\left(\frac{\Omega^2}{\mu_0} - \frac{2}{l_0}\right)\sin(\Omega t)\right]\tilde{u}_{\xi\xi} - \frac{\mu_0}{l_0}\tilde{u}_\xi \right.$$
$$\left. + \frac{2\beta_0\Omega\cos(\Omega t)}{l_0}(\xi - 1)\tilde{u}_{\xi t}\right\} + \mathcal{O}(\varepsilon^2),$$

(5.9a)

for $0 < \xi < 1$ and $t > 0$, with the BCs:

$$\tilde{u}(0, t) = \tilde{u}(1, t) = 0,$$

(5.9b)

for $t > 0$, with the ICs:

$$\tilde{u}(\xi, 0) = \tilde{\phi}(\xi),$$
$$\tilde{u}_t(\xi, 0) = \tilde{\psi}(\xi) + \varepsilon\frac{\Omega\beta_0}{l_0}\xi\tilde{\phi}'(\xi),$$

(5.9c)

for $0 < \xi < 1$. In accordance with the boundary conditions (5.9b), we will later use the Fourier series approach. Beforehand we need to satisfy the orthogonality properties of the trigonometric functions involved in the series. To do so, we assume that $\tilde{u}$ is odd with respect to $\xi = 0$ and $\xi = 1$, and it is 2-periodic. Additionally, it is convenient to extend the finite domain $[0, 1]$ to infinity. Correspondingly, the initial-boundary value problem (5.9a-5.9c) transforms to an initial value problem. Thus, in the right-hand side of (5.9a) we have in principle three terms that need to be extended in odd and 2-periodic functions in ξ, and there is only one term needed for the extension in the equation for the initial velocity (5.9c). The rest of terms in (5.9a-5.9c) satisfy to the periodicity and additive properties. The extension can be accomplished with the help

of the following 2-periodic functions:

$$h_1(\xi) := \frac{1}{2} - \frac{4}{\pi^2} \sum_{r=1}^{\infty} \frac{\cos([2r-1]\pi\xi)}{(2r-1)^2}, \tag{5.10}$$

$$h_2(\xi) := -\frac{2}{\pi} \sum_{r=1}^{\infty} \frac{\sin(r\pi\xi)}{r}, \tag{5.11}$$

$$h_3(\xi) := \frac{4}{\pi} \sum_{r=1}^{\infty} \frac{\sin([2r-1]\pi\xi)}{2r-1}, \tag{5.12}$$

$$h_4(\xi) := -\frac{2}{\pi} \sum_{r=1}^{\infty} \frac{(-1)^r \sin(r\pi\xi)}{r}. \tag{5.13}$$

Remark that (5.10) is an *even extension* of the function "ξ" which is a factor of $\tilde{u}_{\xi\xi}$; (5.11) is an *odd extension* of the function "$\xi - 1$" which is a factor of $\tilde{u}_{\xi t}$; (5.12) is an *odd extension* of the function "1" which is a factor of $\tilde{u}_{\xi}$; and (5.13) is an *odd extension* of the function "ξ" which is a factor of $\tilde{\phi}'(\xi)$ in the initial velocity. With these Fourier extensions, we arrive at the following initial value problem:

$$\tilde{u}_{tt} - \frac{1}{l_0^2}\tilde{u}_{\xi\xi} = \varepsilon\left\{\frac{1}{l_0^2}\left[\mu_0 l_0(1-h_1(\xi)) - \mu_0 + \beta_0\left(\frac{\Omega^2}{\mu_0} - \frac{2}{l_0}\right)\sin(\Omega t)\right]\tilde{u}_{\xi\xi}\right.$$
$$\left. + \frac{2\beta_0\Omega\cos(\Omega t)}{l_0}h_2(\xi)\tilde{u}_{\xi t} - \frac{\mu_0}{l_0}h_3(\xi)\tilde{u}_{\xi}\right\} + \mathcal{O}(\varepsilon^2), \tag{5.14a}$$

for $\xi \in (-\infty, \infty)$ and $t > 0$, with the ICs:

$$\tilde{u}(\xi, 0) = \tilde{\phi}(\xi),$$
$$\tilde{u}_t(\xi, 0) = \tilde{\psi}(\xi) + \varepsilon\frac{\Omega\beta_0}{l_0}h_4(\xi)\tilde{\phi}'(\xi), \tag{5.14b}$$

for $\xi \in (-\infty, \infty)$.

5.3.2 Two timescales

To construct an approximation for the solution $\tilde{u}(\xi, t)$ of (5.14a,5.14b), we use a two-timescales perturbation method. First of all, let us introduce an extra timescale $\tau = \varepsilon t$. As a consequence, $\tilde{u}(\xi, t)$ becomes a function of ξ, t, and τ, i.e. $\tilde{u}(\xi, t) := w(\xi, t, \tau)$. This new function has to satisfy the following initial value problem:

$$w_{tt} - \frac{1}{l_0^2}w_{\xi\xi} = \varepsilon\left\{\frac{1}{l_0^2}\left[\mu_0 l_0(1-h_1(\xi)) - \mu_0 + \beta_0\left(\frac{\Omega^2}{\mu_0} - \frac{2}{l_0}\right)\sin(\Omega t)\right]w_{\xi\xi}\right.$$
$$\left. - 2w_{t\tau} + \frac{2\beta_0\Omega\cos(\Omega t)}{l_0}h_2(\xi)w_{\xi t} - \frac{\mu_0}{l_0}h_3(\xi)w_{\xi}\right\} + \mathcal{O}(\varepsilon^2), \tag{5.15a}$$

for $\xi \in (-\infty, \infty)$, $t > 0$, and $\tau > 0$ with the ICs:

$$w(\xi, 0, 0) = \tilde{\phi}(\xi),$$

$$w_t(\xi, 0, 0) = \tilde{\psi}(\xi) + \varepsilon\left(\frac{\Omega\beta_0}{l_0}h_4(\xi)\tilde{\phi}'(\xi) - w_\tau(\xi, 0, 0)\right), \tag{5.15b}$$

for $\xi \in (-\infty, \infty)$. Next, we represent w in a Fourier sine series form $w(\xi, t, \tau) = \sum_{n=1}^{\infty} w_n(t, \tau)\sin(n\pi\xi)$ and assume that w_n can be approximated by the formal perturbation expansion $w_{n0}(t, \tau) + \varepsilon w_{n1}(t, \tau) + \mathcal{O}(\varepsilon^2)$. In order to prevent secular terms appearing in the perturbation expansion over the introduced timescales, we proceed with the standard procedure. First, we substitute these expansions into (5.15a); second, we multiply this equation with a fixed eigenfunction, then integrate the so-obtained equation with respect to ξ over the period 2 using the orthogonality of the eigenfunctions; finally, we collect the coefficients of like powers in ε. Thus, we obtain that $w_{k,0}$ should satisfy

$$\frac{\partial^2 w_{k,0}}{\partial t^2} + \frac{k^2\pi^2}{l_0^2}w_{k,0} = 0,$$

which has the well-known solution

$$w_{k,0}(t, \tau) = A_{k,0}(\tau)\cos\left(\frac{k\pi}{l_0}t\right) + B_{k,0}(\tau)\sin\left(\frac{k\pi}{l_0}t\right), \tag{5.16}$$

where $A_{k,0}$ and $B_{k,0}$ are arbitrary functions. To find the equation for $w_{k,1}$, the following orthogonality properties will be useful

$$\int_{-1}^{1} \sin(k\pi\xi)\sin(r\pi\xi)\cos(n\pi\xi)\mathrm{d}\xi = -\frac{1}{2}I_{k+r-n} + \frac{1}{2}I_{r+n-k} + \frac{1}{2}I_{n+k-r},$$

$$\int_{-1}^{1} \sin(n\pi\xi)\cos([2r-1]\pi\xi)\sin(k\pi\xi)\mathrm{d}\xi = \frac{1}{2}I_{2r-1+k-n} + \frac{1}{2}I_{-k+2r-1+n} - \frac{1}{2}I_{n+k-2r+1},$$

$$\int_{-1}^{1} \sin(k\pi\xi)\sin([2r-1]\pi\xi)\cos(n\pi\xi)\mathrm{d}\xi = -\frac{1}{2}I_{k+2r-1-n} + \frac{1}{2}I_{2r-1+n-k} - \frac{1}{2}I_{n+k-2r+1},$$

with $I_j = 1$ for $j = 0$, otherwise $I_j = 0$. Hence, using these integrals and the notations (5.10-5.12), after equating the coefficients of ε, we obtain that $w_{k,1}$ should satisfy

$$\frac{\partial^2 w_{k,1}}{\partial t^2} + \frac{k^2\pi^2}{l_0^2}w_{k,1} = -2\frac{\partial w_{k,0}}{\partial t \partial \tau} - \frac{k^2\pi^2}{l_0^2}\left[\mu_0\left(\frac{l_0}{2} - 1\right) + \beta_0\left(\frac{\Omega^2}{\mu_0} - \frac{2}{l_0}\right)\sin(\Omega t)\right]w_{k,0}$$

$$+ 2\frac{\beta_0}{l_0}\Omega\cos(\Omega t)\left\{\sum_{\substack{n=1 \\ n\neq k}}^{\infty}\frac{n}{n-k}\delta_{r,\pm(n-k)} - \sum_{\substack{n=1 \\ n\neq k}}^{\infty}\frac{n}{n+k}\delta_{r,n+k}\right\}\frac{\partial w_{n0}}{\partial t}$$

$$- 2\frac{\mu_0}{l_0}\left\{\sum_{\substack{n=1 \\ n\neq k}}^{\infty}\frac{nk}{(n-k)^2}\delta_{r,\pm(n-k)} + \sum_{\substack{n=1 \\ n\neq k}}^{\infty}\frac{nk}{(n+k)^2}\delta_{r,n+k}\right\}w_{n0}, \tag{5.17}$$

where $r \in \mathbb{N}$ and $\delta_{i,j}$ is a *Kronecker delta*[2].

Resonance frequency

First of all, it should be noted that $\Omega_s = \frac{s\pi}{l_0}$, where $s \in \mathbb{N}$, causes internal resonance. It is straightforward in the right-hand side of (5.17) that $\frac{k^2\pi^2}{l_0^2}\beta_0\left(\frac{2}{l_0} - \frac{\Omega^2}{\mu_0}\right)\sin(\Omega t)w_{k,0}$ and the last three terms, comprised of the infinite sums, do not lead to secular. The rest of the terms require a more thorough analysis. For this purpose, we substitute (5.16) into (5.17) and use Table 5.1 for the the infinite sums containing terms that might lead to unbounded terms in $w_{k,1}$. Note that "ST" and "NST" stand for secular and nonsecular terms in Table 5.1, respectively.

$\cos(\Omega_s t)\sum\limits_{\substack{n=1 \\ n \neq k}}^{\infty} \dfrac{n}{r}\dfrac{\partial w_{n,0}}{\partial t}$	$r = n - k$	$r = k - n$	$r = n + k$
$n = s + k$	NST	NST	ST
$n = s - k$	NST	ST	ST
$n = -s - k$	ST	NST	NST
$n = -s + k$	ST	ST	ST

Table 5.1: Analysis of the terms in the infinite sums in (5.17) that might lead to secular terms in the function $w_{k,1}$.

Thus, collecting all terms in the right-hand side of (5.17) that might lead to secular terms in the function $w_{k,1}$, we obtain:

$$
\begin{aligned}
\frac{\partial^2 w_{k,1}}{\partial t^2} + \frac{k^2\pi^2}{l_0^2}w_{k,1} = & \; 2\frac{k\pi}{l_0}\left(\frac{dA_{k,0}}{d\tau}\sin\left(\frac{k\pi}{l_0}t\right) - \frac{dB_{k,0}}{d\tau}\cos\left(\frac{k\pi}{l_0}t\right)\right) \\
& - k^2\pi^2\frac{\mu_0}{l_0^2}\left(\frac{l_0}{2} - 1\right)\left(A_{k,0}\cos\left(\frac{k\pi}{l_0}t\right) + B_{k,0}\sin\left(\frac{k\pi}{l_0}t\right)\right) \\
& - \frac{\beta_0\pi^2}{l_0^3}\frac{2k(s+k)^2}{2k+s}\left(A_{s+k,0}\sin\left(\frac{k\pi}{l_0}t\right) - B_{s+k,0}\cos\left(\frac{k\pi}{l_0}t\right)\right) \\
& + \frac{\beta_0\pi^2}{l_0^3}\frac{2k(s-k)^2}{2k-s}\left(A_{k-s,0}\sin\left(\frac{k\pi}{l_0}t\right) - B_{k-s,0}\cos\left(\frac{k\pi}{l_0}t\right)\right) \\
& + \frac{\beta_0\pi^2}{l_0^3}\frac{s+2k}{s-2k}(s-k)^2\left(A_{s-k,0}\sin\left(\frac{k\pi}{l_0}t\right) + B_{s-k,0}\cos\left(\frac{k\pi}{l_0}t\right)\right) \\
& + \text{"NST"}.
\end{aligned}
\tag{5.18}
$$

To avoid secular terms in $w_{k,1}$ it follows from (5.18) that $A_{k,0}(\tau)$ and $B_{k,0}(\tau)$ have to satisfy the following infinite dimensional ($k \in \mathbb{N}$) system of coupled ordinary differential

---

[2]Kronecker delta is a function $\delta(i,j) = 1$ if $i = j$ and 0 otherwise.

equations

$$\frac{dA_{k,0}}{d\tilde{\tau}} = \gamma k B_{k,0} + \frac{(k+s)^2}{2k+s}A_{k+s,0} - \frac{(k-s)^2}{2k-s}A_{k-s,0} + \frac{2k+s}{2k-s}\frac{(k-s)^2}{2k}A_{s-k,0},$$
$$\frac{dB_{k,0}}{d\tilde{\tau}} = -\gamma k A_{k,0} + \frac{(k+s)^2}{2k+s}B_{k+s,0} - \frac{(k-s)^2}{2k-s}B_{k-s,0} - \frac{2k+s}{2k-s}\frac{(k-s)^2}{2k}B_{s-k,0},$$

$$(5.19)$$

where $\tilde{\tau} = \frac{\beta_0\pi}{l_0^2}\tau$ and $\gamma = \frac{\mu_0 l_0(l_0-2)}{4\beta_0}$. It should be noted that the correctness of the obtained system can be checked by investigating the initial value problem (5.14a,5.14b) in characteristic coordinates. Remark that in some cases this approach allows to solve the obtained infinite dimensional system analytically providing the approximate solution for the infinite number of oscillation modes (see [39, 61]).

Resonance detuning

In order to describe the resonance regions more clearly, the frequency detuning is useful to study. Let us consider a small detuning of the resonance frequency $\Omega_d = \Omega_s + \varepsilon\alpha$, where $\Omega_s = \frac{s\pi}{l_0}$ (for $s \in \mathbb{N}$) is the resonant frequency and α is the detuning parameter. We start with the $\mathcal{O}(\varepsilon)$-equation (5.17) for a detuned frequency Ω_d:

$$\frac{\partial^2 w_{k,1}}{\partial t^2} + \frac{k^2\pi^2}{l_0^2}w_{k,1} = -2\frac{\partial w_{k,0}}{\partial t\partial\tau} - \frac{k^2\pi^2}{l_0^2}\mu_0\left(\frac{l_0}{2}-1\right)w_{k,0} + 2\frac{\beta_0}{l_0}\Omega_s\cos(\Omega_d t)$$

$$\times \left\{\sum_{\substack{n=1\\n\neq k}}^{\infty}\frac{n}{n-k}\delta_{r,\pm(n-k)} - \sum_{\substack{n=1\\n\neq k}}^{\infty}\frac{n}{n+k}\delta_{r,n+k}\right\}\frac{\partial w_{n0}}{\partial t} + \text{"NST"}, \quad (5.20)$$

where $\Omega_d t = \Omega_s t + \alpha\tau$. As in the previous subsection, by using the $\mathcal{O}(1)$-solution $w_{k,0}$ and Table 5.1, we collect all terms in the right-hand side of (5.20) that lead to secular terms in $w_{k,1}$. Thus, we obtain the following solvability conditions for the resonance detuning case

$$\frac{dA_{k,0}}{d\tilde{\tau}} = \gamma k B_{k,0} + \cos(\alpha\tau)\left[\frac{(k+s)^2}{2k+s}A_{k+s,0} - \frac{(k-s)^2}{2k-s}A_{k-s,0} + \frac{2k+s}{2k-s}\frac{(k-s)^2}{2k}A_{s-k,0}\right]$$

$$- \sin(\alpha\tau)\left[\frac{(k+s)^2}{2k+s}B_{k+s,0} + \frac{(k-s)^2}{2k-s}B_{k-s,0} + \frac{2k+s}{2k-s}\frac{(k-s)^2}{2k}B_{s-k,0}\right],$$

$$\frac{dB_{k,0}}{d\tilde{\tau}} = -\gamma k A_{k,0} + \cos(\alpha\tau)\left[\frac{(k+s)^2}{2k+s}B_{k+s,0} - \frac{(k-s)^2}{2k-s}B_{k-s,0} - \frac{2k+s}{2k-s}\frac{(k-s)^2}{2k}B_{s-k,0}\right]$$

$$+ \sin(\alpha\tau)\left[\frac{(k+s)^2}{2k+s}A_{k+s,0} + \frac{(k-s)^2}{2k-s}A_{k-s,0} - \frac{2k+s}{2k-s}\frac{(k-s)^2}{2k}A_{s-k,0}\right],$$

$$(5.21)$$

where $\tilde{\tau} = \frac{\beta_0\pi}{l_0^2}\tau$ and $\gamma = \frac{\mu_0 l_0(l_0-2)}{4\beta_0}$. One can see that if $\alpha = 0$, then system (5.21) equals (5.19).

5.4   Truncation and eigenvalue analysis

The Galerkin method is a traditional approach in engineering to deal with infinite dimensional systems. By using this method we compute here the approximate eigenvalues of system (5.19), given in Tables 5.2-5.6, up to a certain number of oscillation modes. In some cases these eigenvalues can give some information about the stability of the problem.

First of all, from Tables 5.2-5.4 one can see that the eigenvalues constructed up to the first ten vibration modes are purely imaginary. This means that the solution of the truncated system is bounded for the first three resonance frequencies, Ω_1, Ω_2, and Ω_3, on a timescale of $\mathcal{O}(\varepsilon^{-1})$. As a confirmation, it can be additionally observed for Ω_1 and Ω_2 that the constant matrix of the truncated system,

$$\begin{cases} \dot{A}_{k,0} & = \gamma k B_{k,0} + \dfrac{(k+s)^2}{2k+s} A_{k+s,0} - \dfrac{(k-s)^2}{2k-s} A_{k-s,0}, \\ \dot{B}_{k,0} & = -\gamma k A_{k,0} + \dfrac{(k+s)^2}{2k+s} B_{k+s,0} - \dfrac{(k-s)^2}{2k-s} B_{k-s,0}, \end{cases} \tag{5.22}$$

where the overdot notation stands for the differentiation with respect to $\tilde{\tau}$, is similar to a *skew-symmetric* matrix. To prove that, we turn to some basic theorems from linear algebra. To begin with, let us denote the truncated square matrix of size $2n$ by $\mathbf{X}$, where n is a number of oscillation modes. In addition, we define another $2n$-square matrix $\mathbf{Y}$ which is *similar*[3] to $\mathbf{X}$. By using *mathematical induction* for a given n it can be shown that there always exists such a non-singular matrix $\mathbf{P}$ that transforms the matrix $\mathbf{X}$ to a similar skew-symmetric matrix $\mathbf{Y}$ in the scope of our problem. For an illustrative example on the construction of a skew-symmetric matrix for three modes of oscillations (i.e., for $n = 3$), the reader is referred to Appendix A. Furthermore, it is well-known that *the eigenvalues of a skew-symmetric matrix are purely imaginary or zero*. The latter and the fact that similar matrices have equal eigenvalues prove that the eigenvalues of the matrix $\mathbf{X}$ are purely imaginary or zero too. Tables 5.2-5.4 confirm that the eigenvalues of the truncated system of equations (5.22) are purely imaginary. In fact, when after truncation at least one eigenvalue has a real part zero, stability of the solution cannot be determined [11]. In our case, as it has been mentioned before, all eigenvalues are purely imaginary, so a small perturbation of the system can still give instability by the presence of the eigenvalues with positive real parts. As a result, *we need to provide an additional stability analysis of the cable's motion*.

Next, Table 5.5 shows that for the fourth resonance frequency, Ω_4, starting from seven oscillation modes of truncation, the natural motion of the cable is unstable due to a contribution of positive real parts in the approximate eigenvalues. Likewise, for the fifth resonance frequency, Ω_5, in Table 5.6 we see a similar contribution of negative real parts. It can also be noticed from these tables that by increasing the number of modes, there is no convergence in the eigenvalues to any particular value. Consequently, these eigenvalues do not provide an accurate approximation of the solution. All in all, *Galerkin's method seems to be not applicable for the construction of the approximate*

---

[3]Matrices $\mathbf{X}$ and $\mathbf{Y}$ are called similar if there exists a non-singular matrix $\mathbf{P}$ such that $\mathbf{Y=PXP}^{-1}$.

№ Modes	Eigenvalues for Ω_1
1	$\pm 0.5i$
2	$\pm 0.0391i$, $\pm 1.46i$
3	$\pm 0.325i$, $\pm 0.76i$, $\pm 2.57i$
4	$\pm 0.348i$, $\pm 0.69i$, $\pm 1.6i$, $\pm 3.74i$
5	$\pm 0.033i$, $\pm 1.02i$, $\pm 1.07i$, $\pm 2.55i$, $\pm 4.96i$
6	$\pm 0.26i$, $\pm 0.615i$, $\pm 1.45i$, $\pm 1.81i$, $\pm 3.57i$, $\pm 6.21i$
7	$\pm 0.301i$, $\pm 0.562i$, $\pm 1.28i$, $\pm 1.84i$, $\pm 2.69i$, $\pm 4.65i$, $\pm 7.48i$
8	$\pm 0.0298i$ $\pm 0.874i$, $\pm 0.878i$, $\pm 2.05i$, $\pm 2.25i$, $\pm 3.64i$, $\pm 5.76i$, $\pm 8.78i$
9	$\pm 0.23i$, $\pm 0.55i$, $\pm 1.21i$, $\pm 1.54i$, $\pm 2.65i$, $\pm 2.89i$, $\pm 4.63i$, $\pm 6.9i$, $\pm 10.1i$
10	$\pm 0.275i$, $\pm 0.501i$, $\pm 1.13i$, $\pm 1.54i$, $\pm 2.29i$, $\pm 3.07i$, $\pm 3.78i$, $\pm 5.66i$, $\pm 8.07i$, $\pm 11.4i$

Table 5.2: Eigenvalues of the truncated system (5.19) with $\gamma = 0.5$ for the first resonance frequency $\Omega_1 = \frac{\pi}{l_0}$.

№ Modes	Eigenvalues for Ω_2
1	$\pm 0.5i$
2	$\pm 0.5i$, $\pm i$
3	$\pm 0.0986i$, $\pm i$, $\pm 1.9i$
4	$\pm 0.0749i$, $\pm 0.0986i$, $\pm 1.9i$, $\pm 2.93i$
5	$\pm 0.0749i$, $\pm 0.367i$, $\pm 0.871i$, $\pm 2.93i$, $\pm 4i$
6	$\pm 0.367i$, $\pm 0.654i$, $\pm 0.871i$, $\pm 1.52i$, $\pm 4i$, $\pm 5.13i$
7	$\pm 0.412i$, $\pm 0.654i$, $\pm 1.01i$, $\pm 1.52i$, $\pm 2.31i$, $\pm 5.13i$, $\pm 6.29i$
8	$\pm 0.412i$, $\pm 0.698i$, $\pm 1.01i$, $\pm 1.38i$, $\pm 2.31i$, $\pm 3.2i$, $\pm 6.29i$, $\pm 7.48i$
9	$\pm 0.0895i$, $\pm 0.698i$, $\pm 1.34i$, $\pm 1.38i$, $\pm 1.74i$, $\pm 3.2i$, $\pm 4.12i$ $\pm 7.48i$, $\pm 8.69i$
10	$\pm 0.0634i$, $\pm 0.0895i$, $\pm 1.34i$, $\pm 1.74i$, $\pm 2.04i$, $\pm 2.13i$ $\pm 4.12i$, $\pm 5.1i$, $\pm 8.69i$, $\pm 9.92i$

Table 5.3: Eigenvalues of the truncated system (5.19) with $\gamma = 0.5$ for the second resonance frequency $\Omega_2 = \frac{2\pi}{l_0}$.

№ Modes	Eigenvalues for Ω_3
1	$\pm 0.5i$
2	$\pm 4i$, $\pm 4.5i$
3	$\pm 1.5i$, $\pm 4i$, $\pm 4.5i$
4	$\pm 1.5i$, $\pm 1.87i$, $\pm 4.18i$, $\pm 4.54i$
5	$\pm 1.5i$, $\pm 1.89i$, $\pm 2.15i$, $\pm 4.29i$, $\pm 5.03i$
6	$\pm 0.114i$, $\pm 1.89i$, $\pm 2.15i$, $\pm 4.29i$, $\pm 4.39i$, $\pm 5.03i$
7	$\pm 0.0942i$, $\pm 0.114i$, $\pm 2.16i$, $\pm 4.09i$, $\pm 4.39i$, $\pm 5.03i$, $\pm 5.51i$
8	$\pm 0.114i$, $\pm 0.159i$, $\pm 0.189i$, $\pm 4.11i$, $\pm 4.39i$, $\pm 4.48i$, $\pm 5.51i$, $\pm 6.67i$
9	$\pm 0.159i$, $\pm 0.189i$, $\pm 0.979i$, $\pm 2.28i$, $\pm 4.11i$, $\pm 4.48i$, $\pm 5.51i$, $\pm 6.67i$, $\pm 7.7i$
10	$\pm 0.0466i$, $\pm 0.979i$, $\pm 1.23i$, $\pm 2.28i$, $\pm 2.75i$, $\pm 4.33i$, $\pm 4.48i$, $\pm 6.67i$, $\pm 7.7i$, $\pm 8.85i$

Table 5.4: Eigenvalues of the truncated system (5.19) with $\gamma = 0.5$ for the third resonance frequency $\Omega_3 = \frac{3\pi}{l_0}$.

№ Modes	Eigenvalues for Ω_4
1	$\pm 0.5i$
2	$\pm 0.5i$, $\pm i$
3	$\pm i$, $\pm 3i$, $\pm 4i$
4	$\pm i$, $\pm 2i$, $\pm 3i$, $\pm 4i$
5	$\pm i$, $\pm 2i$, $\pm 2.515i$, $\pm 2.971i$, $\pm 4.012i$
6	$\pm 0.6408i$, $\pm 2i$, $\pm 2.515i$, $\pm 2.971i$, $\pm 3.097i$, $\pm 4.012i$
7	$\pm 0.6408i$, $\pm 2i$, $\pm 2.107i$, $\pm 3.097i$, $-0.881 \pm 3.122i$, $0.881 \pm 3.122i$, $\pm 4.595i$
8	$\pm 0.6408i$, $\pm 0.8352i$, $\pm 2.107i$, $-0.881 \pm 3.122i$, $0.881 \pm 3.122i$, $\pm 3.097i$, $\pm 4.393i$, $\pm 4.595i$
9	$\pm 0.6408i$, $\pm 0.8352i$, $\pm 0.8934i$, $-0.7753 \pm 2.922i$, $0.7753 \pm 2.922i$, $\pm 3.097i$, $\pm 4.393i$, $\pm 4.477i$, $\pm 5.2i$
10	$\pm 0.8352i$, $\pm 0.8934i$, $-1.154 \pm 1.07i$, $1.154 \pm 1.07i$, $\pm 4.393i$, $\pm 4.477i$, $-0.7753 \pm 2.922i$, $0.7753 \pm 2.922i$, $\pm 5.2i$, $\pm 5.948i$

Table 5.5: Eigenvalues of the truncated system (5.19) with $\gamma = 0.5$ for the fourth resonance frequencies $\Omega_4 = \frac{4\pi}{l_0}$.

№ Modes	Eigenvalues for Ω_5
1	$\pm 0.5i$
2	$\pm 0.5i, \pm i$
3	$\pm 0.5i, \pm 12i, \pm 12.5i$
4	$\pm 2.667i, \pm 4.167i, \pm 12i, \pm 12.5i$
5	$\pm 2.5i, \pm 2.667i, \pm 4.167i, \pm 12i, \pm 12.5i$
6	$\pm 2.5i, \pm 2.685i, \pm 2.97i, \pm 4.177i, \pm 12i, \pm 12.5i$
7	$\pm 2.685i, \pm 2.97i, \pm 3.5i, \pm 4.177i, \pm 11.98i, \pm 12.52i$
8	$\pm 2.5i, \pm 2.685i, \pm 2.97i, \pm 3.097i, \pm 3.361i, \pm 4.177i, \pm 4.152i,$ $\pm 11.83i, \pm 12.65i$
9	$\pm 2.336i, \pm 2.5i, -0.9087 \pm 3.282i, 0.9087 \pm 3.282i, \pm 3.361i,$ $\pm 4.152i, \pm 5.327i, \pm 11.83i, \pm 12.65i$
10	$\pm 1.042i, \pm 2.336i, \pm 3.361i, -0.9087 \pm 3.282i, 0.9087 \pm 3.282i,$ $\pm 4.152i, \pm 5.327i, \pm 5.492i, \pm 11.83i, \pm 12.65i$

Table 5.6: Eigenvalues of the truncated system (5.19) with $\gamma = 0.5$ for the fifth resonance frequency $\Omega_5 = \frac{5\pi}{l_0}$.

solution in this problem. To proceed with the a stability analysis, we will evaluate the energy integral of the governing equation in the following section.

5.5 Energetics

The systems (5.19) and (5.21) ensure the boundedness of the approximate solution of some truncated systems up to $\mathcal{O}(\varepsilon)$ for some resonance cases and their detuning, respectively. However, these truncated systems do not provide the boundedness of the energy of vibrations for time-variable problems (see also [24, 56]). In order to give more information about the dynamic stability of the solution, we proceed with the investigation of the energy.

5.5.1 Energy

The total mechanical energy of the cable is given by (see [36, 46])

$$E(t, \tau) = \frac{1}{2} \int_0^1 \left(\tilde{u}_t^2(\xi, t, \tau) + \frac{1}{l_0^2} \tilde{u}_\xi^2(\xi, t, \tau) \right) d\xi + \mathcal{O}(\varepsilon), \tag{5.23}$$

where $\tilde{u}$ is given by

$$\tilde{u}(\xi, t, \tau) = \sum_{n=1}^{\infty} \left[A_{n,0}(\tau) \cos\left(\frac{n\pi}{l_0} t \right) + B_{n,0}(\tau) \sin\left(\frac{n\pi}{l_0} t \right) \right] \sin(n\pi\xi) + \mathcal{O}(\varepsilon). \tag{5.24}$$

By substituting (5.24) into (5.23), we obtain the following simplified expression for the energy

$$E(\tau) = \frac{\pi^2}{4l_0^2} \sum_{n=1}^{\infty} n^2 \left[A_{n,0}^2(\tau) + B_{n,0}^2(\tau) \right] + \mathcal{O}(\varepsilon). \tag{5.25}$$

5.5.2 Rate of change of the energy

Next, we proceed with the time rate of change of the energy (5.25) for both resonance and its detuning.

Resonance frequency

For this, we employ the system (5.19) for $\Omega = \frac{N\pi}{l_0}$, where $N \in \mathbb{Z}_+$. By putting $X_k(\tau) = kA_{k,0}(\tau)$ and $Y_k(\tau) = kB_{k,0}(\tau)$, we rewrite (5.19) as follows:

$$\begin{cases} \dot{X}_k &= \gamma k Y_k + \dfrac{k(k+N)}{2k+N} X_{k+N} - \dfrac{k(k-N)}{2k-N} X_{k-N} + \dfrac{2k+N}{2k-N}\dfrac{N-k}{2} X_{N-k}, \\ \dot{Y}_k &= -\gamma k X_k + \dfrac{k(k+N)}{2k+N} Y_{k+N} - \dfrac{k(k-N)}{2k-N} Y_{k-N} - \dfrac{2k+N}{2k-N}\dfrac{N-k}{2} Y_{N-k}, \end{cases} \tag{5.26}$$

where $\gamma = \frac{\mu_0 l_0 (l_0 - 2)}{4\beta_0}$ and the overdot stands for the differentiation with respect to τ. From where it readily follows that

$$\frac{\mathrm{d}}{\mathrm{d}\tau} \sum_{n=1}^{\infty} (X_n^2 + Y_n^2) = N \sum_{\substack{n=1 \\ n \neq N/2}}^{N-1} (Y_n Y_{N-n} - X_n X_{N-n}).$$

Consequently, the rate of change of the energy is given by

$$\frac{\mathrm{d}E(\tau)}{\mathrm{d}\tau} = \frac{\pi^2}{4l_0^2} \sum_{\substack{n=1 \\ n \neq N/2}}^{N-1} nN(n-N)(A_{n,0}A_{N-n,0} - B_{n,0}B_{N-n,0}) + \mathcal{O}(\varepsilon), \tag{5.27}$$

for $N \in \mathbb{Z}_+$. It should be observed that for the first and the second resonance frequencies the energy is conserved. That is, for $\Omega_1 = \frac{\pi}{l_0}$ and $\Omega_2 = \frac{2\pi}{l_0}$ from (5.25) and (5.27), it follows that $E(\tau) = E(0) + \mathcal{O}(\varepsilon)$ for $\tau = \mathcal{O}(1)$. For the resonant frequencies Ω_N, when $N \geq 3$, the behavior of the energy is defined by the expression (5.27) in combination with system (5.19) tending to infinitely many interactions among modes of oscillations as $N \to \infty$. No conclusions so far can be drawn for $N \geq 3$.

Resonance detuning

For detuned resonant frequencies, the rate of change of the energy of the system (5.21) is given by

$$\frac{\mathrm{d}E(\tau)}{\mathrm{d}\tau} = \frac{\pi^2}{4l_0^2} \sum_{\substack{n=1 \\ n \neq s/2}}^{s-1} ns(n-s)[\cos(\alpha\tau)(A_{n,0}A_{s-n,0} - B_{n,0}B_{s-n,0})$$

$$- \sin(\alpha\tau)(A_{s-n,0}B_{n,0} + B_{s-n,0}A_{n,0})] + \mathcal{O}(\varepsilon). \tag{5.28}$$

From (5.28) similar conclusions as for the resonance case hold. That is, for the first two detuning frequencies the energy is constant up to $\mathcal{O}(\varepsilon)$ for $\tau = \mathcal{O}(1)$. For the frequencies higher than two, the energy is defined by the interaction of the lower oder modes and by the value of the detuning parameter α. Also we can draw no general conclusions when $N \geq 3$.

5.6   Conclusions

In this chapter we have studied the transverse vibrations of a vertically moving string with harmonically changing length, $l(t) = l_0 + \beta \sin \Omega t$. To investigate this problem, we have used a two-timescales perturbation method in combination with a Fourier series expansion of the solution. By using this approach we obtained the non-secularity conditions for the amplitudes of vibration. Those conditions are represented by the infinite dimensional system of coupled ordinary differential equations. In other words, there is an infinite number of interactions among the oscillation modes of the cable. Moreover, the natural frequencies, at which resonance occurs, were given by $\Omega = \frac{s\pi}{l_0}$ for $s \in \mathbb{N}$.

Further, Galerkin's method was applied in order to tackle the infinite dimensional system (5.19). The truncation provided purely imaginary eigenvalues for the first three resonance frequencies, which required a further stability analysis. For the higher order resonance frequencies, it turned out that the boundedness of the solution depends on the level of truncation. Moreover, we showed by an eigenvalue analysis that the Galerkin truncation method cannot be used for the construction of approximations which are valid on long timescales in our problem. In general, this problem is a good example to show that the infinite dimensional system cannot be studied by a truncation to a finite system of ordinary differential equations. Remark that in some cases the use of characteristic coordinates allows one to solve the infinite dimensional system analytically resulting in an approximation of the solution containing an infinite number of oscillation modes; see, for instance, [39, 61]. To this end we could only show the validity of the obtained system (5.19) through the characteristic coordinates. The proof that (5.19) can be solved analytically is not trivial and requires more study.

Since an eigenvalue analysis did not give enough information about the stability of the solution, we considered the problem from the energy view point. This approach allowed to draw some conclusions for the first two resonance frequencies, Ω_1 and Ω_2. More precisely, it has been shown that the energy is conserved for them on the timescale of order ε^{-1}. For the higher order resonance frequencies, the energy can behave differently which requires further investigation numerically. Additionally, detuning of resonance frequencies was considered producing similar conclusions as for the purely resonance case.

Appendix C

C.1 Skew-symmetric matrix

In this appendix, we construct a skew-symmetric matrix $\mathbf{Y}$ that is similar to the truncated matrix $\mathbf{X}$ of system (5.22). First of all, the truncated matrix for this system for $k = 1, 2, 3$ is given by

$$
\mathbf{X} =
\begin{bmatrix}
0 & \gamma & {}^4\!/_3 & 0 & 0 & 0 \\
-\gamma & 0 & 0 & {}^4\!/_3 & 0 & 0 \\
-{}^1\!/_3 & 0 & 0 & 2\gamma & {}^9\!/_5 & 0 \\
0 & -{}^1\!/_3 & -2\gamma & 0 & 0 & {}^9\!/_5 \\
0 & 0 & -{}^4\!/_5 & 0 & 0 & 3\gamma \\
0 & 0 & 0 & -{}^4\!/_5 & -3\gamma & 0
\end{bmatrix}.
$$

Next, we need to find the non-singular matrix $\mathbf{P} = (p_{ii})$ for $i = 1, 2, \ldots, 6$ transforming $\mathbf{X}$ to $\mathbf{Y}$. Using $\mathbf{Y} = \mathbf{P}\mathbf{X}\mathbf{P}^{-1}$, where $\mathbf{P}^{-1} = \left(\frac{1}{p_{ii}}\right)$ for $i = 1, 2, \ldots, 6$, we obtain

$$
\mathbf{Y} =
\begin{bmatrix}
0 & \frac{\gamma p_{11}}{p_{22}} & \frac{4}{3}\frac{p_{11}}{p_{33}} & 0 & 0 & 0 \\
-\frac{\gamma p_{22}}{p_{11}} & 0 & 0 & \frac{4}{3}\frac{p_{22}}{p_{44}} & 0 & 0 \\
-\frac{1}{3}\frac{p_{33}}{p_{11}} & 0 & 0 & \frac{2\gamma p_{33}}{p_{44}} & \frac{9}{5}\frac{p_{33}}{p_{55}} & 0 \\
0 & -\frac{1}{3}\frac{p_{44}}{p_{22}} & -\frac{2\gamma p_{44}}{p_{33}} & 0 & 0 & \frac{9}{5}\frac{p_{44}}{p_{66}} \\
0 & 0 & -\frac{4}{5}\frac{p_{55}}{p_{33}} & 0 & 0 & \frac{3}{5}\frac{\gamma p_{55}}{p_{66}} \\
0 & 0 & 0 & -\frac{4}{5}\frac{p_{66}}{p_{44}} & -\frac{3\gamma p_{66}}{p_{55}} & 0
\end{bmatrix}
$$

and, consequently,

$$
-\mathbf{Y}^T =
\begin{bmatrix}
0 & \frac{\gamma p_{22}}{p_{11}} & \frac{1}{3}\frac{p_{33}}{p_{11}} & 0 & 0 & 0 \\
-\frac{\gamma p_{11}}{p_{22}} & 0 & 0 & \frac{1}{3}\frac{p_{44}}{p_{22}} & 0 & 0 \\
-\frac{4}{3}\frac{p_{11}}{p_{33}} & 0 & 0 & \frac{2\gamma p_{44}}{p_{33}} & \frac{4}{5}\frac{p_{55}}{p_{33}} & 0 \\
0 & -\frac{4}{3}\frac{p_{22}}{p_{44}} & -\frac{2\gamma p_{33}}{p_{44}} & 0 & 0 & \frac{4}{5}\frac{p_{66}}{p_{44}} \\
0 & 0 & -\frac{9}{5}\frac{p_{33}}{p_{55}} & 0 & 0 & \frac{3}{5}\frac{\gamma p_{66}}{p_{55}} \\
0 & 0 & 0 & -\frac{9}{5}\frac{p_{44}}{p_{66}} & -\frac{3\gamma p_{55}}{p_{66}} & 0
\end{bmatrix}.
$$

If the entry of $\mathbf{Y}$ in the i-th row and j-th column is y_{ij}, then the skew symmetric condition is given by $y_{ij} = -y_{ji}$. From where, for p_{11} being arbitrary, we obtain the matrix $\mathbf{Y}$ as follows:

$$\mathbf{Y} = \begin{bmatrix} 0 & \gamma & {}^2\!/_3 & 0 & 0 & 0 \\ -\gamma & 0 & 0 & {}^2\!/_3 & 0 & 0 \\ -{}^2\!/_3 & 0 & 0 & 2\gamma & {}^6\!/_5 & 0 \\ 0 & -{}^2\!/_3 & -2\gamma & 0 & 0 & {}^6\!/_5 \\ 0 & 0 & -{}^6\!/_5 & 0 & 0 & 3\gamma \\ 0 & 0 & 0 & -{}^6\!/_5 & -3\gamma & 0 \end{bmatrix},$$

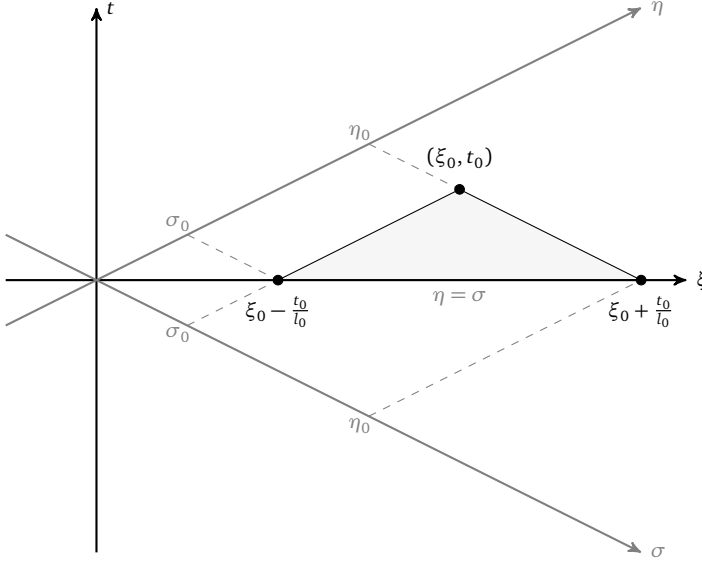which is skew-symmetric and similar to $\mathbf{X}$.

Figure C.1: The triangle of dependence of the point (ξ_0, t_0) in the characteristic coordinates.

C.2 Characteristic coordinates

Here, we start with the initial value problem (5.14a,5.14b) for the resonant frequencies $\Omega = \frac{s\pi}{l_0}$, where $s \in \mathbb{N}$. As an alternative to an infinite series representation of the solution, we will study this problem in characteristic coordinates $\sigma = \xi - \frac{1}{l_0}t$ and $\eta = \xi + \frac{1}{l_0}t$. Further, as in the previous section, we will use the two-timescales perturbation method, because a straightforward perturbation expansion contains secular terms. As a result, the solution $\tilde{u}(\xi, t)$ becomes a function of the characteristic coordinates (σ and η), and a new slow timescale $\tau = \varepsilon t$, i.e., $\tilde{u}(\xi, t) = \tilde{w}(\sigma, \eta, \tau)$. In accordance with these new variables, the derivatives take the following form

$$\tilde{u}_t = \frac{1}{l_0}(\tilde{w}_\eta - \tilde{w}_\sigma) + \varepsilon\tilde{w}_\tau, \; \tilde{u}_{tt} = \frac{1}{l_0^2}(\tilde{w}_{\sigma\sigma} - 2\tilde{w}_{\sigma\eta} + \tilde{w}_{\eta\eta}) - \frac{2\varepsilon}{l_0}(\tilde{w}_{\sigma\tau} - \tilde{w}_{\eta\tau}) + \varepsilon^2\tilde{w}_{\tau\tau},$$

$$\tilde{u}_\xi = \tilde{w}_\sigma + \tilde{w}_\eta, \; \tilde{u}_{\xi\xi} = \tilde{w}_{\sigma\sigma} + 2\tilde{w}_{\sigma\eta} + \tilde{w}_{\eta\eta}, \; \tilde{u}_{\xi t} = \tilde{u}_{t\xi} = \frac{1}{l_0}(\tilde{w}_{\eta\eta} - \tilde{w}_{\sigma\sigma}) + \varepsilon(\tilde{w}_{\sigma\tau} + \tilde{w}_{\eta\tau}).$$
$$(C.1)$$

Substituting (C.1) into (5.14a,5.14b) and introducing the following notations for convenience,

$$H_1(\sigma, \eta) := \mu_0 l_0\left[1 - h_1\left(\frac{\sigma + \eta}{2}\right)\right] - \mu_0 + \beta_0\left(\frac{s^2\pi^2}{l_0^2}\frac{1}{\mu_0} - \frac{2}{l_0}\right)\sin\left(\frac{s\pi[\eta - \sigma]}{2}\right), \; (C.2)$$

$$H_2(\sigma, \eta) := 2\beta_0\frac{s\pi}{l_0}\cos\left(\frac{s\pi[\eta - \sigma]}{2}\right)h_2\left(\frac{\sigma + \eta}{2}\right), \quad (C.3)$$

where h_1 and h_2 are given by (5.10) and (5.11), respectively, we obtain a modified initial value problem in terms of characteristic coordinates:

$$-4\tilde{w}_{\sigma\eta} = \varepsilon[(H_1 - H_2)\tilde{w}_{\sigma\sigma} + (H_1 + H_2)\tilde{w}_{\eta\eta} + 2H_1\tilde{w}_{\sigma\eta} - \mu_0 l_0 h_3\left(\frac{\sigma + \eta}{2}\right)(\tilde{w}_\sigma + \tilde{w}_\eta)$$
$$+ 2l_0(\tilde{w}_{\sigma\tau} - \tilde{w}_{\eta\tau})] + \mathcal{O}(\varepsilon^2), \tag{C.4a}$$

for $-\infty < \sigma < \eta < \infty$ and $\tau > 0$, with the ICs:

$$\tilde{w}(\sigma, \eta, 0) = \tilde{\phi}(\sigma),$$
$$-\frac{1}{l_0}(\tilde{w}_\sigma(\sigma, \eta, 0) - \tilde{w}_\eta(\sigma, \eta, 0)) + \varepsilon\tilde{w}_\tau(\sigma, \eta, 0) = \tilde{\psi}(\sigma) + 2\varepsilon\frac{\Omega\beta_0}{l_0}h_4(\sigma)\tilde{\phi}'(\sigma), \tag{C.4b}$$

for $-\infty < \sigma = \eta < \infty$, where h_3 and h_4 are given by (5.12) and (5.13), respectively.

Next, we expand the solution in a formal perturbation series in ε as $\tilde{w}(\sigma, \eta, \tau; \varepsilon) = w_0(\sigma, \eta, \tau) + \varepsilon w_1(\sigma, \eta, \tau) + \mathcal{O}(\varepsilon^2)$. Substituting this expansion into (C.4a-C.4b) and collecting terms of like powers of ε, we obtain that w_0 should satisfy

$$w_{0_{\sigma\eta}} = 0, \tag{C.5a}$$

for $-\infty < \sigma < \eta < \infty$ and $\tau > 0$, with the ICs:

$$w_0(\sigma, \eta, 0) = \phi_0(\sigma),$$
$$w_{0_\eta}(\sigma, \eta, 0) - w_{0_\sigma}(\sigma, \eta, 0) = l_0\psi_0(\sigma), \tag{C.5b}$$

for $-\infty < \sigma = \eta < \infty$. To integrate (C.5a), we need to fix a point (ξ_0, t_0). This point has the coordinates (σ_0, η_0) in the characteristic variables. To find the value of the solution at this point, we first integrate (C.5a) in terms of σ from η to σ_0. Then we integrate the so-obtained identity with respect to η from σ_0 to η_0. In general, we take the double integral over the triangle of dependence of the fixed point (ξ_0, t_0) as illustrated in Figure C.1. Thus, the initial value problem (C.5a,C.5b) has the following general solution

$$w_0(\sigma, \eta, \tau) = f_0(\sigma, \tau) + g_0(\sigma, \tau), \tag{C.6}$$

where

$$f_0(\sigma, \tau) = \frac{1}{2}\sum_{k=1}^{\infty}[A_k(\tau)\sin(k\pi\sigma) + B_k(\tau)\cos(k\pi\sigma)], \tag{C.7}$$

$$g_0(\eta, \tau) = \frac{1}{2}\sum_{k=1}^{\infty}[A_k(\tau)\sin(k\pi\eta) - B_k(\tau)\cos(k\pi\eta)]. \tag{C.8}$$

The initial conditions (C.5b) imply that f_0 and g_0 have to satisfy $f_0(\sigma, 0) + g_0(\sigma, 0) = \phi_0(\sigma)$ and $g_0'(\sigma, 0) - f_0'(\sigma, 0) = l_0\psi_0(\sigma)$. Additionally, from the 2-periodic odd extension, it follows that $f_0(\sigma, \tau) = f_0(\sigma + 2, \tau)$ and $g_0(\sigma, \tau) = -f_0(-\sigma, \tau)$ for $-\infty <$

$\sigma < \infty$ and $\tau \geq 0$. Proceeding with the construction of a formal approximation for the solution $\tilde{w}(\sigma, \eta, \tau)$, we obtain from (C.4a-C.4b), by using (C.6), that w_1 should satisfy

$$
\begin{aligned}
-4w_{1_{\sigma\eta}} = &(H_1 - H_2)f_{0_{\sigma\sigma}} + (H_1 + H_2)g_{0_{\eta\eta}} - \mu_0 l_0 h_3\left(\frac{\sigma+\eta}{2}\right)(f_{0_\sigma} + g_{0_\eta}) \\
&+ 2l_0(f_{0_{\sigma\tau}} - g_{0_{\eta\tau}}),
\end{aligned}
\tag{C.9a}
$$

for $-\infty < \sigma < \eta < \infty$ and $\tau > 0$, with the ICs:

$$
\begin{aligned}
&w_1(\sigma, \eta, 0) = \phi_1(\sigma), \\
&-\frac{1}{l_0}[w_{1_\sigma}(\sigma, \eta, 0) - w_{1_\eta}(\sigma, \eta, 0)] + w_{0_\tau}(\sigma, \eta, 0) = \psi_1(\sigma) + 2\frac{\Omega\beta_0}{l_0}h_4(\sigma)\phi_0'(\sigma),
\end{aligned}
\tag{C.9b}
$$

for $-\infty < \sigma = \eta < \infty$. Next, we integrate (C.9a) with respect to η from $\eta = \sigma$ to $\eta = \eta$ as follows:

$$
\begin{aligned}
-4w_{1_\sigma}(\sigma, \eta, \tau) = &-4w_{1_\sigma}(\sigma, \sigma, \tau) + 2l_0(\eta - \sigma)f_{0\sigma\tau}(\sigma, \tau) - 2l_0[g_{0_\tau}(\eta, \tau) - g_{0_\tau}(\sigma, \tau)] \\
&- f_{0_{\sigma\sigma}}(\sigma, \tau)\int_\sigma^\eta [H_1(\sigma, \theta) - H_2(\sigma, \theta)]\,\mathrm{d}\theta + \mu_0 l_0 f_{0_\sigma}(\sigma, \tau)\int_\sigma^\eta h_3\left(\frac{\sigma+\theta}{2}\right)\mathrm{d}\theta \\
&+ \int_\sigma^\eta [H_1(\sigma, \theta) + H_2(\sigma, \theta)]g_{0_{\theta\theta}}(\theta, \tau)\,\mathrm{d}\theta - \mu_0 l_0 \int_\sigma^\eta h_3\left(\frac{\sigma+\theta}{2}\right)g_{0_\theta}(\theta, \tau)\,\mathrm{d}\theta.
\end{aligned}
\tag{C.10}
$$

Let us consider, for example, the integral $\int_\sigma^\eta H_1(\sigma, \theta)g_{0_{\theta\theta}}(\theta, \tau)\mathrm{d}\theta$ in the right hand side of (C.10). It turns out that if we subtract from the integrand its average value over the period 2, the obtained result is bounded for all values σ and η. Hence, the integrand can be represented by two summands, one of which is $\mathcal{O}(1)$ and the other one is linear in $\eta - \sigma = \frac{2}{l_0}t$, that is, it is of $\mathcal{O}(\varepsilon^{-1})$ on a timescale of $\mathcal{O}(\varepsilon^{-1})$:

$$
\begin{aligned}
\int_\sigma^\eta H_1(\sigma, \theta)g_{0_{\theta\theta}}(\theta, \tau)\,\mathrm{d}\theta = &\int_\sigma^\eta \left[H_1(\sigma, \theta)g_{0_{\theta\theta}}(\sigma, \tau) - \frac{1}{2}\int_{-1}^1 H_1(\sigma, \lambda)g_{0_{\lambda\lambda}}(\lambda, \tau)\mathrm{d}\lambda\right]\mathrm{d}\theta \\
&+ \frac{\eta - \sigma}{2}\int_{-1}^1 H_1(\sigma, \theta)g_{0_{\theta\theta}}(\theta, \tau)\,\mathrm{d}\theta.
\end{aligned}
$$

So, in (C.10), proceeding with integration of the remaining terms in the same way and

collecting the unbounded ones, we obtain the following equation

$$-4w_{1_\sigma}(\sigma,\eta,\tau) = -4w_{1_\sigma}(\sigma,\sigma,\tau) + (\eta-\sigma)\left\{\left(\frac{\mu_0 l_0}{2} - \mu_0 + \frac{2\beta_0}{l_0}\sin(s\pi\sigma)\right) f_{0_{\sigma\sigma}}(\sigma,\tau)\right.$$

$$+ 2l_0 f_{0_{\sigma\tau}}(\sigma,\tau) + \frac{\beta_0 s}{2l_0}\sum_{n=1}^{\infty}\frac{n^2\pi^2}{2n-s}[A_n(\tau)\cos((n-s)\pi\sigma) - B_n(\tau)\sin((n-s)\pi\sigma)]$$

$$+ \frac{\beta_0 s}{2l_0}\sum_{n=1}^{\infty}\frac{n^2\pi^2}{2n+s}[A_n(\tau)\cos((n+s)\pi\sigma) - B_n(\tau)\sin((n+s)\pi\sigma)]$$

$$\left. - \frac{\beta_0 s}{2l_0}\sum_{n=1}^{\infty}\frac{n^2\pi^2}{s-2n}[A_n(\tau)\cos((s-n)\pi\sigma) + B_n(\tau)\sin((s-n)\pi\sigma)]\right\} + \text{"NST"},$$

where "NST" contains bounded terms. Thus, to avoid unbounded terms, we have to set:

$$\left(\frac{\mu_0 l_0}{2} - \mu_0 + \frac{2\beta_0}{l_0}\sin(s\pi\sigma)\right) f_{0_{\sigma\sigma}}(\sigma,\tau) + 2l_0 f_{0_{\sigma\tau}}(\sigma,\tau)$$

$$+ \frac{\beta_0 s}{2l_0}\sum_{n=1}^{\infty}\frac{n^2\pi^2}{2n-s}[A_n(\tau)\cos((n-s)\pi\sigma) - B_n(\tau)\sin((n-s)\pi\sigma)]$$

$$+ \frac{\beta_0 s}{2l_0}\sum_{n=1}^{\infty}\frac{n^2\pi^2}{2n+s}[A_n(\tau)\cos((n+s)\pi\sigma) - B_n(\tau)\sin((n+s)\pi\sigma)]$$

$$- \frac{\beta_0 s}{2l_0}\sum_{n=1}^{\infty}\frac{n^2\pi^2}{s-2n}[A_n(\tau)\cos((s-n)\pi\sigma) + B_n(\tau)\sin((s-n)\pi\sigma)] = 0. \qquad \text{(C.11)}$$

It should be observed that by substituting (C.7) into (C.11) and using orthogonality of trigonometric functions, one obtains exactly the same infinite dimensional system as (5.19), what confirms its correctness. Finally, it follows that both w_{1_η} and w_{1_σ} are $\mathcal{O}(1)$ on a timescale of $\mathcal{O}(\varepsilon^{-1})$ if f_0 and g_0 satisfy the following solvability conditions

$$\left(\frac{\mu_0 l_0}{2} - \mu_0 + \frac{2\beta_0}{l_0}\sin(s\pi\sigma)\right) f_{0_{\sigma\sigma}} + 2l_0 f_{0_{\sigma\tau}} + \int_{-1}^{1} H_2(\sigma,\theta)g_{0_{\theta\theta}}(\theta,\tau)\mathrm{d}\theta = 0,$$

$$\left(\frac{\mu_0 l_0}{2} - \mu_0 - \frac{2\beta_0}{l_0}\sin(s\pi\eta)\right) g_{0_{\eta\eta}} + 2l_0 g_{0_{\eta\tau}} + \int_{-1}^{1} H_2(\theta,\eta)f_{0_{\theta\theta}}(\theta,\tau)\mathrm{d}\theta = 0,$$

which are actually equivalent due to $g_0(\sigma,\tau) = -f_0(-\sigma,\tau)$ and where H_2 is given by (C.3). It should be noted that these PDEs can be solved analytically if one can get rid of the infinite sums representation; consequently, providing an analytical solution of the infinite dimensional system (5.19) for infinitely many modes of oscillations. Thus, analytical solvability of the infinite dimensional system is still an open problem.

Chapter 6

Resonances and vibrations in an elevator cable system due to boundary sway

In this chapter, an analytical method is presented to study an initial-boundary value problem describing the transverse displacements of a vertically moving beam under boundary excitation. The length of the beam is linearly varying in time, i.e., the axial, vertical velocity of the beam is assumed to be constant. The bending stiffness of the beam is assumed to be small. This problem may be regarded as a model describing the lateral vibrations of an elevator cable excited at its boundaries by the wind-induced building sway. Slow variation of the cable length leads to a singular perturbation problem which is expressed in slowly changing, time-dependent coefficients in the governing differential equation. By providing an interior layer analysis, infinitely many resonance manifolds are detected. Further, the initial-boundary value problem is studied in detail using a three-timescales perturbation method. The constructed formal approximations of the solutions are in agreement with the numerical results.

6.1   Introduction

Within the last decade, high-rise buildings have entered a new era of "megatall" buildings, which are over 600 meters in height. The construction of such tall buildings has many practical limitations due to various issues. The higher buildings rise, the more vulnerable they become to wind influence. This wind-force can lead to building sway, which can initiate the motion of elevator cables. Resonances in elevator cables can damage shaft devices or cause entanglements in the shaft. In fact, internal transportation systems play a crucial role in the building functionality. That is why considerable attention should be paid to improvement of elevator technologies to prevent any damage, and consequently downtime of elevators. However, the increasing complexity of the engineering structures increases the complexity of their analysis. Therefore, it is also important to develop advanced analytical models in order to tackle this complexity; one of which is presented in this chapter.

This work is an extension of the study by Sandilo and van Horssen [45], where the lateral vibrations of an elevator cable system with a small sinusoidal excitation at its upper end was studied. The results showed that $\mathscr{O}(\varepsilon)$ excitation at the upper end of the cable resulted in $\mathscr{O}(\sqrt{\varepsilon})$ autoresonance responses. In contrast to that work, a mathematical model developed in the current chapter is made closer to reality. One of the reasons is that the formulation of the problem includes bending stiffness of the cable allowing to obtain more accurate results for higher-order frequencies. The other reason is that both boundaries of the cable are excited by a harmonic function representing wind-induced sway of the building. In reality, when the building is acted upon by high velocity winds, it tends to sway in the lateral direction. This lateral motion translates into lateral motion of the cable. Note that in our mathematical model the sway related harmonic function changes with the travel height of the elevator.

A lot of other research has been conducted on similar types of problems. Kaczmarczyk [48] analyzed resonance in a catenary-vertical cable with slowly varying length under a periodic external excitation. Zhu and Ni [56] investigated a class of axially moving continua with arbitrarily varying length. Zhu and Xu [64] studied the dynamics of elevator cables with small bending stiffness. Zhu and Teppo [58] developed a new scaled model describing the lateral vibrations of an elevator cable with a variable length for a high-rise, high-speed elevator. Kaczmarczyk and Ostachowicz derived a mathematical model [49] and provided a numerical simulation of the dynamic response [50] for transient vibrations in deep mine hoisting cables. Zhu and Chen [60] presented a control method to dissipate the vibratory energy of the cable. Moreover, the authors introduced a new experimental method to validate the theoretical results for the (un)controlled lateral vibrations. Kimura et al. [18] studied forced vibrations of an elevator rope with both ends excited by wind-induced displacement sway of the building. Kaczmarczyk [47] developed a model describing the lateral dynamics of long vertically moving ropes for high-rise transportation. Crespo et al. [41] investigated nonlinear responses of an elevator rope system coupled with the elevator car sheave motion. Bao et al. [29] studied the nonlinear response of a flexible hoisting rope with time-varying length. Gaiko and van Horssen [37] considered lateral vibrations of a vertically moving string with in time harmonically varying length.
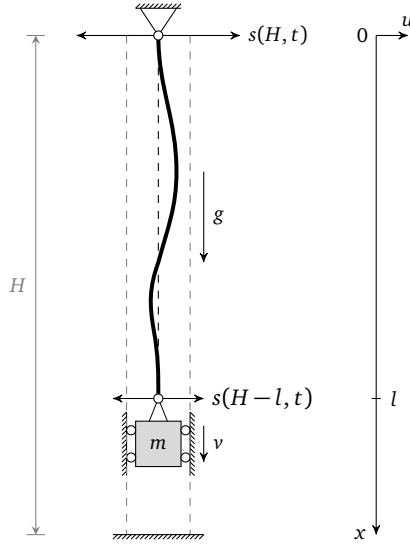
Figure 6.1: Schematic of a vertically moving cable with an attached elevator car at the lower end in a swaying building

In this chapter we study, in particular, the lateral vibrations of a vertically moving beam (with linearly in time varying length) excited at both boundaries by a harmonic function in the horizontal direction (see Figure 6.1). From the physical point of view, the motivation of this work is described as follows. When the fundamental frequency of the building sway matches one of the natural frequencies of elevator cable oscillations, then resonance emerges. This match happens due to a slow variation of the cable's length. In order to describe this phenomenon, an analytical methodology is developed in this chapter. First, an internal layer analysis is provided to study the behavior of the solution in the neighborhood of resonance. To perform this analysis we introduce local variables in the vicinity of resonance and shift out of it on a value which follows from a certain balancing principle. Note that this value determines the size of the resonance interior layer. Next we proceed with a detailed three-timescales perturbation method. The crucial step in the construction of an approximation by this method is removing unbounded terms by providing the so-called secularity conditions. So, in order to obtain asymptotically valid approximations of the solution, one should distinguish between the behavior outside and inside resonance zones.

This chapter is organized as follows. In Section 6.2 we make some assumptions and present an initial-boundary value problem describing the motion of the cable. Next, some transformations are introduced in order to simplify the construction of the approximation of the solution in Section 6.3. Further, we proceed with an internal layer analysis to study resonance in Section 6.4. Then, in Section 6.5 three-timescales are introduced to construct an accurate approximation of the solution on long timescales. Section 6.6 summarizes the results and provides some numerical experiments for the cable with small bending stiffness. Finally, in Section 6.7 we draw some conclusions

based on both analytical and numerical results and also discuss future work.

6.2   Assumptions and a mathematical model

In order to restrict the complexity of the analysis of the problem, it is necessary to make some assumptions:

- the mass of the cable is small compared to the mass of the elevator car (otherwise, oscillations of the building have to be coupled with the lateral motion of the elevator car);

- the elevator car is assumed to be a point mass;

- the cable is modeled as a uniform Euler-Bernoulli beam with small bending stiffness;

- the length of the cable is varying linearly in time, that is, $l = l_0 + \varepsilon t$, where l_0 is a constant, pretensioned length of the cable, ε is a small parameter, and t is time;

- the motion of both ends of the cable in lateral direction is defined by the fundamental frequency of the building sway;

- the speed of the elevator car is smaller than the velocity of the wave propagation in the cable;

- the acceleration of the elevator car is smaller than the gravitational acceleration.

The lateral displacement, u, of the elevator cable modeled as a beam is governed by [56]

$$\rho(u_{tt} + 2vu_{xt} + v^2 u_{xx} + \dot{v}u_x) - [P(x,t)u_x]_x + EIu_{xxxx} = 0, \qquad (6.1)$$

where the overdot notation means differentiation with respect to time, and the axial loading, comprised of the car's and the cable's weights and the longitudinal acceleration, is given by

$$P(x,t) := (m + \rho[l-x])(g - \dot{v}),$$

where $v = v(t)$ is the axial velocity of the cable, ρ is the mass-density of the cable, m is the mass of the car, g is the gravitational acceleration, EI is the flexural rigidity, where E is Young's modulus and I is the second moment of inertia of the cable. The governing equation (6.1) can be rewritten as

$$\rho(u_{tt} + 2vu_{xt} + v^2 u_{xx}) + \rho g u_x - P(x,t)u_{xx} + EIu_{xxxx} = 0. \qquad (6.2)$$

Using the following dimensionless quantities

$$x^* = \frac{x}{L}, \ u^* = \frac{u}{L}, \ l^* = \frac{l}{L}, \ \mu^* = \frac{\rho L}{m}, \ t^* = \frac{t}{L}\sqrt{\frac{mg}{\rho}}, \ v^* = v\sqrt{\frac{\rho}{mg}}, \ p = \frac{1}{L^2}\frac{EI}{mg}, \quad (6.3)$$

we further rewrite (6.2) in a dimensionless form, omitting the asterisk notation,

$$u_{tt} + 2vu_{xt} + v^2 u_{xx} + \mu u_x - (\mu - \dot{v})\left(l - x + \frac{1}{\mu}\right)u_{xx} + pu_{xxxx} = 0.$$

We also introduce the sway related term as follows (see Appendix A):

$$s(x,t) := A\big(\sin(\lambda x) - \sinh(\lambda x) - \alpha[\cos(\lambda x) - \cosh(\lambda x)]\big)\sin(\lambda^2 t), \qquad (6.4)$$

where

$$\alpha = \frac{\sin(\lambda H) + \sinh(\lambda H)}{\cos(\lambda H) + \cosh(\lambda H)},$$

and $\lambda = \frac{1.875}{H}$ is the fundamental frequency of the building sway, and H is the elevator travel height (or a height of the building). In summary, we obtain the following initial-boundary value problem describing the vibratory dynamics of the elevator cable pinned (i.e., the rotary inertia is zero) at its boundaries.

The governing PDE is given by

$$u_{tt} + 2vu_{xt} + v^2 u_{xx} - (\mu - \dot{v})\left(l - x + \frac{1}{\mu}\right)u_{xx} + \mu u_x + pu_{xxxx} = 0, \qquad (6.5a)$$

for $0 < x < l(t)$, and $t > 0$, subject to the BCs:

$$u(0,t) = s(H,t), \text{ and } u_{xx}(0,t) = 0,$$
$$u(l,t) = s(H-l,t), \text{ and } u_{xx}(l,t) = 0, \qquad (6.5b)$$

for $t > 0$, and with the ICs:

$$u(x,0) = f(x),$$
$$u_t(x,0) = g(x), \qquad (6.5c)$$

for $0 < x < l_0$.

Note that according to the stated assumptions, the following orders of smallness (for the dimensionalized system parameters) will be used further in the analysis of the problem

$$\mu := \varepsilon\mu_0, \ p := \varepsilon p_0, \ A := \varepsilon A_0, \ v = \mathcal{O}(\varepsilon), \ \dot{v} = \mathcal{O}(\varepsilon).$$

Initial displacement and velocity are also assumed to be small, that is

$$f = \mathcal{O}(\varepsilon), \ g = \mathcal{O}(\varepsilon).$$

6.3 Problem transformation

For the sake of convenience, we slightly modify the initial-boundary value problem (6.5a-6.5c) in this section. First, we will introduce a space coordinate transformation

in order to be able to expand the solution in a Fourier series. Then, the WKBJ method will be applied to remove the variable coefficients from the higher order terms in the initial value problem.

6.3.1 Notation

This work contains lengthy computations and sometimes some cumbersome expressions. Some of these terms are used repeatedly through out this chapter. That is why we introduce the most frequent notations here. First of all, we denote the sway related terms as

$$S_0 := \frac{A_0 \lambda^2}{l_0}\big(\beta[1 - l_0] + \Phi(\lambda l_0)\big), \tag{6.6}$$

$$S_1(t) := \frac{A_0 \lambda^4}{l}\big(2\beta[1 - l] + \Phi(\lambda l)\big)\sin(\lambda^2 t), \tag{6.7}$$

$$S_2(t) := -\frac{A_0 \lambda^2}{l}\big(2\beta + \Phi(\lambda l)\big)\cos(\lambda^2 t), \tag{6.8}$$

where

$$\beta := \frac{\sin(\lambda H)\cosh(\lambda H) - \cos(\lambda H)\sinh(\lambda H)}{\cos(\lambda H) + \cosh(\lambda H)}, \tag{6.9}$$

$$\Phi(t) := -\beta[\cosh(t) + \cos(t)] - \gamma_1 \sinh(t) + \gamma_2 \sin(t), \tag{6.10}$$

and where

$$\gamma_i := \frac{\cos(\lambda H)\cosh(\lambda H) + (-1)^i \sin(\lambda H)\sinh(\lambda H) + 1}{\cos(\lambda H) + \cosh(\lambda H)} \quad \text{for } i = 1, 2. \tag{6.11}$$

Related to (6.7) and (6.8) the following functions are defined:

$$S_{k1}(t) := A_0 \lambda^4 f_k^{[1]}\big(2\beta[1 - l] + \Phi(\lambda l)\big)\sin(\lambda^2 t), \tag{6.12}$$

$$S_{k2}(t) := -\frac{A_0 \lambda^2 f_k^{[2]}}{l}\big(2\beta + \Phi(\lambda l)\big)\cos(\lambda^2 t), \tag{6.13}$$

which depend on the mode number k, and terms which will follow from orthogonality properties:

$$f_k^{[1]} := \frac{(-1)^k}{k\pi}, \; f_k^{[2]} := \frac{1 - (-1)^k}{k\pi}, \; f_{nk}^{[3]} := \frac{2nk}{n^2 - k^2}, \tag{6.14}$$

$$f_{nk}^{[4]} := [(-1)^{n+k} - 1]\frac{nk(n^2 + k^2)}{(n^2 - k^2)^2}, \; f_{nk}^{[5]} := \frac{(-1)^{n+k} nk}{(n^2 - k^2)}, \tag{6.15}$$

where the superscripts are solely meant for notational purposes. In addition,

$$L_k(t) := p_0 \frac{k^2 \pi^2}{l^2} + \frac{\mu_0}{2}l. \tag{6.16}$$

6.3.2 A transformation to homogeneous boundary conditions on a fixed domain

The initial-boundary value problem with inhomogeneous boundary conditions can be put into a simpler form with homogeneous boundary conditions by introducing a transformation for the dependent variable. Moreover, the method of eigenfunction expansion which will be used further needs homogeneous boundary conditions. Let us use the following transformation

$$\hat{u}(x,t) := u(x,t) - s(H,t) - \frac{s(H-l,t) - s(H,t)}{l}x, \tag{6.17}$$

where s is given by (6.4). Next, we substitute (6.17) into (6.5a-6.5c), and change the spatial coordinate by $\xi = x/l$. Hence $\hat{u}(x,t;\varepsilon)$ becomes a new function $\bar{u}(\xi,t;\varepsilon)$, and the initial conditions change as follows $f(x) = \bar{f}(\xi)$ and $g(x) = \bar{g}(\xi)$. So, the initial-boundary value problem becomes

$$\bar{u}_{tt} - \frac{1}{l^2}\bar{u}_{\xi\xi} = -\varepsilon\left(\frac{p_0}{l^4}\bar{u}_{\xi\xi\xi\xi} - \frac{2}{l}(1-\xi)\bar{u}_{\xi t} + \frac{\mu_0}{l}(1-\xi)\bar{u}_{\xi\xi} + \frac{\mu_0}{l}\bar{u}_\xi + \xi l S_1 + S_2\right)$$
$$+ \mathcal{O}(\varepsilon^2), \tag{6.18a}$$

for $0 < \xi < 1$ and $t > 0$, subject to the BCs:

$$\bar{u}(0,t;\varepsilon) = \bar{u}_{\xi\xi}(0,t;\varepsilon) = 0,$$
$$\bar{u}(1,t;\varepsilon) = \bar{u}_{\xi\xi}(1,t;\varepsilon) = 0, \tag{6.18b}$$

for $t > 0$, and subject to the ICs:

$$\bar{u}(\xi,0;\varepsilon) = \varepsilon\bar{f}(\xi) + \mathcal{O}(\varepsilon^2),$$
$$\bar{u}_t(\xi,0;\varepsilon) = \varepsilon\left(\bar{g}(\xi) + S_0 + \frac{\xi}{l_0}\bar{u}_\xi(\xi,0;\varepsilon)\right) + \mathcal{O}(\varepsilon^2), \tag{6.18c}$$

for $0 < \xi < l_0$.

6.3.3 The Fourier series expansion

In accordance with the homogeneous boundary conditions, we expand all functions in (6.18a-6.18c) in a Fourier sine series

$$\bar{u}(\xi,t;\varepsilon) = \sum_{n=1}^{\infty} u_n(t;\varepsilon)\sin(n\pi\xi). \tag{6.19}$$

Substituting (6.19) into (6.18a-6.18c), multiplying the so-obtained equations by $\sin(k\pi\xi)$, integrating with respect to ξ from 0 to 1, and using the orthogonality of the sin-functions on $0 < \xi < 1$, we obtain the following ODEs for $k \in \mathbb{N}$,

$$\ddot{u}_k + \frac{k^2\pi^2}{l^2}u_k = -\varepsilon\left(\frac{1}{l}\dot{u}_k + \frac{k^2\pi^2}{l^2}L_k u_k + 2S_{k1} + 2S_{k2} + \frac{2}{l}\sum_{\substack{n=1 \\ n\neq k}}^{\infty}\left[f_{nk}^{[3]}\dot{u}_n + \mu_0 f_{nk}^{[4]}u_n\right]\right)$$
$$+ \mathcal{O}(\varepsilon^2), \tag{6.20a}$$

for $t > 0$, subject to the ICs:

$$u_k(0; \varepsilon) = 2\varepsilon F_k + \mathcal{O}(\varepsilon^2),$$

$$\dot{u}_k(0; \varepsilon) = 2\varepsilon \left(G_k + f_k^{[2]} S_0 + \frac{1}{l_0} \sum_{\substack{n=1 \\ n \neq k}}^{\infty} f_{nk}^{[5]} u_n(0; \varepsilon) \right) + \mathcal{O}(\varepsilon^2), \tag{6.20b}$$

where $l = l(t)$, and the Fourier coefficients are given by

$$F_k := \int_0^1 \bar{f}(\xi) \sin(k\pi\xi) \, d\xi, \quad G_k := \int_0^1 \bar{g}(\xi) \sin(k\pi\xi) \, d\xi.$$

6.3.4 The Liouville-Green transformation

The homogeneous equation for (6.20a),

$$\ddot{u}_k + \frac{k^2\pi^2}{l^2} u_k = 0, \tag{6.21}$$

can be interpreted as a linear oscillator (spring) with a slowly varying restoring force. Recall that $l = l_0 + \varepsilon t$. Equation (6.21) has an infinite sequence of large eigenvalues corresponding to rapid oscillations. The high oscillatory behavior implies that the variable coefficients in (6.21) may be approximated by constant ones over a few periods. Note that the periods are small due to large frequencies. Thus, let us approximate equation (6.20a) by one with constant coefficients by using the Liouville-Green transformation following from the *WKBJ method*[1]:

$$\tilde{t}(t) = \int_0^t \frac{ds}{l(s)} = \frac{1}{\varepsilon} \ln\left(1 + \frac{\varepsilon t}{l_0}\right). \tag{6.22}$$

In accordance with a new time variable, $u_k(t; \varepsilon)$ becomes a new function $\tilde{u}_k(\tilde{t}; \varepsilon)$. The initial value problem (6.20a-6.20b) becomes

$$\frac{d^2 \tilde{u}_k}{d\tilde{t}^2} + (k\pi)^2 \tilde{u}_k$$

$$= -\varepsilon \left(k^2\pi^2 \tilde{L}_k \tilde{u}_k + 2\tilde{l}^2 \left[\tilde{S}_{k1} + \tilde{S}_{k2} \right] + 2 \sum_{\substack{n=1 \\ n \neq k}}^{\infty} \left[f_{nk}^{[3]} \frac{d\tilde{u}_n}{d\tilde{t}} + \mu_0 f_{nk}^{[4]} \tilde{l} \tilde{u}_n \right] \right) + \mathcal{O}(\varepsilon^2), \tag{6.23a}$$

with the ICs:

$$\tilde{u}_k(0; \varepsilon) = 2\varepsilon F_k + \mathcal{O}(\varepsilon^2),$$

$$\frac{d\tilde{u}_k}{d\tilde{t}}(0; \varepsilon) = 2\varepsilon \left(l_0 G_k + f_k^{[2]} l_0 S_0 + \sum_{\substack{n=1 \\ n \neq k}}^{\infty} f_{nk}^{[5]} \tilde{u}_n(0; \varepsilon) \right) + \mathcal{O}(\varepsilon^2), \tag{6.23b}$$

---

[1] The WKBJ method is a method for finding approximate solutions to linear differential equations with varying coefficients [25, 1].

where $\tilde{l} = \tilde{l}(\varepsilon\tilde{t}) := l_0 e^{\varepsilon\tilde{t}}$, $\tilde{L}_k = \tilde{L}_k(\tilde{t}) := L_k(t)$, $\tilde{S}_{k1} = \tilde{S}_{k1}(\tilde{t}) := S_{k1}(t)$, and $\tilde{S}_{k2} = \tilde{S}_{k2}(\tilde{t}) := S_{k2}(t)$, where $t(\tilde{t}) = \frac{l_0}{\varepsilon}\left(e^{\varepsilon\tilde{t}} - 1\right)$.

6.4 Internal layer analysis

In this section, we determine resonance manifolds and their corresponding timescales. Beforehand, one should observe that the terms under the summation sign in the right-hand side of (6.23a) are nonsecular and can be omitted. At the same time, the rest of the terms require a thorough analysis. Continuing with the analysis of the secular terms, we consider

$$\frac{d^2\tilde{u}_k}{d\tilde{t}^2} + (k\pi)^2\tilde{u}_k = -\varepsilon\left(k^2\pi^2\tilde{L}_k\tilde{u}_k + 2\tilde{l}^2\left[\tilde{S}_{k1} + \tilde{S}_{k2}\right]\right), \tag{6.24}$$

instead of (6.23a).

6.4.1 Variation of constants

When $\varepsilon = 0$, the solution for (6.24) is well known, and it is given by a linear combination of $\sin(k\pi t)$ and $\cos(k\pi t)$. For $\varepsilon \neq 0$, according to the Lagrange variation of constants method [11], we assume that the general solution to the equation (6.24) has a similar form,

$$\tilde{u}_k(\tilde{t}) = A_k(\tilde{t})\cos(k\pi\tilde{t}) + B_k(\tilde{t})\sin(k\pi\tilde{t}), \tag{6.25}$$

where A_k and B_k are arbitrary functions. Further we need the following derivative,

$$\frac{d\tilde{u}_k}{d\tilde{t}}(\tilde{t}) = -k\pi A_k(\tilde{t})\sin(k\pi\tilde{t}) + k\pi B_k(\tilde{t})\cos(k\pi\tilde{t}), \tag{6.26}$$

where without loss of generality were assumed that

$$\dot{A}_k\cos(k\pi\tilde{t}) + \dot{B}_k\sin(k\pi\tilde{t}) = 0. \tag{6.27}$$

Then, substituting (6.25) and (6.26) into (6.24), we obtain

$$\dot{A}_k\sin(k\pi\tilde{t}) - \dot{B}_k\cos(k\pi\tilde{t}) = \varepsilon\left(k\pi\tilde{L}_k\left[A_k\cos(k\pi\tilde{t}) + B_k\sin(k\pi\tilde{t})\right] + \frac{2\tilde{l}^2}{k\pi}\left[\tilde{S}_{k1} + \tilde{S}_{k2}\right]\right). \tag{6.28}$$

Equations (6.27) and (6.28) constitute a system of two algebraic equations with respect to $\dot{A}_k$ and $\dot{B}_k$. By solving this system and using trigonometric identities, we find

$$\dot{A}_k = \varepsilon\left(\frac{k\pi\tilde{L}_k}{2}\big[A_k \sin(2k\pi\tilde{t}) - B_k \cos(2k\pi\tilde{t})\big] + \frac{k\pi\tilde{L}_k}{2}B_k\right.$$
$$\left. + \frac{2\tilde{l}^2}{k\pi}\big[\tilde{S}_{k1} + \tilde{S}_{k2}\big]\sin(k\pi\tilde{t})\right), \tag{6.29}$$

$$\dot{B}_k = -\varepsilon\left(\frac{k\pi\tilde{L}_k}{2}\big[A_k \cos(2k\pi\tilde{t}) + B_k \sin(2k\pi\tilde{t})\big] + \frac{k\pi\tilde{L}_k}{2}A_k\right.$$
$$\left. + \frac{2l^2}{k\pi}\big[\tilde{S}_{k1} + \tilde{S}_{k2}\big]\cos(k\pi\tilde{t})\right). \tag{6.30}$$

In (6.29) one should observe that $\big(\tilde{S}_{k1} + \tilde{S}_{k2}\big)\sin(k\pi\tilde{t})$ and $\big(\tilde{S}_{k1} + \tilde{S}_{k2}\big)\cos(k\pi\tilde{t})$ both contain products of trigonometric functions which lead to secular terms in $\tilde{u}_k(\tilde{t})$.

6.4.2 Resonance manifold detection

To study resonances in the system, we introduce the following time-like variables

$$\tau := \varepsilon\tilde{t}, \ \phi_k := k\pi\tilde{t}, \ \psi := \frac{\lambda^2 l_0}{\varepsilon}(e^\tau - 1), \text{ and } \theta := \lambda l_0 e^\tau. \tag{6.31}$$

Note that these time-like variables monotonically increase with time. Accordingly, we rewrite system (6.29) as

$$\dot{A}_k = \varepsilon\left(\frac{k\pi\tilde{L}_k}{2}\big[A_k \sin 2\phi_k - B_k \cos 2\phi_k\big] + \frac{k\pi\tilde{L}_k}{2}B_k\right.$$
$$\left. + \frac{2\tilde{l}^2}{k\pi}\big[\check{S}_{k1} \sin\psi + \check{S}_{k2} \cos\psi\big]\sin\phi_k\right), \tag{6.32}$$

$$\dot{B}_k = -\varepsilon\left(\frac{k\pi\tilde{L}_k}{2}\big[A_k \cos 2\phi_k + B_k \sin 2\phi_k\big] + \frac{k\pi\tilde{L}_k}{2}A_k\right.$$
$$\left. + \frac{2\tilde{l}^2}{k\pi}\big[\check{S}_{k1} \sin\psi + \check{S}_{k2} \cos\psi\big]\cos\phi_k\right), \tag{6.33}$$

combined with the slow/fast variables

$$\dot{\tau} = \varepsilon, \qquad\qquad \tau(0) = 0, \tag{6.34}$$
$$\dot{\theta} = \varepsilon\lambda l_0 e^\tau, \qquad\qquad \theta(0) = \lambda l_0, \tag{6.35}$$
$$\dot{\phi}_k = k\pi, \qquad\qquad \phi_k(0) = 0, \tag{6.36}$$
$$\dot{\psi} = \lambda^2 l_0 e^\tau, \qquad\qquad \psi(0) = 0. \tag{6.37}$$

Remark that we introduced θ more for convenience than necessity in the slow-fast analysis. Note that here the dot notation means differentiation with respect to $\tilde{t}$ and not to t, $\tilde{l} = \tilde{l}(\tau)$, $\tilde{L} = \tilde{L}(\tau)$, and $\check{S}_{k1}$, $\check{S}_{k2}$ are given by

$$\check{S}_{k1}(\tau, \theta) := A_0 \lambda^4 f_k^{[1]} \big(2\beta[1 - \tilde{l}] + \Phi(\theta)\big), \tag{6.38}$$

$$\check{S}_{k2}(\tau, \theta) := -\frac{A_0 \lambda^2}{\tilde{l}} f_k^{[2]} \big(2\beta + \Phi(\theta)\big). \tag{6.39}$$

Note the last two variables ϕ_k and ψ in (6.32) are fast-varying, while the rest, τ and θ, are slow. Keep in mind that the system can be averaged over the fast variables [11]. Combining $\sin\phi_k$ and $\cos\phi_k$ with $\sin\psi$ and $\cos\psi$, we obtain the following combinations of arguments $\phi_k + \psi$, $\phi_k - \psi$. So the resonance zone is active when

$$\dot{\phi}_k - \dot{\psi} \approx 0, \tag{6.40}$$

corresponding to the manifold $\tau \approx \ln\left(\frac{k\pi}{\lambda^2 l_0}\right)$, where $k\pi > \lambda^2 l_0$ for $k \in \mathbb{N}$. Note that when $k\pi = \lambda^2 l_0$, resonance occurs at time $\tau = 0$ and the system can stabilize after the timescale of order $\varepsilon^{-\frac{1}{2}}$. In case when $k\pi < \lambda^2 l_0$, the system is stable for that particular k-th mode. Observe that ϕ_k, ψ, and $\phi_k + \psi$ are time-like; consequently, they do not play a part in resonance. Next, the size of the emerged resonance zones has to be established. Note that this size will also be used as a new asymptotic scale in the subsequent section for the construction of a formal approximation.

6.4.3 Averaging inside the resonance zone

For the sake of convenience let us introduce the following combination argument $\chi_k = \phi_k - \psi$, and a distinguished parameter $\delta(\varepsilon) = o(1)$ as $\varepsilon \to 0$ to be determined later. In order to study the behavior of the solution in the resonance zone, we rescale τ as follows:

$$\tau = \delta(\varepsilon)\tau_k + \ln\left(\frac{k\pi}{\lambda^2 l_0}\right), \tag{6.41}$$

where τ_k is a new local variable. Observe that

$$\dot{\chi}_k = \dot{\phi}_k - \dot{\psi}_k = -\delta(\varepsilon)k\pi\tau_k + \mathcal{O}\big(\delta^2(\varepsilon)\big).$$

Let us rewrite system (6.32), using trigonometric identities, as

$$\dot{A}_k = \varepsilon\bigg(\frac{k\pi\tilde{L}_k}{2}\big[A_k\sin 2\phi_k - B_k\cos 2\phi_k\big] + \frac{k\pi\tilde{L}_k}{2}B_k + \frac{\tilde{l}^2}{k\pi}\bar{S}_{k1}[\cos\chi_k - \cos(\phi_k + \psi_k)]$$

$$+ \frac{\tilde{l}^2}{k\pi}\bar{S}_{k2}[\sin\chi_k + \sin(\phi_k + \psi_k)]\bigg), \tag{6.42}$$

$$\dot{B}_k = -\varepsilon\bigg(\frac{k\pi\tilde{L}_k}{2}\big[A_k\cos 2\phi_k + B_k\sin 2\phi_k\big] + \frac{k\pi\tilde{L}_k}{2}A_k + \frac{\tilde{l}^2}{k\pi}\bar{S}_{k1}[\sin(\phi_k + \psi_k) - \sin\chi_k]$$

$$+ \frac{\tilde{l}^2}{k\pi}\bar{S}_{k2}[\cos\chi_k + \cos(\phi_k + \psi_k)]\bigg), \tag{6.43}$$

combined with the slow/fast variables

$$\dot{\tau}_k = \frac{\varepsilon}{\delta(\varepsilon)}, \qquad\qquad \tau_k(0) = -\frac{1}{\delta(\varepsilon)}\ln\left(\frac{k\pi}{\lambda^2 l_0}\right), \qquad (6.44)$$

$$\dot{\theta}_k = \varepsilon\lambda l_0 e^{\delta(\varepsilon)\tau_k}, \qquad\qquad \theta_k(0) = \lambda l_0, \qquad\qquad (6.45)$$

$$\dot{\chi}_k = -\delta(\varepsilon)k\pi\tau_k, \qquad\qquad \chi_k(0) = 0, \qquad\qquad (6.46)$$

$$\dot{\phi}_k = k\pi, \qquad\qquad \phi_k(0) = 0, \qquad\qquad (6.47)$$

$$\dot{\psi}_k = \lambda^2 l_0 e^{\delta(\varepsilon)\tau_k}, \qquad\qquad \psi_k(0) = 0. \qquad\qquad (6.48)$$

Note that the dot notation means differentiation with respect to $\tilde{t}$, and the arguments of the following notations are omitted, $\tilde{l} = \tilde{l}(\tau_k)$, $\bar{S}_{k1} = \check{S}_{k1}(\tau_k, \theta_k)$, and $\bar{S}_{k2} = \check{S}_{k2}(\tau_k, \theta_k)$. In order to balance the equations of the system (6.42), we have to choose $\delta(\varepsilon) = \sqrt{\varepsilon}$. This value determines the size of the resonance layer. With this choice, the equations for the time-like variables become

$$\dot{\tau}_k = \sqrt{\varepsilon}, \ \dot{\chi}_k = -\sqrt{\varepsilon}k\pi\tau_k + \mathcal{O}(\varepsilon), \ \dot{\psi}_k = \lambda^2 l_0 e^{\sqrt{\varepsilon}\tau_k}, \text{ and } \dot{\theta}_k = \varepsilon\lambda l_0 e^{\sqrt{\varepsilon}\tau_k}. \qquad (6.49)$$

The right-hand sides of the equations for A_k and B_k in (6.42) are 2π-periodic in ϕ_k and ψ_k. So let us average system (6.42), taking into account (6.49), over the fast variables. The system takes the following form

$$\dot{A}_k^a = \varepsilon\left(\frac{k\pi\tilde{L}_k^a}{2}B_k^a + \frac{\tilde{l}_a^2}{k\pi}\left[S_{k1}^a\cos\chi_k^a + S_{k2}^a\sin\chi_k^a\right]\right), \qquad (6.50)$$

$$\dot{B}_k^a = -\varepsilon\left(\frac{k\pi\tilde{L}_k^a}{2}A_k^a + \frac{\tilde{l}_a^2}{k\pi}\left[-S_{k1}^a\sin\chi_k^a + S_{k2}^a\cos\chi_k^a\right]\right), \qquad (6.51)$$

combined with the slow/fast variables

$$\dot{\tau}_k^a = \sqrt{\varepsilon}, \qquad\qquad \tau_k^a(0) = -\frac{1}{\sqrt{\varepsilon}}\ln\left(\frac{k\pi}{\lambda^2 l_0}\right), \qquad (6.52)$$

$$\dot{\theta}_k^a = \varepsilon\lambda l_0 e^{\sqrt{\varepsilon}\tau_k^a}, \qquad\qquad \theta_k^a(0) = \lambda l_0, \qquad\qquad (6.53)$$

$$\dot{\chi}_k^a = -\sqrt{\varepsilon}k\pi\tau_k^a, \qquad\qquad \chi_a(0) = 0, \qquad\qquad (6.54)$$

where $\tilde{l} = \tilde{l}_a(\tau_k^a)$, $S_{k1}^a = \check{S}_{k1}(\tau_k^a, \theta_k^a)$, and $S_{k2}^a = \check{S}_{k2}(\tau_k^a, \theta_k^a)$. Note that we have replaced A_k, B_k, τ_k, θ_k, χ_k, $\tilde{l}$, and $\tilde{L}_k$ by A_k^a, B_k^a, τ_k^a, θ_k^a, χ_k^a, $\tilde{l}_a$, and $\tilde{L}_k^a$ respectively, since the averaged equations define different vector functions but are still valid on the timescale of $\mathcal{O}(\varepsilon^{-\frac{1}{2}})$ as long as we do not leave the $\mathcal{O}(\sqrt{\varepsilon})$-neighborhood of the resonance manifold.

6.4.4 Averaging outside the resonance zone

Outside the resonance manifold, we average the right-hand side of the first equations in (6.32) over ϕ_k and ψ while keeping A_k and B_k fixed. Note that second terms, $\frac{k\pi}{2}\tilde{L}_k B_k$ and $\frac{k\pi}{2}\tilde{L}_k A_k$, are slowly varying, therefore they will not average out; at the same time the average of the first terms over ϕ_k is zero. The last terms consist of the fast varying

terms outside the resonance zone. Thus, averaging of (6.32) over ϕ_k and ψ results in the following approximate equations

$$\frac{dA_k^a}{d\tilde{t}} - \varepsilon \frac{k\pi\tilde{L}_k^a}{2}B_k^a = 0,$$
$$\frac{dB_k^a}{d\tilde{t}} + \varepsilon \frac{k\pi\tilde{L}_k^a}{2}A_k^a = 0,$$

(6.55)

with $A_k^a(0) = A_k(0)$ and $B_k^a(0) = B_k(0)$, and where $\tilde{L}_k^a$ is a function of $\varepsilon\tilde{t}$. The solution of system (6.55) can be readily found by using the method of separation of variables, and it is given by

$$A_k^a(\tilde{t}) = \sqrt{A_k^2(0) + B_k^2(0)} \cos\left(-\frac{k\pi}{4}r_k(\tilde{t}) + q_k\right),$$
$$B_k^a(\tilde{t}) = \sqrt{A_k^2(0) + B_k^2(0)} \sin\left(-\frac{k\pi}{4}\tilde{t}_k(t) + q_k\right),$$

where r_k and q_k are given by

$$r_k(\tilde{t}) = \left(-p_0\frac{k^2\pi^2}{\tilde{l}^2(\varepsilon\tilde{t})} + \mu_0\tilde{l}(\varepsilon\tilde{t})\right),$$
$$q_k = \arctan\left(\frac{B_k(0)}{A_k(0)}\right) + \frac{k\pi}{4}\left(-p_0\frac{k^2\pi^2}{l_0^2} + \mu_0 l_0\right),$$

for $k \in \mathbb{N}$.

6.5 Formal approximation

In the previous section we found that the resonances emerged repeatedly in the neighborhood of time instants τ_k for $k \in \mathbb{N}$. First of all, in order to construct accurate approximations in the neighborhood of τ_k, we rescale it as follows:

$$\tau_k = \hat{t} + \frac{1}{\varepsilon}\ln\left(\frac{k\pi}{\lambda^2 l_0}\right),$$

(6.56)

where $\hat{t}$ is a new local variable. Consequently, $\tilde{u}_k(\tilde{t}; \varepsilon)$ becomes a new function $y_k(\hat{t}; \varepsilon)$ in (6.23a-6.23b). Correspondingly, the initial-value problem takes the following form up to $\mathcal{O}(\varepsilon)$. The ODE is given by

$$\ddot{y}_k + (k\pi)^2 y_k = -\varepsilon\left(k^2\pi^2\hat{L}_k y_k + 2\hat{l}_k^2[\hat{S}_{k1} + \hat{S}_{k2}] + 2\sum_{\substack{n=1 \\ n \neq k}}^{\infty}\left[f_{nk}^{[3]}\dot{y}_n + \mu_0 f_{nk}^{[4]}\hat{l}_n y_n\right]\right),$$

(6.57a)

for $t > 0$, subject to the ICs:

$$y_k(a_k; \varepsilon) = 2\varepsilon F_k,$$

$$\dot{y}_k(a_k; \varepsilon) = 2\varepsilon\left(l_0 G_k + f_k^{[2]} l_0 S_0 + \sum_{\substack{n=1 \\ n \neq k}}^{\infty} f_{nk}^{[5]} y_n(a_n; \varepsilon)\right), \tag{6.57b}$$

where $a_k := -\frac{1}{\varepsilon} \ln\left(\frac{k\pi}{\lambda^2 l_0}\right)$, $\hat{l}_k(\varepsilon\hat{t}) := \frac{k\pi}{\lambda^2} e^{\varepsilon\hat{t}}$, and

$$\hat{L}_k(\varepsilon\hat{t}) := p_0 \frac{k^2\pi^2}{\hat{l}^2(\varepsilon\hat{t})} + \frac{\mu_0}{2}\hat{l}(\varepsilon\hat{t}), \tag{6.58}$$

$$\hat{S}_{k1}(\hat{t}) := A_0\lambda^4 f_k^{[1]}\big(2\beta[1 - \hat{l}_k] + \Phi(\hat{\theta}_k)\big)\sin\hat{\psi}_k, \tag{6.59}$$

$$\hat{S}_{k2}(\hat{t}) := -\frac{A_0\lambda^2 f_k^{[2]}}{\hat{l}_k}\big(2\beta + \Phi(\hat{\theta}_k)\big)\cos\hat{\psi}_k, \tag{6.60}$$

where the time-like variables $\hat{\psi}_k$ and $\hat{\theta}_k$ have the form, respectively,

$$\hat{\psi}_k = \frac{1}{\varepsilon}\big(k\pi e^{\varepsilon\hat{t}} - \lambda^2 l_0\big), \text{ and } \hat{\theta}_k = \frac{k\pi}{\lambda} e^{\varepsilon\hat{t}}, \tag{6.61}$$

respectively.

It has been shown in the previous section that the $\mathcal{O}(\varepsilon)$ excitations produce an unexpected timescale of $\mathcal{O}\left(\varepsilon^{-\frac{1}{2}}\right)$. Therefore we introduce the following three timescales

$$t_0 = \hat{t}, \ t_1 = \sqrt{\varepsilon}\hat{t}, \text{ and } t_2 = \varepsilon\hat{t} \tag{6.62}$$

as natural timescales for this problem. As a consequence, the solution $y_k(\hat{t}; \varepsilon)$ is rewritten as a function of three timescales $w_k(t_0, t_1, t_2; \sqrt{\varepsilon})$. Time derivatives of y_k will transform, correspondingly, as follows:

$$\dot{y}_k = \frac{\partial w_k}{\partial t_0} + \sqrt{\varepsilon}\frac{\partial w_k}{\partial t_1} + \varepsilon\frac{\partial w_k}{\partial t_2}, \tag{6.63}$$

$$\ddot{y}_k = \frac{\partial^2 w_k}{\partial t_0^2} + 2\sqrt{\varepsilon}\frac{\partial^2 w_k}{\partial t_0 \partial t_1} + \varepsilon\left(\frac{\partial^2 w_k}{\partial t_1^2} + 2\frac{\partial^2 w_k}{\partial t_0 \partial t_2}\right) + 2\varepsilon\sqrt{\varepsilon}\frac{\partial^2 w_k}{\partial t_1 \partial t_2}. \tag{6.64}$$

As a next step, according to the three-timescales perturbation method, w_k can be approximated by the following formal asymptotic expansion

$$w_k(t_0, t_1, t_2; \sqrt{\varepsilon}) \sim \sqrt{\varepsilon}w_{k0}(t_0, t_1, t_2) + \varepsilon w_{k1}(t_0, t_1, t_2) + \varepsilon\sqrt{\varepsilon}w_{k2}(t_0, t_1, t_2) + \cdots. \tag{6.65}$$

Substituting (6.65) into the recently obtained initial value problem and collecting terms of like powers of ε, we will obtain a set of problems of different order of smallness. Note that one has to distinguish between the solutions inside and outside the resonance zones while constructing a formal approximation.

6.5.1 The $\mathcal{O}(\sqrt{\varepsilon})$-problem

Equating the coefficients of like powers of $\sqrt{\varepsilon}$, we obtain an equation which can be interpreted as a simple harmonic oscillator for the k-th oscillation mode of the PDE:

$$\frac{\partial^2 w_{k0}}{\partial t_0^2} + (k\pi)^2 w_{k0} = 0, \tag{6.66a}$$

for $t > 0$, with the ICs:

$$w_{k0}(a_k, b_k, c_k) = 0,$$
$$\frac{\partial w_{k0}}{\partial t_0}(a_k, b_k, c_k) = 0, \tag{6.66b}$$

where a_k is introduced in (6.57b), $b_k := -\frac{\sqrt{\varepsilon}}{\varepsilon}\ln\left(\frac{k\pi}{\lambda^2 l_0}\right)$, and $c_k := -\ln\left(\frac{k\pi}{\lambda^2 l_0}\right)$. The general solution of this problem is given by

$$w_{k0}(t_0, t_1, t_2) = A_{k0}(t_1, t_2)\cos(k\pi t_0) + B_{k0}(t_1, t_2)\sin(k\pi t_0), \tag{6.67}$$

where A_{k0} and B_{k0} are unknown functions yet, and can be obtained from the secularity conditions for the higher-order problems. It can be observed from the initial conditions (6.66b) that $A_{k0}(b_k, c_k) = B_{k0}(b_k, c_k) = 0$.

6.5.2 The $\mathcal{O}(\varepsilon)$-problem

By collecting terms of equal powers in ε, we obtain the following problem to solve:

$$\frac{\partial^2 w_{k1}}{\partial t_0^2} + (k\pi)^2 w_{k1} = -2\frac{\partial^2 w_{k0}}{\partial t_0 \partial t_1} - 2\hat{l}_k^2\left[\hat{S}_{k1} + \hat{S}_{k2}\right], \tag{6.68a}$$

for $t > 0$, with the ICs:

$$w_{k1}(a_k, b_k, c_k) = 2F_k,$$
$$\frac{\partial w_{k1}}{\partial t_0}(a_k, b_k, c_k) = -\frac{\partial w_{k0}}{\partial t_1}(a_k, b_k, c_k) + 2l_0 G_k - f_k^{[2]} l_0 S_0. \tag{6.68b}$$

Using (6.67), we rewrite (6.68a) as follows:

$$\frac{\partial^2 w_{k1}}{\partial t_0^2} + (k\pi)^2 w_{k1} = 2k\pi\left[\frac{\partial A_{k0}}{\partial t_1}\sin(k\pi t_0) - \frac{\partial B_{k0}}{\partial t_1}\cos(k\pi t_0)\right] - 2\hat{l}_k^2\left[\hat{S}_{k1} + \hat{S}_{k2}\right]. \tag{6.69}$$

We will find an explicit solution for this problem inside and outside the resonance zone.

Inside the resonance zone

First of all let us take a closer look at the functions $\hat{S}_{k1}$ and $\hat{S}_{k2}$ given by (6.59) and (6.60), respectively. They contain products of trigonometric functions, which might cause secular terms. These products lead to sums or differences of their arguments namely $\hat{\psi}_k + \hat{\theta}_k$ or $\hat{\psi}_k - \hat{\theta}_k$, respectively. In accordance with the timescale of $\mathcal{O}\left(\varepsilon^{-\frac{1}{2}}\right)$, it is convenient to expand these arguments in a Taylor series in ε:

$$\hat{\psi}_k = k\pi t_0 + \frac{1}{2}k\pi t_1^2 + \sigma_k^{[0]} + \mathcal{O}(\sqrt{\varepsilon}) \text{ with } \sigma_k^{[0]} := \frac{1}{\varepsilon}(k\pi - \lambda^2 l_0),$$

$$\hat{\psi}_k - \hat{\theta}_k = k\pi t_0 + \frac{1}{2}k\pi t_1^2 + \sigma_k^{[-]} + \mathcal{O}(\sqrt{\varepsilon}) \text{ with } \sigma_k^{[-]} := \frac{1}{\varepsilon}(k\pi - \lambda^2 l_0) - \frac{k\pi}{\lambda},$$

$$\hat{\psi}_k + \hat{\theta}_k = k\pi t_0 + \frac{1}{2}k\pi t_1^2 + \sigma_k^{[+]} + \mathcal{O}(\sqrt{\varepsilon}) \text{ with } \sigma_k^{[+]} := \frac{1}{\varepsilon}(k\pi - \lambda^2 l_0) + \frac{k\pi}{\lambda},$$

where $\sigma_k^{[0]}$, $\sigma_k^{[-]}$, $\sigma_k^{[+]}$ are the phases. With these new notations, we rewrite (6.69) as follows

$$\frac{\partial^2 w_{k1}}{\partial t_0^2} + (k\pi)^2 w_{k1} = \left(2k\pi \frac{\partial A_{k0}}{\partial t_1} + \hat{S}_{k1}^{[1]} - \hat{S}_{k2}^{[2]}\right)\sin(k\pi t_0) - \left(2k\pi \frac{\partial B_{k0}}{\partial t_1} - \hat{S}_{k1}^{[2]} + \hat{S}_{k2}^{[1]}\right)$$
$$\times \cos(k\pi t_0),$$

where

$$\hat{S}_{k1}^{[1]}(t_1, t_2) := A_0 \lambda^4 \hat{l}_k^2 f_k^{[1]}\left(4\beta \hat{l}_k \cos\left(\frac{1}{2}k\pi t_1^2 + \sigma_k^{[0]}\right) - \hat{S}_{k2}^{[1]}\right), \tag{6.70}$$

$$\hat{S}_{k1}^{[2]}(t_1, t_2) := A_0 \lambda^4 \hat{l}_k^2 f_k^{[1]}\left(4\beta \hat{l}_k \sin\left(\frac{1}{2}k\pi t_1^2 + \sigma_k^{[0]}\right) - \hat{S}_{k2}^{[2]}\right), \tag{6.71}$$

where $\hat{l} = \hat{l}_k(t_2)$, and

$$\hat{S}_{k2}^{[1]}(t_1, t_2) := 2\left[2\beta - \beta \cosh \hat{\theta}_k - \gamma_1 \sinh \hat{\theta}_k\right]\cos\left(\frac{1}{2}k\pi t_1^2 + \sigma_k^{[0]}\right)$$
$$+ \beta\left[\cos\left(\frac{1}{2}k\pi t_1^2 + \sigma_k^{[-]}\right) + \cos\left(\frac{1}{2}k\pi t_1^2 + \sigma_k^{[+]}\right)\right]$$
$$+ \gamma_2\left[\sin\left(\frac{1}{2}k\pi t_1^2 + \sigma_k^{[-]}\right) - \sin\left(\frac{1}{2}k\pi t_1^2 + \sigma_k^{[+]}\right)\right], \tag{6.72}$$

$$\hat{S}_{k2}^{[2]}(t_1, t_2) := 2\left[2\beta - \beta \cosh \hat{\theta}_k - \gamma_1 \sinh \hat{\theta}_k\right]\sin\left(\frac{1}{2}k\pi t_1^2 + \sigma_k^{[0]}\right)$$
$$- \beta\left[\sin\left(\frac{1}{2}k\pi t_1^2 + \sigma_k^{[-]}\right) + \sin\left(\frac{1}{2}k\pi t_1^2 + \sigma_k^{[+]}\right)\right]$$
$$+ \gamma_2\left[\cos\left(\frac{1}{2}k\pi t_1^2 + \sigma_k^{[-]}\right) - \cos\left(\frac{1}{2}k\pi t_1^2 + \sigma_k^{[+]}\right)\right]. \tag{6.73}$$

The solution w_{k1} produces unbounded terms in t_0 unless

$$\frac{\partial A_{k0}}{\partial t_1} + \frac{1}{2k\pi}\left(\hat{S}_{k1}^{[1]} - \hat{S}_{k2}^{[2]}\right) = 0, \tag{6.74}$$

$$\frac{\partial B_{k0}}{\partial t_1} - \frac{1}{2k\pi}\left(\hat{S}_{k1}^{[2]} + \hat{S}_{k2}^{[1]}\right) = 0. \tag{6.75}$$

By straightforward integration we obtain

$$A_{k0}(t_1, t_2) = -\frac{A_0 \lambda^4 \hat{l}_k}{2k\sqrt{k}\pi}\left(f_k^{[1]}\hat{I}_{k1}^{[1]} + f_k^{[2]}\hat{I}_{k2}^{[2]}\right) + C_{k0}(t_2), \tag{6.76}$$

$$B_{k0}(t_1, t_2) = \frac{A_0 \lambda^4 \hat{l}_k}{2k\sqrt{k}\pi}\left(f_k^{[1]}\hat{I}_{k1}^{[2]} + f_k^{[2]}\hat{I}_{k2}^{[1]}\right) + D_{k0}(t_2), \tag{6.77}$$

where C_{k0} and D_{k0} are unknown functions which can be obtained from the $\mathcal{O}(\varepsilon\sqrt{\varepsilon})$-problem, and where

$$\hat{I}_{k1}^{[1]}(t_1, t_2) := \hat{l}_k\left[4\beta\hat{l}_k\left(\cos\sigma_k^{[0]}\mathrm{C}_{\mathrm{Fr}}(\sqrt{k}t_1) - \sin\sigma_k^{[0]}\mathrm{S}_{\mathrm{Fr}}(\sqrt{k}t_1)\right) - \hat{I}_{k2}^{[1]}\right], \tag{6.78}$$

$$\hat{I}_{k1}^{[2]}(t_1, t_2) := \hat{l}_k\left[4\beta\hat{l}_k\left(\cos\sigma_k^{[0]}\mathrm{S}_{\mathrm{Fr}}(\sqrt{k}t_1) + \sin\sigma_k^{[0]}\mathrm{C}_{\mathrm{Fr}}(\sqrt{k}t_1)\right) + \hat{I}_{k2}^{[2]}\right], \tag{6.79}$$

where

$$\hat{I}_{k2}^{[1]}(t_1, t_2) := 2\left[2\beta - \beta\cosh\hat{\theta}_k - \gamma_1\sinh\hat{\theta}_k\right]\left[\cos\sigma_k^{[0]}\mathrm{C}_{\mathrm{Fr}}(\sqrt{k}t_1) - \sin\sigma_k^{[0]}\mathrm{S}_{\mathrm{Fr}}(\sqrt{k}t_1)\right]$$
$$- \beta\left[(\cos\sigma_k^{[-]} + \cos\sigma_k^{[+]})\mathrm{C}_{\mathrm{Fr}}(\sqrt{k}t_1) - (\sin\sigma_k^{[-]} + \sin\sigma_k^{[+]})\mathrm{S}_{\mathrm{Fr}}(\sqrt{k}t_1)\right]$$
$$- \gamma_2\left[(\cos\sigma_k^{[-]} - \cos\sigma_k^{[+]})\mathrm{S}_{\mathrm{Fr}}(\sqrt{k}t_1) + (\sin\sigma_k^{[-]} - \sin\sigma_k^{[+]})\mathrm{C}_{\mathrm{Fr}}(\sqrt{k}t_1)\right], \tag{6.80}$$

$$\hat{I}_{k2}^{[2]}(t_1, t_2) := -2\left[2\beta - \beta\cosh\hat{\theta}_k - \gamma_1\sinh\hat{\theta}_k\right]\left[\cos\sigma_k^{[0]}\mathrm{S}_{\mathrm{Fr}}(\sqrt{k}t_1) + \sin\sigma_k^{[0]}\mathrm{C}_{\mathrm{Fr}}(\sqrt{k}t_1)\right]$$
$$+ \beta\left[(\cos\sigma_k^{[-]} + \cos\sigma_k^{[+]})\mathrm{S}_{\mathrm{Fr}}(\sqrt{k}t_1) + (\sin\sigma_k^{[-]} + \sin\sigma_k^{[+]})\mathrm{C}_{\mathrm{Fr}}(\sqrt{k}t_1)\right]$$
$$- \gamma_2\left[(\cos\sigma_k^{[-]} - \cos\sigma_k^{[+]})\mathrm{C}_{\mathrm{Fr}}(\sqrt{k}t_1) - (\sin\sigma_k^{[-]} - \sin\sigma_k^{[+]})\mathrm{S}_{\mathrm{Fr}}(\sqrt{k}t_1)\right], \tag{6.81}$$

where S_{Fr} and C_{Fr} are the Fresnel integrals given by

$$\mathrm{S}_{\mathrm{Fr}}(t) := \int_0^t \sin\left(\frac{1}{2}\pi x^2\right)\mathrm{d}x, \text{ and } \mathrm{C}_{\mathrm{Fr}}(t) := \int_0^t \cos\left(\frac{1}{2}\pi x^2\right)\mathrm{d}x. \tag{6.82}$$

Actually the presence of the Fresnel integrals in the expressions for amplitudes of vibrations cause resonance jumps in the system causing the effect of autoresonance. The integrals $\mathrm{S}_{\mathrm{Fr}}(\sqrt{k}t_1)$ and $\mathrm{C}_{\mathrm{Fr}}(\sqrt{k}t_1)$ are plotted for the third oscillation mode with $l_0 = 0.7$ and $\lambda = 1.875$ in Figure 6.2.
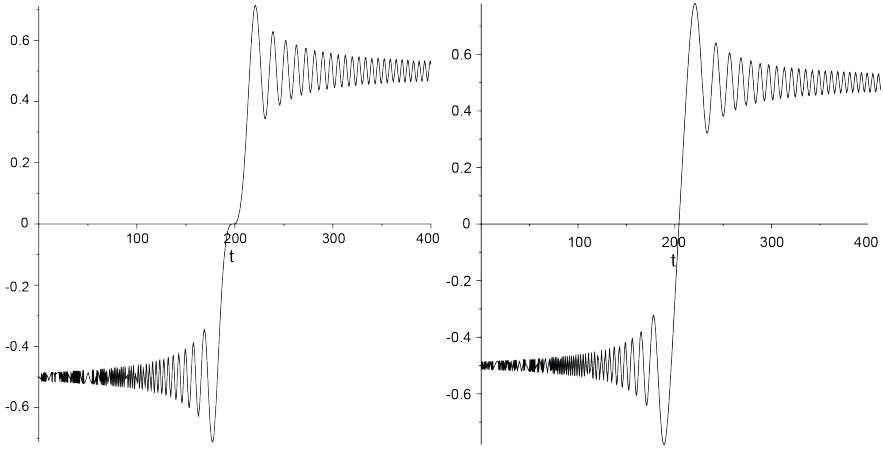
Figure 6.2: Fresnel integrals (a) $S_{Fr}(\sqrt{k}t_1)$ and (b) $C_{Fr}(\sqrt{k}t_1)$ for the third oscillation mode ($k = 3$).

Outside the resonance zone

It should be observed that the last two terms in (6.69) do not give rise to secular terms in w_{k1}. To prevent secular terms there, A_{k0} and B_{k0} have to satisfy the following conditions

$$\frac{\partial A_{k0}}{\partial t_1} = 0, \text{ and } \frac{\partial B_{k0}}{\partial t_1} = 0, \tag{6.83}$$

which have, respectively, the following solutions

$$A_{k0}(t_1, t_2) = \tilde{C}_{k0}(t_2), \text{ and } B_{k0}(t_1, t_2) = \tilde{D}_{k0}(t_2), \tag{6.84}$$

where $\tilde{C}_{k0}$ and $\tilde{D}_{k0}$ are unknown functions and can be obtained by removing secular terms from the $\mathcal{O}(\varepsilon\sqrt{\varepsilon})$-problem. From the initial conditions (6.66b), it follows that $\tilde{C}_{k0}(c_k) = \tilde{D}_{k0}(c_k) = 0$.

General solution

Taking into account the secularity conditions (6.74) and (6.75), the general solution for (6.68a) is given by

$$w_{k1}(t_0, t_1, t_2) = A_{k1}(t_1, t_2)\cos(k\pi t_0) + B_{k1}(t_1, t_2)\sin(k\pi t_0), \tag{6.85}$$

where A_{k1} and B_{k1} are unknown functions and may be determined from higher-order problems. The initial values of A_{k1} and B_{k1} are found from the initial conditions (6.68b)

as follows:

$$A_{k1}(b_k, c_k) = 2F_k \cos(k\pi a_k) + \frac{\sin(k\pi a_k)}{k\pi}\left(\frac{\partial A_{k0}}{\partial t_1}(b_k, c_k)\cos(k\pi a_k)\right.$$

$$\left. + \frac{\partial B_{k0}}{\partial t_1}(b_k, c_k)\sin(k\pi a_k) - 2l_0 G + f_k^{[2]} l_0 S_0 \right),$$

$$B_{k1}(b_k, c_k) = 2F_k \sin(k\pi a_k) - \frac{\cos(k\pi a_k)}{k\pi}\left(\frac{\partial A_{k0}}{\partial t_1}(b_k, c_k)\cos(k\pi a_k)\right.$$

$$\left. + \frac{\partial B_{k0}}{\partial t_1}(b_k, c_k)\sin(k\pi a_k) - 2l_0 G + f_k^{[2]} l_0 S_0 \right),$$

where, *inside* the resonance manifold,

$$\frac{\partial A_{k0}}{\partial t_1}(b_k, c_k) = -\frac{1}{2k\pi}\left(\hat{S}_{k1}^{[1]}(b_k, c_k) - \hat{S}_{k2}^{[2]}(b_k, c_k)\right),$$

$$\frac{\partial B_{k0}}{\partial t_1}(b_k, c_k) = \frac{1}{2k\pi}\left(\hat{S}_{k1}^{[2]}(b_k, c_k) + \hat{S}_{k2}^{[1]}(b_k, c_k)\right),$$

where $\hat{S}_{k1}^{[i]}$ and $\hat{S}_{k2}^{[i]}$ for $i = 1, 2$ are given by (6.70-6.73). *Outside* the resonance manifold, $\frac{\partial A_{k0}}{\partial t_1}(b_k, c_k)$ and $\frac{\partial B_{k0}}{\partial t_1}(b_k, c_k)$ are equal to zero.

6.5.3 The $\mathcal{O}(\varepsilon\sqrt{\varepsilon})$-problem

Here we collect terms of equal powers of $\varepsilon^{\frac{3}{2}}$ and consider the last problem in this chapter finalizing the construction of the formal approximation:

$$\frac{\partial^2 w_{k2}}{\partial t_0^2} + (k\pi)^2 w_{k2} = -2\frac{\partial^2 w_{k1}}{\partial t_0 \partial t_1} - 2\frac{\partial^2 w_{k0}}{\partial t_0 \partial t_2} - \frac{\partial^2 w_{k0}}{\partial t_1^2} - (k\pi)^2 \hat{L}_k w_{k0}$$

$$+ 2\sum_{\substack{n=1 \\ n \neq k}}^{\infty}\left(f_{nk}^{[3]}\frac{\partial w_{n0}}{\partial t_0} + \mu_0 f_{nk}^{[4]} \hat{l}_n w_{n0}\right), \quad (6.86a)$$

for $t > 0$, subject to the ICs:

$$w_{k2}(a_k, b_k, c_k) = 0,$$

$$\frac{\partial w_{k2}}{\partial t_0}(a_k, b_k, c_k) = -\frac{\partial w_{k1}}{\partial t_1}(a_k, b_k, c_k) - \frac{\partial w_{k0}}{\partial t_2}(a_k, b_k, c_k). \quad (6.86b)$$

Substituting (6.67) and (6.85) into (6.86a) and rearranging the so-obtained equation,

we obtain

$$
\frac{\partial^2 w_{k2}}{\partial t_0^2} + (k\pi)^2 w_{k2} = 2k\pi\left(\frac{\partial A_{k1}}{\partial t_1} + \frac{\partial A_{k0}}{\partial t_2} - \frac{1}{2k\pi}\frac{\partial B_{k0}^2}{\partial t_1^2} - \frac{k\pi}{2}\hat{L}_k B_{k0}\right)\sin(k\pi t_0)
$$
$$
- 2k\pi\left(\frac{\partial B_{k1}}{\partial t_1} + \frac{\partial B_{k0}}{\partial t_2} + \frac{1}{2k\pi}\frac{\partial A_{k0}^2}{\partial t_1^2} + \frac{k\pi}{2}\hat{L}_k A_{k0}\right)\cos(k\pi t_0)
$$
$$
+ 2\sum_{\substack{n=1 \\ n\neq k}}^{\infty}\left(\left(\mu_0 f_{nk}^{[4]}\hat{l}_n B_{n0} - n\pi f_{nk}^{[3]}A_{n0}\right)\sin(n\pi t_0) + \left(\mu_0 f_{nk}^{[4]}\hat{l}_n A_{n0} + n\pi f_{nk}^{[3]}B_{n0}\right)\cos(n\pi t_0)\right).
$$

$$(6.87)$$

Next, we analyze this equation inside and outside the resonance manifold.

Inside the resonance zone

$$
\frac{\partial^2 w_{k2}}{\partial t_0^2} + (k\pi)^2 w_{k2} = 2k\pi\left(\frac{\partial A_{k1}}{\partial t_1} + \frac{\partial A_{k0}}{\partial t_2} - \frac{1}{2k\pi}\frac{\partial B_{k0}^2}{\partial t_1^2} - \frac{k\pi}{2}\hat{L}_k B_{k0}\right)\sin(k\pi t_0)
$$
$$
- 2k\pi\left(\frac{\partial B_{k1}}{\partial t_1} + \frac{\partial B_{k0}}{\partial t_2} + \frac{1}{2k\pi}\frac{\partial A_{k0}^2}{\partial t_1^2} + \frac{k\pi}{2}\hat{L}_k A_{k0}\right)\cos(k\pi t_0) + \text{``NST''}, \quad (6.88)
$$

where "NST" stands for nonsecular terms. Substituting (6.76) and (6.77) into (6.88), we obtain the following secularity conditions:

$$
\frac{dC_{k0}}{dt_2} - \frac{k\pi}{2}\hat{L}_k D_{k0} + \frac{\partial A_{k1}}{\partial t_1} + \frac{A_0\lambda^2 \hat{l}_k}{\sqrt{k}}\left\{\frac{1}{2k\pi}\left(\lambda^2\hat{l}_k f_k^{[1]}\frac{\partial \hat{I}_{k2}^{[1]}}{\partial t_2} - f_k^{[2]}\frac{\partial \hat{I}_{k2}^{[2]}}{\partial t_2}\right) - \frac{\hat{L}_k f_k^{[2]}}{4}(\hat{I}_{k2}^{[2]}
$$
$$
+ \hat{I}_{k2}^{[1]}) - \frac{1}{4(k\pi)^2}\left(\lambda^2\hat{l}_k f_k^{[1]}\left[4k\sqrt{k}\pi\beta\hat{l}_k t_1\cos\left(\frac{1}{2}k\pi t_1^2 + \sigma^{[0]}\right) + \frac{\partial^2\hat{I}_{k2}^{[2]}}{\partial t_1^2}\right]\right.
$$
$$
\left.\left. - f_k^{[2]}\frac{\partial^2\hat{I}_{k2}^{[1]}}{\partial t_1^2}\right)\right\} = 0,
$$

$$(6.89)$$

and

$$
\frac{dD_{k0}}{dt_2} + \frac{k\pi}{2}\hat{L}_k C_{k0} + \frac{\partial B_{k1}}{\partial t_1} + \frac{A_0\lambda^2 \hat{l}_k}{\sqrt{k}}\left\{\frac{1}{2k\pi}\left(\lambda^2\hat{l}_k f_k^{[1]}\frac{\partial \hat{I}_{k2}^{[2]}}{\partial t_2} + f_k^{[2]}\frac{\partial \hat{I}_{k2}^{[1]}}{\partial t_2}\right) + \frac{\hat{L}_k f_k^{[2]}}{4}(\hat{I}_{k2}^{[1]}
$$
$$
+ \hat{I}_{k2}^{[2]}) - \frac{1}{4(k\pi)^2}\left(\lambda^2\hat{l}_k f_k^{[1]}\left[4k\sqrt{k}\pi\beta\hat{l}_k t_1\sin\left(\frac{1}{2}k\pi t_1^2 + \sigma^{[0]}\right) + \frac{\partial^2\hat{I}_{k2}^{[1]}}{\partial t_1^2}\right]\right.
$$
$$
\left.\left. - f_k^{[2]}\frac{\partial^2\hat{I}_{k2}^{[2]}}{\partial t_1^2}\right)\right\} = 0.
$$

$$(6.90)$$

Observe that integration of these equations with respect to t_1 produces unbounded solutions because of t_2 depending terms. Hence, from (6.89) and (6.90) the secularity

conditions follow:

$$\frac{\mathrm{d}C_{k0}}{\mathrm{d}t_2} - \frac{k\pi}{2}\hat{L}_k D_{k0} = 0,$$
$$\frac{\mathrm{d}D_{k0}}{\mathrm{d}t_2} + \frac{k\pi}{2}\hat{L}_k C_{k0} = 0,$$
(6.91)

together with

$$\frac{\partial A_{k1}}{\partial t_1} + \frac{A_0\lambda^2\hat{l}_k}{\sqrt{k}}\left\{\frac{1}{2k\pi}\left(\lambda^2\hat{l}_k f_k^{[1]}\frac{\partial \hat{I}_{k2}^{[1]}}{\partial t_2} - f_k^{[2]}\frac{\partial \hat{I}_{k2}^{[2]}}{\partial t_2}\right) - \frac{\hat{L}_k f_k^{[2]}}{4}\left(\hat{I}_{k2}^{[2]} + \hat{I}_{k2}^{[1]}\right)\right.$$
$$\left. - \frac{1}{4(k\pi)^2}\left(\lambda^2\hat{l}_k f_k^{[1]}\left[4k\sqrt{k}\pi\beta\hat{l}_k t_1\cos\left(\frac{1}{2}k\pi t_1^2 + \sigma_k^{[0]}\right) + \frac{\partial^2 \hat{I}_{k2}^{[2]}}{\partial t_1^2}\right] - f_k^{[2]}\frac{\partial^2 \hat{I}_{k2}^{[1]}}{\partial t_1^2}\right)\right\} = 0,$$
(6.92)

and

$$\frac{\partial B_{k1}}{\partial t_1} + \frac{A_0\lambda^2\hat{l}_k}{\sqrt{k}}\left\{\frac{1}{2k\pi}\left(\lambda^2\hat{l}_k f_k^{[1]}\frac{\partial \hat{I}_{k2}^{[2]}}{\partial t_2} + f_k^{[2]}\frac{\partial \hat{I}_{k2}^{[1]}}{\partial t_2}\right) + \frac{\hat{L}_k f_k^{[2]}}{4}\left(\hat{I}_{k2}^{[1]} + \hat{I}_{k2}^{[2]}\right)\right.$$
$$\left. - \frac{1}{4(k\pi)^2}\left(\lambda^2\hat{l}_k f_k^{[1]}\left[4k\sqrt{k}\pi\beta\hat{l}_k t_1\sin\left(\frac{1}{2}k\pi t_1^2 + \sigma_k^{[0]}\right) + \frac{\partial^2 \hat{I}_{k2}^{[1]}}{\partial t_1^2}\right] - f_k^{[2]}\frac{\partial^2 \hat{I}_{k2}^{[2]}}{\partial t_1^2}\right)\right\} = 0,$$
(6.93)

where $\hat{L}_k = \hat{L}_k(t_2)$ is given by (6.58). A_{k1} and B_{k1} can be readily found by straightforward integration of (6.92) and (6.93), but we omit the details because of cumbersome expressions. One should only observe that after integration, the arbitrary functions depending on t_2 appear in the expressions for A_{k1} and B_{k1}. These functions may be determined from the $\mathcal{O}(\varepsilon^2)$-problem. Similar to (6.55), system (6.91) can be readily solved analytically. Imposing the secularity conditions, we obtain the following inhomogeneous equation inside the resonance zone

$$\frac{\partial^2 w_{k2}}{\partial t_0^2} + (k\pi)^2 w_{k2} = 2\sum_{\substack{n=1 \\ n\neq k}}^{\infty}\left(\left(\mu_0 f_{nk}^{[4]}\hat{l}_n B_{n0} - n\pi f_{nk}^{[3]} A_{n0}\right)\sin(n\pi t_0)\right.$$
$$\left. + \left(\mu_0 f_{nk}^{[4]}\hat{l}_n A_{n0} + n\pi f_{nk}^{[3]} B_{n0}\right)\cos(n\pi t_0)\right).$$

The solution of this equation readily follows

$$w_{k2} = A_{k2}\cos(k\pi t_0) + B_{k2}\sin(k\pi t_0) + 2\sum_{\substack{n=1 \\ n\neq k}}^{\infty}\frac{1}{\pi^2(k^2 - n^2)}$$
$$\times\left(\left(\mu_0 f_{nk}^{[4]}\hat{l}_n B_{n0} - n\pi f_{nk}^{[3]} A_{n0}\right)\sin(n\pi t_0) + \left(\mu_0 f_{nk}^{[4]}\hat{l}_n A_{n0} + n\pi f_{nk}^{[3]} B_{n0}\right)\cos(n\pi t_0)\right),$$
(6.94)

where A_{k2} and B_{k2} are arbitrary functions of (t_1, t_2) which can be determined from the solution $w_{k3}(t_0, t_1, t_2)$, and where A_{n0} and B_{n0} are given by (6.76) and (6.77), respectively.

Outside the resonance zone

In the $\mathcal{O}(\varepsilon)$-problem we obtained that outside the resonance zone $A_{k0} = \tilde{C}_{k0}(t_2)$, and $B_{k0} = \tilde{D}_{k0}(t_2)$; see (6.84). Hence, (6.87) takes the following form

$$\frac{\partial^2 w_{k2}}{\partial t_0^2} + (k\pi)^2 w_{k2} = 2k\pi \left(\frac{\partial A_{k1}}{\partial t_1} + \frac{d\tilde{C}_{k0}}{dt_2} - \frac{k\pi}{2}\hat{L}_k\tilde{D}_{k0} \right) \sin(k\pi t_0)$$

$$- 2k\pi \left(\frac{\partial B_{k1}}{\partial t_1} + \frac{d\tilde{D}_{k0}}{dt_2} + \frac{k\pi}{2}\hat{L}_k\tilde{C}_{k0} \right) \cos(k\pi t_0) + \text{"NST"}.$$

To avoid secular terms the following should hold

$$\frac{\partial A_{k1}}{\partial t_1} + \frac{d\tilde{C}_{k0}}{dt_2} - \frac{k\pi}{2}\hat{L}_k\tilde{D}_{k0} = 0, \tag{6.95}$$

$$\frac{\partial B_{k1}}{\partial t_1} + \frac{d\tilde{D}_{k0}}{dt_2} + \frac{k\pi}{2}\hat{L}_k\tilde{C}_{k0} = 0. \tag{6.96}$$

Likewise in the previous case, solving these equations with respect to t_1 will produce unbounded solutions because of t_2 depending terms unless $\tilde{C}_{k0}$ and $\tilde{D}_{k0}$ satisfy to

$$\frac{d\tilde{C}_{k0}}{dt_2} - \frac{k\pi}{2}\hat{L}_k\tilde{D}_{k0} = 0, \tag{6.97}$$

$$\frac{d\tilde{D}_{k0}}{dt_2} + \frac{k\pi}{2}\hat{L}_k\tilde{C}_{k0} = 0, \tag{6.98}$$

where $\hat{L}_k = \hat{L}_k(t_2)$ is given by (6.58). Similar to (6.55), this system can be solved analytically. Then, from (6.95) and (6.96) it follows that

$$\frac{\partial A_{k1}}{\partial t_1} = 0, \text{ and } \frac{\partial B_{k1}}{\partial t_1} = 0,$$

for which the solutions are given by $A_{k1}(t_1, t_2) = \tilde{C}_{k1}(t_2)$, and $B_{k1}(t_1, t_2) = \tilde{D}_{k1}(t_2)$, respectively, where $\tilde{C}_{k1}$ and $\tilde{D}_{k1}$ are arbitrary functions which can be determined from the $\mathcal{O}(\varepsilon^2)$-problem. Employing the secularity conditions (6.94), we obtain the following inhomogeneous equation outside the resonance zone

$$\frac{\partial^2 w_{k2}}{\partial t_0^2} + (k\pi)^2 w_{k2} = 2\sum_{\substack{n=1 \\ n\neq k}}^{\infty} \left(\left(\mu_0 f_{nk}^{[4]}\hat{l}_n\tilde{D}_{n0} - n\pi f_{nk}^{[3]}\tilde{C}_{n0} \right) \sin(n\pi t_0) \right.$$

$$\left. + \left(\mu_0 f_{nk}^{[4]}\hat{l}_n\tilde{C}_{n0} + n\pi f_{nk}^{[3]}\tilde{D}_{n0} \right) \cos(n\pi t_0) \right).$$

The solution has a similar form as the solution inside the resonance zone:

$$w_{k2} = \tilde{A}_{k2}\cos(k\pi t_0) + \tilde{B}_{k2}\sin(k\pi t_0) + 2\sum_{\substack{n=1 \\ n\neq k}}^{\infty} \frac{1}{\pi^2(k^2-n^2)}$$

$$\times \left(\left(\mu_0 f_{nk}^{[4]}\hat{l}_n\tilde{D}_{n0} - n\pi f_{nk}^{[3]}\tilde{C}_{n0} \right) \sin(n\pi t_0) + \left(\mu_0 f_{nk}^{[4]}\hat{l}_n\tilde{C}_{n0} + n\pi f_{nk}^{[3]}\tilde{D}_{n0} \right) \cos(n\pi t_0) \right),$$

where $\tilde{A}_{k2}$ and $\tilde{B}_{k2}$ are arbitrary functions of (t_1, t_2) which can be determined from the solution $w_{k3}(t_0, t_1, t_2)$.
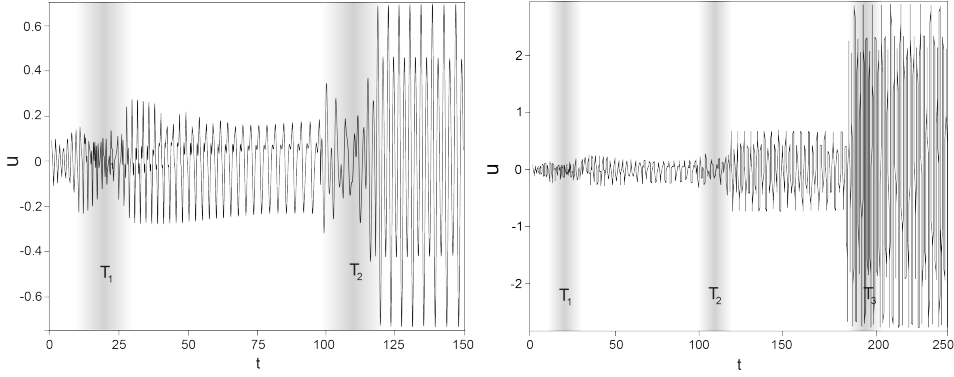
Figure 6.3: Lateral displacements of the middle point of the cable up to the first three oscillation modes on timescales up to (a) $t = 150$, and (b) $t = 250$. The shadowed bands represent the resonance zones.

6.6   Results

In this section, we summarize the results obtained in the previous section. Besides, we compute the lateral displacements and the vibratory energy of the cable by using the constructed formal approximation as well as by applying a numerical scheme to present some numerical results.

6.6.1   Formal approximation

Analytic results

All in all, we constructed a formal approximation in the form (6.65) for $\tilde{u}_k(\tilde{t}; \sqrt{\varepsilon})$. Introducing the following notation

$$\omega_n(t) := \frac{1}{\varepsilon} \ln\left(\frac{\lambda^2(l_0 + \varepsilon t)}{n\pi} \right),$$

and using (6.22) and (6.56), we finally obtain the approximate solution of the initial-boundary value problem (6.18a-6.18c) as

$$\bar{u}(x, t, t_1, t_2; \varepsilon) = \sum_{n=1}^{\infty} \left(\sqrt{\varepsilon} u_{n0}(t, t_1, t_2) + \varepsilon u_{n1}(t, t_1, t_2) + \varepsilon \sqrt{\varepsilon} u_{n2}(t, t_1, t_2) \right)$$
$$\times \sin\left(\frac{n\pi x}{l_0 + \varepsilon t} \right), \tag{6.99}$$

where t_1 and t_2 are given by (6.62), and where

$$u_{n0}(t, t_1, t_2) = A_{n0}(t_1, t_2) \cos(n\pi\omega_n(t)) + B_{n0}(t_1, t_2) \sin(n\pi\omega_n(t)), \tag{6.100}$$

where functions A_{n0} and B_{n0} are given by (6.76,6.77);

$$u_{n1}(t, t_1, t_2) = A_{n1}(t_1, t_2) \cos(n\pi\omega_n(t)) + B_{n1}(t_1, t_2) \sin(n\pi\omega_n(t)), \tag{6.101}$$
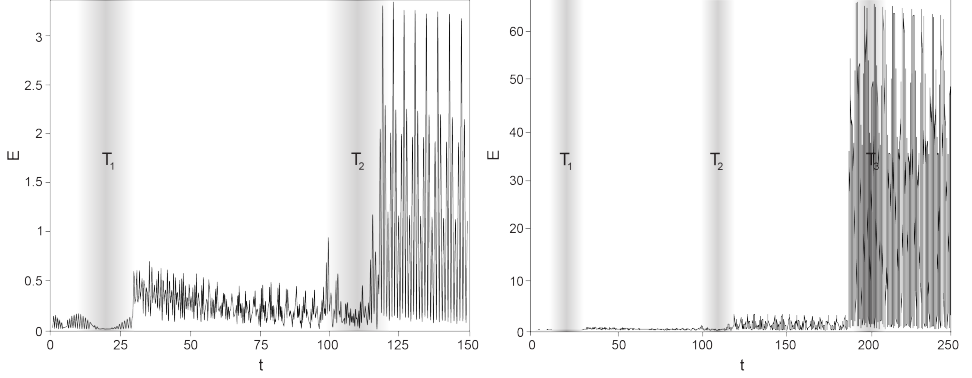
Figure 6.4: Vibratory energy of the cable up to the first three oscillation modes on timescales up to (a) $t = 150$, and (b) $t = 250$. The shadowed bands represent the resonance zones.

where functions A_{n1} and B_{n1} are given by (6.92,6.93);

$$u_{n2}(t, t_1, t_2) = A_{n2}(t_1, t_2) \cos(n\pi\omega_n(t)) + B_{n2}(t_1, t_2) \sin(n\pi\omega_n(t))$$

$$+ 2 \sum_{\substack{k=1 \\ k \neq n}}^{\infty} \frac{1}{\pi^2(n^2 - k^2)} \Big[\big(\mu_0 f_{kn}^{[4]} \hat{l} B_{k0}(t_1, t_2) - k\pi f_{kn}^{[3]} A_{k0}(t_1, t_2) \big) \sin \omega_k(t)$$

$$+ \big(\mu_0 f_{kn}^{[4]} \hat{l} A_{k0}(t_1, t_2) + k\pi f_{kn}^{[3]} B_{k0}(t_1, t_2) \big) \cos \omega_k(t) \Big], \tag{6.102}$$

where functions A_{n2} and B_{n2} can be found from higher-order approximations.

Remark that the constructed formal approximations are asymptotic. Their accuracy is strongly connected with the timescales. Thus, $u_n - (\sqrt{\varepsilon}u_{n0} + \varepsilon u_{n1} + \varepsilon\sqrt{\varepsilon}u_{n2}) = \mathcal{O}(\varepsilon^2)$, $u_n - (\sqrt{\varepsilon}u_{n0} + \varepsilon u_{n1}) = \mathcal{O}(\varepsilon\sqrt{\varepsilon})$, and $u_n - \sqrt{\varepsilon}u_{n0} = \mathcal{O}(\varepsilon)$ on a timescale of order ε^{-1} for $n \in \mathbb{N}$, where u_n is given by (6.19).

Numerical results

The numerical results simulating the vibration response and the energy are computed based on the analytical expressions (6.99,6.100), and (D.8), respectively. The computations are performed by using the following parameters $\varepsilon = 0.01$, $H = 1$, $\lambda = 1.875$, $l_0 = 0.7$, $A_0 = 1$. For simplicity, let us assume only the initial displacement is prescribed, so that $f = \varepsilon \sin^2 \pi\xi$, and the initial velocity $g = 0$ for $0 \leq \xi \leq 1$. In numerical computations we neglect bending stiffness of the cable because its contribution is assumed to be small. It is also worth mentioning that the following numerical results are computed based on $\mathcal{O}(\varepsilon)$ approximations. Higher-order approximations are neglected due to their insignificant contribution into the solution. By using (6.22) and (6.56), we obtain that the resonance occurs periodically in time at time instants

$$T_k = \frac{1}{\varepsilon}\left(\frac{k\pi}{\lambda^2} - l_0\right) \text{ for } k \in \mathbb{N}, \tag{6.103}$$
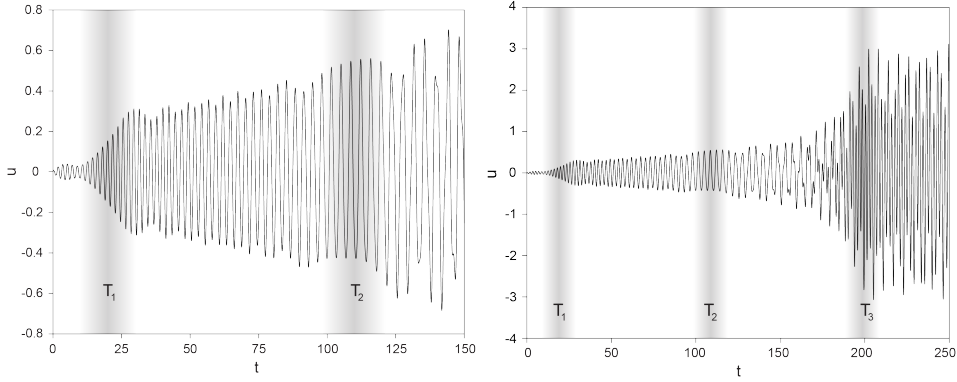
Figure 6.5: Lateral displacements of the middle point of the cable by using a numerical method for timescales up to (a) $t = 150$, and (b) $t = 250$. The shadowed bands represent the resonance zones.

with an interval

$$\Delta T = \frac{\pi}{\varepsilon \lambda^2}. \tag{6.104}$$

Note that the resonance time depends on the mode number k. For the first three oscillation modes, resonance emerges at times $T_1 \approx 19.36$, $T_2 \approx 108.72$, and $T_3 \approx 198.08$ with $\Delta T = 89.36$. They are illustrated in Figures 6.3-6.6.

Figures 6.3-6.4 depict the lateral displacements and the vibratory energy of the cable on timescales up to $t = 150$ and $t = 250$. Note that subfigures (b) are simply enlarged version of subfigures (a), that is why all explanations for (b) are automatically inherent to (a). From the analytical results we can distinguish three main stages in time of resonance evolution such as the transition of the cable to the resonance zone, capture of the cable into resonance, and transition of the cable out of the resonance zone, the autoresonance stage, where the lateral displacements and the vibratory energy of the cable increases to a certain level and remains phase-locked until it meets another resonance zone. One can see this type of behavior in Figures 6.3,6.4, where three resonances are detected corresponding to time instants T_1, T_2, and T_3. The shadowed bands represent the resonance layers which have the size of $\mathcal{O}\left(\varepsilon^{-\frac{1}{2}}\right)$ as was obtained analytically. In the current example the resonance layers are found in the following intervals $|t - T_i| \leq 10$ for $i = 1, 2, 3$. Note that in (a) and (b) these layers are visually different but with respect to the scale of the figures they are the same.

6.6.2 Numerical approximation

Since we neglected by bending stiffness, the governing equation (6.18a) for $0 < \xi < 1$ takes the following form:

$$u_{tt} - \frac{1}{l^2}u_{\xi\xi} = -\varepsilon\left(-\frac{2}{l}(1-\xi)u_{\xi t} + \frac{\mu_0}{l}(1-\xi)u_{\xi\xi} + \frac{\mu_0}{l}u_{\xi} + \xi lS_1 + S_2\right), \tag{6.105}$$
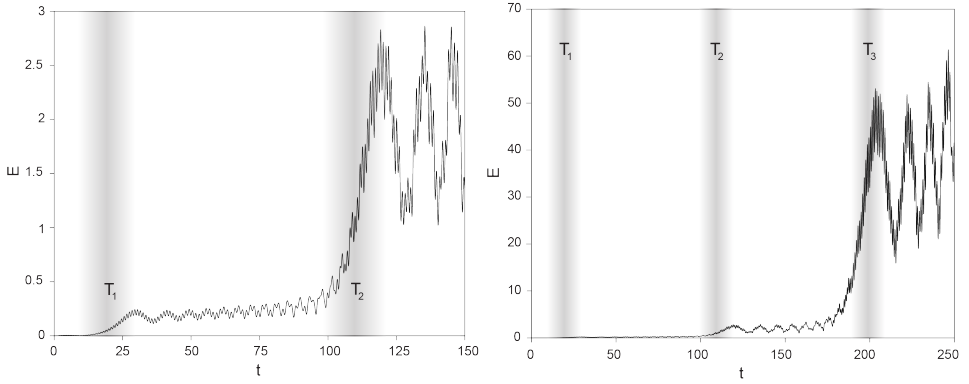
Figure 6.6: Vibratory energy of the cable by using a numerical method for timescales up to (a) $t = 150$, and (b) $t = 250$. The shadowed bands represent the resonance zones.

where the upper bar notation is omitted for convenience, S_1 and S_2 are given by (6.7) and (6.8). To solve (6.105) numerically, we first discretize it in space by using the central finite difference scheme. Then, we rewrite the so-obtained discretized equation in a matrix form and use the numerical time integration by the Crank-Nicolson method (see Appendix B). Note that the same values of parameters as for the analytic approximations are used here for computation. Thus, Figures 6.5-6.6 show the lateral displacements and the vibratory energy of the cable, respectively, on timescales up to $t = 150$ and $t = 250$. Note that as before Figure 6.5 is enlarged Figure 6.6. From these figures one can see that in the resonance zones the lateral displacements and the vibratory energy increase and, between these zones, stay phase-locked. We can make a conclusion that the general dynamic behavior of the solution approximated numerically is in agreement with the analytic approximation.

6.7 Conclusions

In this chapter, the lateral vibrations and resonances emerging in an elevator cable system due to the excitation at its boundaries initiated by the wind-induced building sway were studied. In order to prescribe the boundary conditions of the problem, the exact solution representing the sway of the building was found in Appendix A. Further, an initial-boundary value problem describing the lateral vibrations of a vertically moving beam with small bending stiffness and (in time) linear length variations was considered. In order to tackle the initial-boundary value problem and to construct a formal approximation of the solution, an advanced analytic scheme consisting of many elementary steps has been developed. From an internal layer analysis, it followed that an additional natural timescale inside the resonance zone is $\sqrt{\varepsilon}t$, and outside the resonance layer it is εt. Moreover, we also predicted exact instants of time when resonance emerged. Note that from the physical point of view resonance occurs, when the length

of the cable becomes such that the one of the natural frequencies of its oscillations match with the fundamental frequency of the building sway (or boundary excitation). Further, we constructed an accurate approximation of the solution on a timescale of order ε^{-1} by the three-timescales perturbation method, and the following conclusions could be drawn:

- order ε boundary excitations of the cable result in $\sqrt{\varepsilon}$-order vibration responses;

- the Fresnel integrals involved in the solution cause autoresonance phenomena in the system;

- since the solution contains infinitely many modes, there are infinitely many autoresonances in the system;

- for smaller ε values, more time is needed to catch resonance and more time is needed to pass through a resonance zone;

- higher-order modes have smaller amplitudes (than lower order modes), carrying low impact into the system, due to the factor $k^{-5/2}$ in the expressions for the amplitudes of vibrations in the $\sqrt{\varepsilon}$-order approximation.

The numerical results confirmed these conclusions. Moreover, the constructed analytic approximations are in agreement with the numerical approximations.

The analytical scheme developed for this problem can readily be extended to other, more complicated and realistic, types of elevator motion. For instance, one can investigate the sway dynamics of the elevator cable under three different states of the elevator motion. The first state is acceleration, when the lift begins to accelerate from the resting position. Then, after acceleration, it can move at a constant velocity. Finally, the elevator decelerates before stopping at a certain floor. This example might add extra resonance manifolds and might produce new asymptotic timescales in the dynamics of the cable. One should be also aware of intersection of resonance zones [12], what makes the analysis of the problem even more interesting, but complex. In conclusion, the analytic methodology developed in this chapter can be implemented in other types of gyroscopic systems which are governed by differential equations with in time slowly varying coefficients.

Appendix D

D.1 Boundary sway

As it is mentioned in the introduction of this chapter, the motion of the elevator cable's boundaries in horizontal direction is induced by the building sway. So, to prescribe the boundary conditions for the cable, we need to determine the exact solution of the building motion. We model the building as a vertical clamped Euler-Bernoulli beam of length H (see Figure 6.1).

The PDE representing the motion of the building is given by a beam-like equation as follows:

$$u_{tt} + u_{xxxx} = 0, \tag{D.1a}$$

for $0 < x < H$, and $t > 0$, subject to the BCs:

$$\begin{aligned} u(0,t) = u_x(0,t) &= 0, \\ u_{xx}(H,t) = u_{xxx}(H,t) &= 0, \end{aligned} \tag{D.1b}$$

for $t > 0$, and with the ICs:

$$\begin{aligned} u(x,0) &= \phi_1(x), \\ u_t(x,0) &= \phi_2(x), \end{aligned} \tag{D.1c}$$

for $0 < x < l_0$.

This well-known IBV-problem can be solved by the method of separation of variables, where $u(x,t) = X(x)T(t)$, yielding

$$\frac{X^{(4)}}{X} = -\frac{\ddot{T}}{T} = \nu^2. \tag{D.2}$$

From (D.2) two equations, for T and X, follow. First, the equation for T is given by $\ddot{T} + \nu^2 T = 0$, for which the solution can be readily found as $T(t) = A\cos(\nu t) + B\sin(\nu t)$,

where A and B are constants. For convenience we will use the following notation $\lambda^4 = \nu^2$. The mode-equation for X is given by $X^{(4)} - \lambda^4 X = 0$, which has a well-known solution $X(x) = C_1 \sin(\lambda x) + C_2 \cos(\lambda x) + C_3 \sinh(\lambda x) + C_4 \cosh(\lambda x)$, corresponding to the following roots of the characteristic equation $\pm\lambda$ and $\pm i\lambda$. So using the boundary conditions (D.1b) and the fact of the existence of a non-trivial solution, we obtain the following equation for the eigenvalues $1 + \cos(\lambda_n H) \cosh(\lambda_n H) = 0$, which are actually the natural frequencies of the cantilever beam. This transcendental equation can be solved numerically, providing the following results $\lambda_1 H = 1.875$, $\lambda_2 H = 4.694$, $\lambda_3 H = 7.855$, $\lambda_4 H = 10.996$, $\lambda_5 H = 14.137, \cdots$. Corresponding eigenfunctions are given by

$$X_n(x) = C_{1,n} \sin(\lambda_n x) + C_{2,n} \cos(\lambda_n x) + C_{3,n} \sinh(\lambda_n x) + C_{4,n} \cosh(\lambda_n x).$$

To find the constants of integration, we use the boundary conditions (D.1b). Then, the eigenfunctions are given by

$$X_n(x) = \sin(\lambda_n x) - \sinh(\lambda_n x) - \alpha_n(\cos(\lambda_n x) - \cosh(\lambda_n x)), \tag{D.3}$$

for $n \in \mathbb{N}$, where $\alpha_n := \frac{\sin(\lambda_n H) + \sinh(\lambda_n H)}{\cos(\lambda_n H) + \cosh(\lambda_n H)}$. A solution for T can be also rewritten in accordance with the eigenvalues as follows

$$T_n(t) = A_n \cos(\lambda_n^2 t) + B_n \sin(\lambda_n^2 t), \tag{D.4}$$

where A_n and B_n are constants following from the initial conditions (D.1c). Thus, the sway of the building is given by $u(x,t) = \sum_{n=1}^{\infty} T_n(t) X_n(x)$ or in a full form, using (D.3-D.4), as follows:

$$u(x,t) = \sum_{n=1}^{\infty} \left(\sin(\lambda_n x) - \sinh(\lambda_n x) - \alpha_n[\cos(\lambda_n x) - \cosh(\lambda_n x)] \right)$$
$$\times \left(A_n \cos(\lambda_n^2 t) + B_n \sin(\lambda_n^2 t) \right).$$

D.2   Discretization and time integration

Here we solve (6.105) numerically. In order to make the numerical integration easier, it is more convenient to rewrite this equation as a system of coupled first-order partial differential equations:

$$u_t = v,$$
$$v_t = \frac{1}{l^2} v_{\xi\xi} - \varepsilon \left(-\frac{2}{l}(1-\xi)v_\xi + \frac{\mu_0}{l}(1-\xi)u_{\xi\xi} + \frac{\mu_0}{l}u_\xi + \xi l S_1 + S_2 \right). \tag{D.5}$$

Next, let us use equispaced mesh grids $\xi_j = j\Delta\xi$ for $j = 1, 2, \ldots, n$ with $n\Delta\xi = 1$. Introducing the differences,

$$u_\xi(\xi_j, t) = \frac{u_{j+1} - u_{j-1}}{2\Delta\xi} + \mathcal{O}\left((\Delta\xi)^2\right),$$
$$u_{\xi\xi}(\xi_j, t) = \frac{u_{j+1} - 2u_j + u_{j-1}}{(\Delta\xi)^2} + \mathcal{O}\left((\Delta\xi)^2\right),$$
$$v_\xi(\xi_j, t) = \frac{v_{j+1} - v_{j-1}}{2\Delta\xi} + \mathcal{O}\left((\Delta\xi)^2\right),$$

we discretize (D.5) as follows:

$$\frac{\mathrm{d}u}{\mathrm{d}t}(\xi_j, t) = v_j,$$
$$\frac{\mathrm{d}v}{\mathrm{d}t}(\xi_j, t) = r_j \frac{v_{j+1} - v_{j-1}}{2\Delta\xi} + q_j \frac{u_{j+1} - 2u_j + u_{j-1}}{(\Delta\xi)^2} - h\frac{u_{j+1} - u_{j-1}}{2\Delta\xi} - s_j, \tag{D.6}$$

where $r_j := \frac{2\varepsilon}{l}(1-\xi_j)$, $q_j := \frac{1}{l}\left(\frac{1}{l} - \varepsilon\mu_0(1-\xi_j)\right)$, $h := \frac{\varepsilon\mu_0}{l}$, and $s_j := \varepsilon\xi_j l S_1 + S_2$ for $j = 1, 2, \ldots, n$. Further, we denote a zero matrix by $\emptyset$, the identity matrix by I, and also introduce the following two matrices,

$$Q := \frac{1}{(\Delta\xi)^2}\begin{bmatrix} -2q_1 & q_1 - \frac{\Delta\xi}{2}h & 0 & \cdots & \cdots & 0 \\ q_2 + \frac{\Delta\xi}{2}h & -2q_2 & q_2 - \frac{\Delta\xi}{2}h & \ddots & & \vdots \\ 0 & \ddots & \ddots & \ddots & \ddots & \vdots \\ \vdots & \ddots & \ddots & \ddots & \ddots & 0 \\ \vdots & & \ddots & q_{n-1} + \frac{\Delta\xi}{2}h & -2q_{n-1} & q_{n-1} - \frac{\Delta\xi}{2}h \\ 0 & \cdots & \cdots & 0 & q_n + \frac{\Delta\xi}{2}h & -2q_n \end{bmatrix},$$

and

$$R := \frac{1}{2\Delta\xi} \begin{bmatrix} 0 & r_1 & 0 & \cdots & \cdots & 0 \\ -r_2 & 0 & r_2 & \ddots & & \vdots \\ 0 & \ddots & \ddots & \ddots & \ddots & \vdots \\ \vdots & \ddots & \ddots & \ddots & \ddots & 0 \\ \vdots & & \ddots & -r_{n-1} & 0 & r_{n-1} \\ 0 & \cdots & \cdots & 0 & -r_n & 0 \end{bmatrix},$$

in $\mathbb{R}^{n\times n}$. The introduced four matrices compose a system matrix of (D.6) as follows:

$$M := \begin{bmatrix} \emptyset & I \\ Q & R \end{bmatrix} \in \mathbb{R}^{2n\times 2n}.$$

In addition, let us introduce the following vectors:

$$\boldsymbol{w} = (u_1(\xi_1,t), u_2(\xi_2,t), \ldots, u_n(\xi_n,t), v_1(\xi_1,t), v_2(\xi_2,t), \ldots, v_n(\xi_n,t))^{\mathrm{T}},$$
$$\boldsymbol{s} = (\underbrace{0,0,\ldots,0}_{n \text{ times}}, s_1, s_2, \ldots, s_n)^{\mathrm{T}}.$$

Thus, system (D.6) can be written in a matrix form as follows:

$$\frac{\mathrm{d}\boldsymbol{w}}{\mathrm{d}t} = M\boldsymbol{w} - \boldsymbol{s}. \tag{D.7}$$

In order to perform a time integration of (D.7), we apply the Crank-Nicolson method; note that this method is basically based on the trapezoidal rule. Introducing the equi-spaced mesh grid in time $t_k = k\Delta t$ for $k = 1, 2, \ldots, n$, and using the Crank-Nicolson method, we obtain

$$\boldsymbol{w}^{k+1} = D\boldsymbol{w}^k - \frac{\Delta t}{2} \frac{\boldsymbol{s}^{k+1} + \boldsymbol{s}^k}{I - \frac{\Delta t}{2} M^{k+1}},$$

where $D \in \mathbb{R}^{2n\times 2n}$ is the amplification factor

$$D = \frac{I + \frac{\Delta t}{2} M^k}{I - \frac{\Delta t}{2} M^{k+1}},$$

and where the identity matrix $I \in \mathbb{R}^{2n\times 2n}$.

D.3 Energy

D.3.1 Analytic expressions

The total mechanical energy of the cable is given by

$$E(t) = \frac{1}{2} \int_0^l \left[\rho(u_t + vu_x)^2 + Pu_x^2 + EIu_{xx}^2 \right] dx,$$

where $l = l(t)$, and P is given by (6.2). Using the dimensionless quantities (6.3), we rewrite the energy in a dimensionless form:

$$E(t) = \frac{1}{2} \int_0^l \left((u_t + vu_x)^2 + \left(1 + (\mu - \dot{v})(l - x) - \frac{\dot{v}}{\mu} \right) u_x^2 + pu_{xx}^2 \right) dx.$$

In order to define the energy on the interval $(0, 1)$, we change variables by using the following transformation $x = l\xi$:

$$E(t) = \frac{1}{2} \int_0^1 \frac{1}{l} \left(\left(lu_t + v[1 - \xi]u_\xi \right)^2 + \left(1 + l[\mu - \dot{v}][1 - \xi] - \frac{\dot{v}}{\mu} \right) u_\xi^2 + pu_{\xi\xi}^2 \right) d\xi.$$
$$\tag{D.8}$$

D.3.2 Numerical integration

In order to compute integral (D.8) numerically, let us use the forward differences for u_ξ and $u_{\xi\xi}$, respectively:

$$u_\xi(\xi, t) = \frac{u_{i+1} - u_i}{\Delta \xi} + \mathcal{O}(\Delta \xi), \text{ and } u_{\xi\xi}(\xi, t) = \frac{u_{i+2} - 2u_{i+1} + u_i}{(\Delta \xi)^2} + \mathcal{O}(\Delta \xi),$$

for $i = 1, 2, \ldots, n$, and the trapezoidal rule for u_t:

$$u_t(\xi, t) = \kappa_i v_i + \kappa_{i+1} v_{i+1}, \tag{D.9}$$

where

$$\kappa_i := \frac{\xi - \xi_{i+1}}{\xi_i - \xi_{i+1}}, \text{ and } \kappa_{i+1} := \frac{\xi - \xi_i}{\xi_{i+1} - \xi_i}.$$

The integrals of u_ξ, u_ξ^2, and $u_{\xi\xi}^2$ over ξ can be readily computed. That is why we skip further details for this part and turn to the integration of u_t and u_t^2. Their integrals over

ξ are computed by using (D.9) and the Holand-Bell theorem [23]:

$$\int_0^1 u_t d\xi = \sum_{i=1}^n \int_{\xi_i}^{\xi_{i+1}} (\kappa_i v_i + \kappa_{i+1} v_{i+1}) d\xi$$

$$= \sum_{i=1}^n \frac{v_{i+1} + v_i}{2} \Delta \xi,$$

$$\int_0^1 u_t^2 d\xi = \sum_{i=1}^n \int_{\xi_i}^{\xi_{i+1}} (\kappa_i^2 v_i^2 + 2\kappa_i \kappa_{i+1} v_i v_{i+1} + \kappa_{i+1}^2 v_{i+1}^2) d\xi$$

$$= \sum_{i=1}^n \frac{1}{3} \left(v_i^2 + \frac{1}{4} v_i v_{i+1} + v_{i+1}^2 \right) \Delta \xi.$$

Bibliography

[1]   A.H. Nayfeh and P.F. Pai. *Linear and Nonlinear Structural Mechanics*. Wiley-VCH, 2002.

[2]   A.L. Thurman and C.D. Mote Jr. "Free, periodic, nonlinear oscilation of an axially moving strip." In: *Journal of Applied Mechanics* 36 (1969), pp. 83–91.

[3]   I.V. Andrianov and J. Awrejcewicz. "Dynamics of a string moving with time-varying speed". In: *Journal of Sound and Vibration* 292.3-5 (2006), pp. 935–940.

[4]   H. Benaroya and T. Wei. "Hamilton's principle of external viscous fluid-structure interaction". In: *Journal of Sound and Vibration* 238.1 (2000), pp. 113–145.

[5]   C. Chung and I. Kao. "Green's function and forced vibration response of damped axially moving wire." In: *Journal of Vibration and Control* 18.12 (2012), pp. 1798–1808.

[6]   C. Chung and I. Kao. "Modelling of axially moving wire with damping: Eigenfunctions, orthogonality and applications in slurry wiresaws." In: *Journal of Sound and Vibration* 330 (2011), pp. 2947–2963.

[7]   C.A. Tan and S. Ying. "Dynamic Analysis of the Axially Moving String Based on Wave Propagation". In: *Journal of Applied Mechanics* 64(2) (1997), pp. 394–400.

[8]   D. B. McIver. "Hamilton's principle for systems of changing mass". In: *Journal of Engineering Mathematics* 7.3 (1973), pp. 249–261.

[9]   Darmawijoyo and W.T. van Horssen. "On the weakly damped vibrations of a string attached to a spring-mass-dashpot system". In: *Journal of Vibration and Control* 9(11) (2003), pp. 1231–1248.

[10] E.W. Chen and N.S. Ferguson. "Analysis of energy dissipation in an elastic moving string with a viscous damper at one end". In: *Journal of Sound and Vibration* 128 (2014), pp. 2556–2570.

[11] F. Verhulst. *Nonlinear Differential Equations and Dynamical Systems*. Springer-Verlag, 1996.

[12] F. Verhulst. "Profits and pitfalls of timescales in asymptotics". In: *SIAM Review* 57.2 (2015), pp. 255–274.

[13] G. Suweken and W.T. van Horssen. "On the transversal vibrations of a conveyor belt with a low and time varying velocity. Part I: The string-like case." In: *Journal of Sound and Vibration* 264.1 (2003), pp. 117–133.

[14] N.V. Gaiko and W.T. van Horssen. "On the lateral vibrations of a vertically moving string with a harmonically varying length". In: *ASME International Mechanical Engineering Congress and Exposition, Proceedings (IMECE)* 4B (2015).

[15] N.V. Gaiko and W.T. van Horssen. "On the transverse, low frequency vibrations of a traveling string with boundary damping". In: *Journal of Vibration and Acoustics, Transactions of the ASME* 137.4 (2015), p. 041004.

[16] N.V. Gaiko and W.T. van Horssen. "On transversal oscillations of a vertically translating string with small time-harmonic length variations". In: *Journal of Sound and Vibration* 383 (2016), pp. 339–348.

[17] N.V. Gaiko and W.T. van Horssen. "On wave reflections and energetics for a semi-infinite traveling string with a nonclassical boundary support". In: *Journal of Sound and Vibration* 370 (2016), pp. 336–350.

[18] Y. Fujita H. Kimura H. Ito and T. Nakagawa. "Forced vibration analysis of an elevator rope with both ends moving". In: *Journal of Vibration and Acoustics, Transactions of the ASME* 129.4 (2007), pp. 471–477.

[19] H.H.E. Leipholz. "On an extension of Hamilton's variational principle to nonconservative systems which are conservative in a higher sense". In: *Ingenieur-Archiv* 47(5) (1978), pp. 257–266.

[20] W.T. van Horssen. "On the applicability of the method of separation of variables for partial difference equations". In: *Journal of Difference Equations and Applications* 8.1 (2002), pp. 53–60.

[21] W.T. van Horssen. "On the influence of lateral vibrations of supports for an axially moving string." In: *Journal of Sound and Vibration* 268 (2003), pp. 323–330.

[22] W.T. van Horssen and S.V. Ponomareva. "On the construction of the solution of an equation describing an axially moving string." In: *Journal of Sound and Vibration* 287 (2005), pp. 359–366.

[23] I. Holand and K. Bell eds. *Finite element methods in stress analysis*. Tapir, 1969.

[24] J. Cooper. "Asymptotic Behavior for the Vibrating String with a Moving Boundary". In: *Journal of Mathematical Analysis and Applications* 174.1 (1993), pp. 67–87.

[25] J. Kevorkian and J. D. Cole. *Multiple Scale and Singular Perturbation Methods*. Applied Mathematical Sciences, 1996.

[26] F. Verhulst J.A. Sanders and J. Murdock. *Averaging Methods in Nonlinear Dynamical Systems*. Springer, 2007.

[27] J.A. Wickert and C.D. Mote Jr. "Classical vibration analysis of axially moving continua." In: *Journal of Applied Mechanics* 57 (1990), pp. 738–744.

[28] J.D. Achenbach. *Wave propagation in elastic solids*. North-Holland Publishing Company, 1973.

[29] C.-M. Zhu J.-H. Bao P. Zhang and W.Sun. "Transverse vibration of flexible hoisting rope with time-varying length". In: *Journal of Mechanical Science and Technology* 28.2 (2014), pp. 457–466.

[30] J.W. Hijmissen. *On aspects of boundary damping for cables and vertical beams*. TU Delft, 2008.

[31] K. F. Graff. *Wave motion in elastic solids*. Ohio State University Press, 1975.

[32] L. Q. Chen and X. D. Yang. "Stability in parametric resonance of axially moving viscoelastic beams with time-dependent speed". In: *Journal of Sound and Vibration* 284.3-5 (2005), pp. 879–891.

[33] U. Lee and I. Jang. "On the boundary conditions for axially moving beams". In: *Journal of Sound and Vibration* 306.3-5 (2007), pp. 675–690.

[34] L.-Q. Chen. "Analysis and Control of Transverse Vibrations of Axially Moving Strings". In: *Applied Mechanics Reviews* 58(2) (2005), pp. 91–116.

[35] N. V. Gaiko and W. T. van Horssen. "On the Transverse, Low Frequency Vibrations of a Traveling String with Boundary Damping". In: *Journal of Vibration and Acoustics, Transactions of the ASME* 137.4 (2015), p. 041004.

[36] N. V. Gaiko and W. T. van Horssen. "On the lateral vibrations of a vertically moving string with a harmonically varying length". In: *Proceedings of the ASME 2015* IMECE2015-50449 (2015).

[37] N.V. Gaiko and W.T. van Horssen. "On transversal oscillations of a vertically translating string with small time-harmonic length variation". In: *Journal of Sound and Vibration* 383 (2016), pp. 339–348.

[38] Q.C. Nguyen and K.-S. Hong. "Simultaneous control of longitudinal and transverse vibrations of an axially moving string with velocity tracking". In: *Journal of Sound and Vibration* 331(13) (2012), pp. 3006–3019.

[39] R. A. Malookani and W. T. van Horssen. "On resonances and the applicability of Galerkin's truncation method for an axially moving string with time-varying velocity". In: *Journal of Sound and Vibration* 344 (2015), pp. 1–17.

[40] R. A. Sack. "Transverse oscillations in travelling strings". In: *British Journal of Applied Physics* 5.6 (1954), pp. 224–226.

[41] P. Picton R. Crespo S. Kaczmarczyk and H. Su. "The coupled nonlinear dynamics of a lift system". In: *AIP Conf. Proc.* 1637 (2014), p. 245.

[42] R. D. Swope and W. F. Ames. "Vibrations of a moving threadline". In: *Journal of the Franklin Institute* 275.1 (1963), pp. 36–55.

[43] R. Haberman. *Applied Partial Differential Equations: With Fourier Series and Boundary Value Problems (5th ed.)* Prentice Hall, 2013.

[44] R.E. Greene and S.G. Krantz. *Function Theory of One Complex Variable - 3rd ed.* American Mathematical Society, 2006.

[45] S. H. Sandilo and W. T. van Horssen. "On a cascade of autoresonances in an elevator cable system". In: *Nonlinear Dynamics* 80.3 (2015), pp. 1613–1630.

[46] S. H. Sandilo and W. T. van Horssen. "On variable length induced vibrations of a vertical string". In: *Journal of Sound and Vibration* 333.11 (2014), pp. 2432–2449.

[47] S. Kaczmarczyk. "Nonlinear Sway and Active Stiffness Control of Long Moving Ropes in High-Rise Vertical Transportation Systems". In: *Vibration Problems ICOVP 2011: The 10th International Conference on Vibration Problems, Springer Proceedings in Physics* 139 (2011), pp. 183–188.

[48] S. Kaczmarczyk. "The passage through resonance in a catenary-vertical cable hoisting system with slowly varying length". In: *Journal of Sound and Vibration* 208.2 (1997), pp. 243–265.

[49] S. Kaczmarczyk and W. Ostachowicz. "Transient vibration phenomena in deep mine hoisting cables. Part 1: Mathematical model". In: *Journal of Sound and Vibration* 262.2 (2003), pp. 219–244.

[50] S. Kaczmarczyk and W. Ostachowicz. "Transient vibration phenomena in deep mine hoisting cables. Part 2: Numerical simulation of the dynamic response". In: *Journal of Sound and Vibration* 262.2 (2003), pp. 245–289.

[51] S.H. Sandilo and W.T. van Horssen. "On boundary damping for an axially moving tensioned beam". In: *Journal of Vibration and Acoustics* 134(1) (2012), p. 11005.

[52] S.-Y. Lee and C. D. Mote Jr. "A generalized treatment of the energetics of translating continua, Part I: Strings and second order tensioned pipes". In: *Journal of Sound and Vibration* 204.5 (1997), pp. 717–734.

[53] T. Akkaya and W. T. van Horssen. "Reflection and damping properties for semi-infinite string equations with non-classical boundary conditions". In: *Journal of Sound and Vibration* 336 (2015), pp. 179–190.

[54] T. Yamamoto, K. Yasuda, and M. Kato. "Vibrations of a string with time-variable length". In: *Bull JSME* 21.162 (1978), pp. 1677–1684.

[55] W. D. Zhu and G. Y. Xu. "Vibration of elevator cables with small bending stiffness". In: *Journal of Sound and Vibration* 263.3 (2002), pp. 679–699.

[56] W. D. Zhu and J. Ni. "Energetics and stability of translating media with an arbitrarily varying length". In: *Journal of Vibration and Acoustics, Transactions of the ASME* 122.3 (2000), pp. 295–304.

[57] W. D. Zhu, J. Ni, and J. Huang. "Active control of translating media with arbitrarily varying length". In: *Journal of Vibration and Acoustics, Transactions of the ASME* 123.3 (2001), pp. 347–358.

[58] W. D. Zhu and L. J. Teppo. "Design and analysis of a scaled model of a high-rise, high-speed elevator". In: *Journal of Sound and Vibration* 264.3 (2003), pp. 707–731.

[59] W. D. Zhu and Y. Chen. "Forced response of translating media with variable length and tension: Application to high-speed elevators". In: *Source of the Document Proceedings of the Institution of Mechanical Engineers, Part K: Journal of Multibody Dynamics* 219.1 (2005), pp. 35–53.

[60] W. D. Zhu and Y. Chen. "Theoretical and experimental investigation of elevator cable dynamics and control". In: *Journal of Vibration and Acoustics, Transactions of the ASME* 128.1 (2006), pp. 66–78.

[61] W. T. van Horssen. "Asymptotic theory for a class of initial-boundary value problems for weakly nonlinear wave equations with an application to a model of the galloping oscillations of overhead transmission lines". In: *SIAM Journal of Applied Mathematics* 48.6 (1988), pp. 1227–1243.

[62] W.A. Strauss. *Partial differential equations: An introduction.* Wiley, 1992.

[63] C.D. Mote Jr. W.D. Zhu and B.Z. Guo. "Asymptotic Distribution of Eigenvalues of a Constrained Translating String". In: *Journal of Applied Mechanics* 64(3) (1997), pp. 613–619.

[64] W.D. Zhu and G.Y. Xu. "Vibration of elevator cables with small bending stiffness". In: *Journal of Sound and Vibration* 263 (2003), pp. 679–699.

[65] J.A. Wickert and C.D. Mote Jr. "On the energetics of axially moving continua". In: *The Journal of the Acoustical Society of America* 85.3 (1989), p. 1365.

[66] W.D. Zhu and J. Ni. "Energetics and Stability of Translating Media with an Arbitrary Varying Length". In: *Journal of Vibration and Acoustics* 122.3 (1999), pp. 295–304.

Summary

In this thesis five initial-boundary value problems are studied. These problems describe the motion of axially moving continua such as strings and beams. The developed mathematical models may be regarded in reality as models describing the transverse vibrations of mechanical elastic structures such as conveyor belts and elevator cables.

Chapter 2 starts with a simple model of a damped traveling string between two fixed pulleys. An important distinction of this problem compared to previous research is a contribution of linear viscosity of the material. We tackle this problem by the Laplace transform method due to its straightforwardness. The obtained results show the influence of the transport velocity and the viscous damping to the dynamics of the model.

Chapter 3 continues with the study of the damping generated at the boundary in an axially moving, elastic string with an attached mass-spring-dashpot system. An asymptotic approximation of the low-frequency response of the string is constructed by using a two-timescales perturbation method. Moreover, an alternative implicit exact solution is obtained by the Laplace transform method, where the damping rates and the frequencies of oscillations modes are found. Both approaches, approximate and exact, show agreement. For higher order frequencies, a beam-like model has to be investigated.

Chapter 4 extends the previous study of boundary damping of axially moving systems by considering a semi-infinite span of the string with different types of boundary supports. We employ the classical method of d'Alembert to obtain the response to the initial conditions and analyze the energy to examine the efficiency of the boundary supports. The obtained exact solutions show reflection properties for different types of boundaries.

Chapter 5 is concerned with the study of a vertically moving string with a time-varying length under the gravitational forces. The string length fluctuates periodically about a constant mean length. This chapter mainly studies the dynamic stability of the string oscillations. Moreover, it is shown there that the Fourier-series method combined with the truncation method is not applicable for such type of problems. In order to tackle the problem, the characteristic coordinates may play a part.

Finally, Chapter 6 extends the study of Chapter 5 by considering the sway of the boundaries of a vertically moving beam in horizontal direction. In this problem, the length of the beam linearly changes in time. This problem is referred to as singularly perturbed problems. To tackle the singularly perturbed problem, we developed an advanced analytic scheme and constructed an asymptotic approximation of the lateral response of the cable which is valid on long timescales.

Samenvatting

In dit proefschrift zijn vijf begin-randwaarde problemen bestudeerd. Deze problemen beschrijven de trillingen van axiaal bewegende continua, zoals snaren en balken. De ontwikkelde, mathematische modellen kunnen gezien worden als modellen die de transversale trillingen van elastische, mechanische objecten zoals transportbanden en liftkabels beschrijven.

Hoofdstuk 2 begint met een eenvoudig model voor een gedempte, longitudinaal bewegende snaar tussen twee vaste katrollen. Een belangrijke verschil tussen dit model in vergelijking met voorgaand onderzoek is een bijdrage van lineaire viscositeit van het materiaal. We hebben dit probleem opgelost met behulp van de Laplace transformatie methode vanwege de directe toepasbaarheid ervan. De verkregen resultaten laten de invloed van de transport-snelheid en de visceuze demping op de dynamica van het model zien.

Hoofdstuk 3 gaat verder met de studie van demping gegenereerd door een massaveer-demper systeem op de rand van een axiaal bewegende, elastische snaar. Een asymptotische benadering van de lage-frequentierespons van de snaar is geconstrueerd gebruikmakende van een twee tijdschalen perturbatie methode. Bovendien is een alternatieve, impliciet exacte oplossing verkregen gebruikmakende van de Laplace transformatie methode, waarmee de dempingskarakteristieken en de frequenties van de oscillerende modes gevonden zijn. Beide benaderingen, zowel de benaderde oplossing als de exacte oplossing, zijn in overeenstemming met elkaar. Voor hogere orde frequenties, moet een balk-achtig model worden onderzocht.

Hoofdstuk 4 breidt de vorige studie van dempende systemen voor axiale bewegende systemen uit door het beschouwen van half-oneindige lengtes voor de snaar met verschillende typen van randvoorwaarden. We gebruiken de klassieke methode van d'Alembert om de respons op de beginvoorwaarden te bepalen, en analyseren de energie van het systeem om de efficiëntie van deze dempers op de rand te bepalen. De verkregen exacte oplossingen laten reflectie eigenschappen zien voor verschillende typen van randen.

Hoofdstuk 5 betreft de studie van verticaal bewegende snaren die onderhevig zijn aan gravitatiekrachten. De lengte van de snaar varieert periodiek met een constante gemiddelde lengte. Dit hoofdstuk bestudeert voornamelijk de dynamische stabiliteit van de trillingen van de snaar. Bovendien wordt aangetoond dat de Fourierreeks methode, gecombineerd met de truncation methode, niet toepasbaar is voor dit type problemen. Om toch dit soort problemen te kunnen aanpakken, behoort het gebruik van de ka-

rakteristieke coördinaten methode in combinatie met de twee tijdschalen perturbatie methode tot een mogelijke oplossings strategie.

Het laatste hoofdstuk, hoofdstuk 6, breidt de studie in hoofdstuk 5 uit door het beschouwen van trillingen van de randen van een verticaal bewegende balk in de horizontale richting. Voor dit probleem geldt dat de lengte van de balk verandert in de tijd. Dit probleem behoort tot de klasse van singulier verstoorde problemen. Om deze singulier verstoorde problemen te kunnen aanpakken, hebben we een geavanceerd analytisch schema ontwikkeld, en is een asymptotische benadering van de transversale respons van de kabel geconstrueerd die geldig is op lange tijdschalen.

Acknowledgements

Curriculum Vitæ

Nick V. Gaiko was born in Minsk, Belarus, on August 31, 1989. He completed his secondary education in 2006 at the Lyceum of the Belarusian State University in Minsk. In the same year he started his studies in Mechanics and Applied Mathematics at the Belarusian State University to obtain his Master of Science degree in 2012 under supervision of Prof. dr. M.A. Zhuravkov. Then, from September 1, 2012 he started his PhD research at the Delft Institute of Applied Mathematics of the Delft University of Technology under supervision of Dr. ir. W.T. van Horssen.

List of Publications

1. **N.V. Gaiko & W.T. van Horssen**, *Resonances and vibrations in an elevator cable system due to boundary sway (submitted)*.

2. **N.V. Gaiko & W.T. van Horssen**, *On transversal oscillations of a vertically translating string with small time-harmonic length variations*, Journal of Sound and Vibration, **383**, 339-348 (2016).

3. **N.V. Gaiko & W.T. van Horssen**, *On wave reflections and energetics for a semi-infinite traveling string with a nonclassical boundary support*, Journal of Sound and Vibration, **370**, 336-350 (2016).

4. **N.V. Gaiko & W.T. van Horssen**, *On the lateral vibrations of a vertically moving string with a harmonically varying length*, ASME International Mechanical Engineering Congress and Exposition, Proceedings (IMECE) **IMECE2015-50449**, V04BT04A060 (2015).

5. **N.V. Gaiko & W.T. van Horssen**, *On the transverse, low frequency vibrations of a traveling string with boundary damping*, Journal of Vibration and Acoustics, Transactions of the ASME **137(4)**, 041004-041004-10 (2015).